FOSSIL ENERGY

DOE/BC/14953-19
(DE96001297)

INCREASED OIL PRODUCTION AND RESERVES FROM IMPROVED COMPLETION TECHNIQUES IN THE BLUEBELL FIELD, UINTA BASIN, UTAH

Annual Report 1996

By
Craig D. Morgan

July 1997

Performed Under Contract No. DE-FC22-92BC14953

Utah Geological Survey
Salt Lake City, Utah

National Petroleum Technology Office
U. S. DEPARTMENT OF ENERGY
Tulsa, Oklahoma

INCREASED OIL PRODUCTION AND RESERVES FROM IMPROVED COMPLETION TECHNIQUES IN THE BLUEBELL FIELD, UINTA BASIN, UTAH

Annual Report for the Period
October 1, 1995 to September 30, 1996

By
Craig D. Morgan

Principal Investigator
M. Lee Allison

Performed Under Contract No. DE-FC22-92BC14953

Utah Geological Survey
Salt Lake City, Utah

CONTENTS

ILLUSTRATIONS

TABLES

ABSTRACT

The Bluebell field is productive from the Tertiary lower Green River and Wasatch Formations of the Uinta Basin, Utah. The productive interval consists of thousands of feet of interbedded fractured clastic and carbonate beds deposited in a fluvial-dominated deltaic lacustrine environment. Wells in the Bluebell field are typically completed by perforating 40 or more beds over 1,000 to 3,000 vertical feet (300-900 m), then stimulating the entire interval. This completion technique is believed to leave many potentially productive beds damaged and/or untreated, while allowing water-bearing and low-pressure (thief) zones to communicate with the wellbore. Geologic and engineering characterization has been used to define improved completion techniques.

A two-year characterization study involved detailed examination of outcrop, core, well logs, surface and subsurface fractures, produced oil-field waters, engineering parameters of the two demonstration wells, and analysis of past completion techniques and effectiveness. The characterization study resulted in recommendations for improved completion techniques and a field-demonstration program to test those techniques. The results of the characterization study and the proposed demonstration program are discussed in the second annual technical progress report.

The operator of the wells was unable to begin the field demonstration this project year (October 1, 1995 to September 20, 1996). Correlation and thickness mapping of individual beds in the Wasatch Formation was completed and resulted in a series of maps of each of the individual beds. These data were used in constructing the reservoir models. Non-fractured and fractured geostatistical models and reservoir simulations were generated for a 20-square-mile (51.8-km^2) portion of the Bluebell field. The modeling provides insights into the effects of fracture porosity and permeability in the Green River and Wasatch reservoirs.

EXECUTIVE SUMMARY

The objective of the project is to increase oil production and reserves by the use of improved reservoir characterization and completion techniques in the Uinta Basin, Utah. To accomplish this objective, a two-year geologic and engineering characterization of the Bluebell field was conducted. The study evaluated surface and subsurface data, currently used completion techniques, and common production problems.

Interpreted log data for thicknesses, porosities, and water saturations were used in a 20-square-mile (51.8-km^2) area of the Bluebell field in order to perform geostatistical, stochastic simulations. A total of 64 realizations for about 40 beds were generated and analyzed for initial fluids in place. The analyses provided not only averages of original oil in place but also an idea about data uncertainty, helping delineate the most promising beds in the 20-square-mile (51.8-km^2) area.

The reservoir characterization information, generated using geostatistical modeling, for the five most promising beds was input into a black-oil simulator and ten flow simulations were performed for each of the beds. The potential of oil production (with the uncertainty involved) was computed for each of the five beds over the entire 20-square-mile (51.8-km^2) area and also for Michelle Ute and Malnar Pike demonstration wells. Even though a number of assumptions were made in generating these results, the calculations estimate the intrinsic merit of the producibility of each of the beds in each of the wells.

These analyses were refined to include fracture porosity and permeability. In the base-fracture model, each block had three fractures at 220-feet (67.1-m) spacing. The fractures were vertical and present in both the x-z and y-z planes. With the incorporation of fractures, it was necessary to use a dual-porosity, dual-permeability black-oil simulator.

The modeling indicates that:

1. The overall variability in the flow simulations decreased as fractures were introduced into the reservoir model because the presence of fractures reduces the influence of variability in matrix characteristics.
2. Introduction of fractures affected production from Michelle Ute considerably more than from Malnar Pike because of differences in petrophysical reservoir characteristics around the two wells, such as bed thickness, porosity, and fluid saturation.
3. Increasing the fracture spacing increased oil production but decreased gas production. As a result, the gas-to-oil ratios (GORs) decreased as fracture spacing increased.
4. Increasing fracture porosity increased oil and gas production and thus kept the GOR more or less unchanged. At late stages in reservoir development, reservoirs with lower fracture porosities had higher GOR values.
5. Fracture permeability had the most significant and unexpected effect on production. As the fracture permeability increased, the oil production increased, up to a point; above this point oil production was dwarfed by gas production and the oil-production rates declined precipitously. Thus, for each fractured reservoir with a given matrix permeability there is an optimum fracture permeability (about 3-5 times the matrix permeability) beyond which oil production is unsustainably fast.

ACKNOWLEDGMENTS

This research is performed under the Class I Oil Program of the U. S. Department of Energy (DOE), Bartlesville Project Office contract number DE-FC22-92BC14953. The Contracting Officer's Representatives are Edith Allison and Jerry Casteel, with the DOE Bartlesville Project Office. Additional funding was provided by the Utah Office of Energy and Resource Planning.

1. INTRODUCTION

Craig D. Morgan
Utah Geological Survey
Salt Lake City, Utah

1.1. Project Status

The two-year characterization study of the Bluebell field, Duchesne and Uintah Counties, Utah, consisted of separate, yet related tasks. The characterization tasks were: (1) log analysis and petrophysical investigations, (2) outcrop studies, (3) cuttings and core analysis, (4) subsurface mapping, (5) acquisition and analyses of new logs and cores, (6) fracture analysis, (7) geologic characterization synthesis, (8) analysis of completion techniques, (9) reservoir analysis, (10) best completion technique identification, (11) best zones or areas identification, and (12) technology transfer.

The characterization study resulted in a better understanding of reservoirs in the Tertiary Green River and Wasatch Formations. The study yielded recommendations for improved bed evaluation and completion techniques. The findings of the study and plans for a three-part field demonstration were presented in the second annual technical progress report (Allison and Morgan, 1996).

The operator of the proposed demonstration wells was unable to begin the recompletion work during this project year. The work is scheduled to begin during the next project year (October 1, 1996 to September 30, 1997). Non-fractured and fractured geostatistical models and reservoir simulations were constructed for a 20-square-mile (51.8-km^2) area of eastern Bluebell field. Correlation and mapping of individual beds in the lower Wasatch was completed for the 20-square-mile (51.8-km^2) area. Fluid-entry logs that were run in many of the wells are currently being evaluated.

1.2. Geology and Field Background

The Bluebell field is the largest oil producing field in the Uinta Basin. Bluebell is one of three contiguous oil fields; Bluebell, Altamont, and Cedar Rim (figure 1.1). The basin is an asymmetrical syncline deepest in the north-central area near the basin boundary fault. The Bluebell field produces oil from the Eocene-Paleocene Green River and Wasatch Formations near the basin center.

The Bluebell field covers 251 square miles (650 km^2) and includes all or parts of T. 1 N., T. 1 and 2 S., R. 1 E., and R. 1 through 3 W., Uinta Base Line. Over 136 million barrels of oil (MMBO) (19 million metric tons [MM- MT]) and 174 billion cubic feet (BCF) (4.9 billion cubic meters [B-m^3]) of associated gas have been produced (July 30, 1996). The spacing is two wells per section, but much of the field is still developed at one well per section. The Roosevelt Unit within the Bluebell field operates under the unit agreement. Although some wells have produced over 3 MMBO (420,000 MT), most produce less than 0.5 MMBO (70,000 MT).

The Green River and Wasatch Formations were deposited in intertonguing relationship in and around ancestral Lake Flagstaff and Lake Uinta. Depositional cycles show rapid lake level fluctuations and changes in water chemistry (Fouch and Pitman, 1991, 1992; Fouch and others, 1992). The Green River and Wasatch Formations were deposited in alluvial-fluvial, marginal-lacustrine, and open-lacustrine environments. The depositional environments are described in detail by Fouch (1975, 1976, 1981), Ryder and others (1976), Pitman and others (1982), Pitman and others (1986), Bruhn and others (1983), Stokes (1986), Castle (1991), Fouch and Pitman (1991, 1992), Fouch and others (1990), and Franczyk and others (1992).

The oil production at Bluebell comes from three primary intervals: (1) lower Green River Formation/upper Wasatch transition, (2) Wasatch Formation, and (3) lower Wasatch transition (possible Flagstaff equivalent). The lower Green River/upper Wasatch transition is informally defined as the interval from the middle marker of the Green River to the top of the Wasatch (redbeds). The boundaries of the three intervals are transitional and intertonguing, as a result they are difficult to identity accurately.

The lower Wasatch transition (Flagstaff equivalent?), consists predominately of carbonate with minor sandstone beds that were deposited in marginal to open-lacustrine environments. The lower Wasatch is productive throughout most of the field. In the east portion of the field, lower Wasatch is a primary productive interval, while in the west portion both the Wasatch sandstone and lower Wasatch carbonate beds are productive.

Wasatch production is primarily from sandstone and siltstone beds deposited in alluvial to fluvial-deltaic environments. The sediment source for the Wasatch redbeds (sandstone, siltstone, and red shale) in Bluebell field was the Uinta Mountains to the north. The Wasatch redbeds thin rapidly from north to south through the field, with the best sandstone development present in the west portion of the field.

The lower Green River\upper Wasatch transition production is from interbedded calcareous sandstone, limestone, marlstone, and ostracodal limestone, deposited in fluvial-deltaic and carbonate mud-flat environments. Many of the lower Green River beds are laterally extensive and highly fractured.

Individual beds in the lower Green River and Wasatch producing interval are difficult to evaluate. Fracturing and complex formation-water chemistries make conventional geophysical log analysis highly questionable. Economics have discouraged open hole and/or production testing of individual beds. Therefore, it is not clearly understood which beds in any particular well are potentially significant producers, limited producers, water producers, or thieves. As a result, the common practice is to perforate numerous beds over thousands of vertical feet and apply an acid-frac treatment, generally 20,000 gallons (75,700 l) of hydrochloric acid (HCL). The typical well in the Bluebell field has between 1,500 to 2,000 feet (457-610 m) of gross perforations. As a result, the treatment is being applied to both clastic and carbonate, fractured and non-fractured beds, over-pressured and normally-pressured zones.

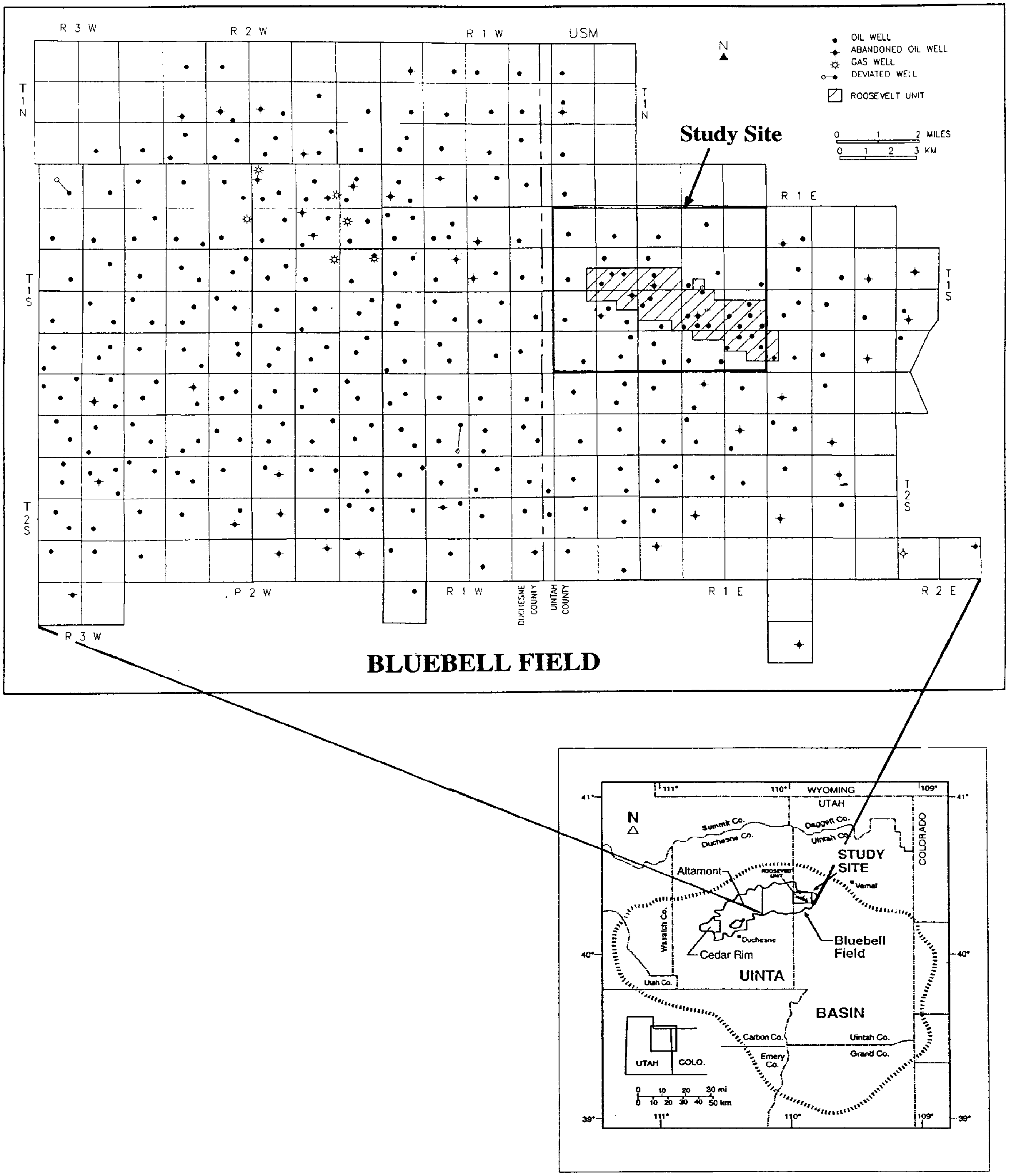

Figure 1.1. Location of Bluebell field, Duchesne and Uintah Counties, Utah.

2. SUBSURFACE MAPPING AND WELL LOG ANALYSIS

Craig D. Morgan
Utah Geological Survey
Salt Lake City, Utah

2.1. Thickness Mapping

Individual beds that met the minimum criteria for long-term production as determined by the characterization study (Allison and Morgan, 1996) have been correlated and mapped throughout the 20-square-mile (51.8-km^2) study area. A thickness map for each of the beds in the lower Wasatch are in the Appendix. Analysis of the thickness maps shows that 50 percent of the beds mapped are 4 feet (1.2 m) or less in thickness and only 12 percent are thicker than 10 feet (3.1 m). The beds typically have a limited areal distribution; 59 percent of the beds mapped cover an area of 640 acres (259.2 ha) or less.

2.2. Fluid-Entry Log Analysis

Fluid-entry (temperature and spinner) logs were evaluated from 29 wells in a 54-square-mile (139.9-km^2) area encompassing the 20-square-mile (51.8-km^2) study area. Based on the fluid-entry logs, 90 percent or more of the oil entry into the well bore of each well came from 1 to 15 beds over a gross vertical interval of 7 to 1,132 feet (2.1-345.3 m). The average productive interval consisted of five beds over a 564-foot (172.0-m) gross vertical thickness. Most wells have 40 to 60 beds over a 1,000-foot (305.0-m) gross vertical interval, open to the well bore. The top of the productive interval dips from south to north, similar to, but at a slightly lower angle, than the structural dip. The top of the productive interval is probably the top of the original over-pressured zone. Each of the fluid-entry logs were run within the first two years of the well's production history. One aspect that will be looked at during the demonstration phase is whether the production continues to come from the same interval late in a well's life as during the initial productive period. If it does, then the original productive beds as determined by fluid-entry logs, may be the beds to concentrate recompletion efforts on, greatly reducing the size of the treated interval.

3. NON-FRACTURED GEOSTATISTICAL MODELING AND RESERVOIR SIMULATIONS

Milind Deo and Rajesh Pawar
Department of Chemical and Fuels Engineering
University of Utah, Salt Lake City, Utah

3.1. Introduction

The objective of geostatistical modeling and reservoir simulation was to use the available geologic information to create realistic reservoir images of the Bluebell field or portions of the field. Once the reservoir characteristics were established, flow simulations were performed to assess oil-production performance. The Bluebell field encompasses several hundred square miles, hence, it was necessary to select a portion of the field for analysis. The geological and engineering characterizations were concentrated in a 20-square-mile (51.8-km^2) area (figure 3.1) containing 27 wells including the Michelle Ute and Malnar Pike demonstration wells. Most of the wells have been perforated over an interval spanning thousands of feet. About 60 different beds (numbered sequentially from shallow to deep) were correlated over the 20-square-mile (51.8-km^2) area. The data for the geostatistical models consists of correlated bed thicknesses, and calculated porosities and saturations from geophysical well logs.

3.2. Approach

The area shown in figure 3.1 was divided into a grid consisting of 41 blocks in the x-direction and 33 blocks in the y-direction. The block dimensions in the both the x and the y directions were 660 feet (201.3 m). Geostatistical methods were then used to generate statistically probable distributions of available reservoir properties in different beds. Porosity and saturation values as functions of spatial locations (x and y) were generated. The thicknesses generated using similar computations were then assigned to appropriate grid blocks. Grid-block thicknesses along with porosities and saturations completed the reservoir description. Using these properties, it was possible to compute the volume of the original fluids in place (oil, gas, and water) for selected beds.

Stochastic simulations allow generation of several equally probable realizations. A number of different realizations were created for selected beds. Using a set of these realizations, it was possible to calculate the variability (minimum, maximum, and standard deviation) in the volumes of the initial fluids in place.

The reservoir properties thus generated were input into a black-oil simulator, IMEX, developed by Computer Modeling Group (CMG), Inc. Simulations were performed individually for selected beds. The initial reservoir pressure was assigned based on a 0.5 pounds per square-inch per foot (psi/ft) (1.05 kPa/m) gradient. In addition to the reservoir properties generated via geostatistical models, the simulator required permeabilities, relative permeabilities, thermodynamic properties, and well constraints. For the purposes of this study, permeabilities were assumed constant at 0.5 millidarcies (mD). Thermodynamic properties were generated using oil and gas compositions and physical properties determined earlier in the study (Allison, 1995). A set of oil-water and oil-gas relative permeabilities were assumed. To assess production variability, data from different realizations were input to the flow simulator.

3.3. Geostatistics

Variograms of thickness, porosity, and saturation for each of the beds were generated and a variogram model was constructed. Most of the models are either spherical or exponential and the properties are correlatable up to about 2,000 to 3,000 feet (610-915 m). The variograms were used for generating property distributions using sequential Gaussian simulations. As an example, the thickness, porosity, and saturation distributions of bed 18 are shown in figures 3.2, 3.3, and 3.4.

The average original oil in place (OOIP) for beds 13 through 44 are tabulated in table 3.1. Most of the wells in the 20-square-mile (51.8-km^2) area produce from below bed 12. The averages were calculated using 64 realizations for each bed. There is a large gap between the minimum and the maximum values for each of the beds. However, since the data was averaged over a large number of realizations, the standard deviations are reasonable. Thus, the OOIP of a certain bed can be narrowed to the mean value plus or minus the standard deviation with a reasonable degree of confidence. The five most promising beds based on this analysis are:

1. bed 23 - average OOIP = 28.8 million stock-tank-barrels (MMstb) (4.03 MM-MT),
2. bed 18 - average OOIP = 23.4 MMstb (3.27 MM-MT),
3. bed 19 - average OOIP = 22.6 MMstb (3.16 MM-MT),
4. bed 30 - average OOIP = 20.3 MMstb (2.84 MM-MT), and
5. bed 20 - average OOIP = 17.1 MMstb (2.39 MM-MT).

The total OOIP in the 20-square-mile (51.8-km^2) area was about 400 MMstb (56 MM-MT), only a fraction of which has been produced to date. Thus, the field has a tremendous amount of oil still in place. Producing this oil economically is a significant technical challenge facing the operators in the field.

3.4. Reservoir Simulations

Reservoir simulations were performed on five of the most promising beds. The beds were considered isolated and simulated individually. Simulations were performed on 10 different realizations in the time period 1981 through 1995. Simulated production results for the five beds are summarized in table 3.2. In most cases the standard deviation is less than 10 percent of the average production. Based on total production, the beds are ranked as follows:

1. bed 23 - 993.23 thousand stock-tank-barrels (Mstb) (139.05 M-MT),
2. bed 19 - 967.11 Mstb (135.39 M-MT),
3. bed 18 - 785.38 Mstb (109.95 M-MT),
4. bed 30 - 431.80 Mstb (60.45 M-MT), and

5. bed 20 - 298.07 Mstb (41.73 M-MT).

This ranking corresponds more or less to the OOIP ranking of the beds except that beds 18 and 19 are reversed. Bed 19 has produced a larger percentage of the OOIP (4.3 percent) than any other bed. Thus, a recovery of only about two to four percent of the OOIP can be expected from these reservoirs with low permeabilities and no fractures.

In the demonstration wells, the most productive beds are:

1. bed 19 - 96.25 Mstb (13.48 M-MT),
2. bed 20 - 28.43 Mstb (3.98 M-MT),
3. bed 30 - 21.73 Mstb (3.04 M-MT),
4. bed 18 - 20.48 Mstb (2.87 M-MT), and
5. bed 23 - 1.71 Mstb (0.24 M-MT), for the Michelle Ute and
1. bed 20 - 36.67 Mstb (5.13 M-MT),
2. bed 18 - 35.53 Mstb (4.97 M-MT),
3. bed 19 - 29.11 Mstb (4.08 M-MT),
4. bed 23 - 18.24 Mstb (2.55 M-MT), and
5. bed 30 - 15.71 Mstb (2.19 M-MT), for the Malnar Pike well.

Thus, even though bed 23 contains a considerable amount of oil in place, according to the model, it has not been a productive interval in Michelle Ute because of high water saturations. No single bed in the Malnar Pike well contains a large volume of OOIP, even though the total production from all the five beds under ideal conditions should exceed 100 Mstb (14.0 M-MT).

3.5. Summary

Interpreted log data for thicknesses, porosities, and water saturations were used in a 20-square-mile (51.8-km^2) area of the Bluebell field in order to perform geostatistical stochastic simulations. A total of 64 realizations for about 40 beds were generated and analyzed for initial fluids in place. The analyses provided not only averages of OOIP but also an idea about data uncertainty. The most promising beds in the 20-square-mile (51.8-km^2) area were thus determined.

The reservoir characterization information generated using geostatistical modeling for the five most promising beds was input into a black-oil simulator and ten flow simulations were performed for each of the beds. The potential of oil production (with the uncertainty involved) was computed for each of the five beds over the entire 20-square-mile (51.8-km^2) area and also for Michelle Ute and Malnar Pike demonstration wells. Even though a number of assumptions were adopted in generating these results, the calculations provide an estimate of the producibility of each of the beds in each of the wells.

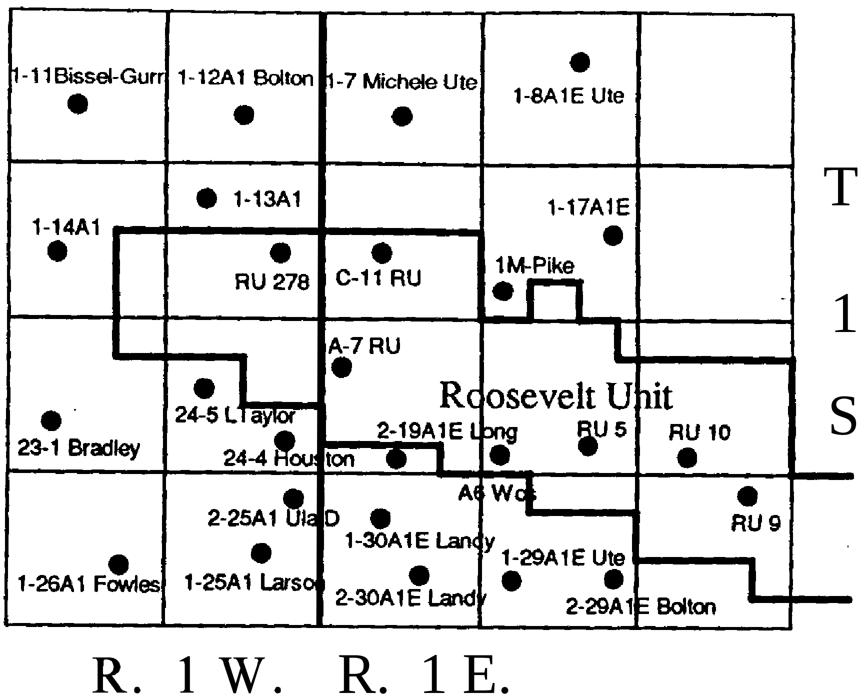

Figure 3.1. Map of the 20-square-mile (51.8-km^2) area showing well locations and names.

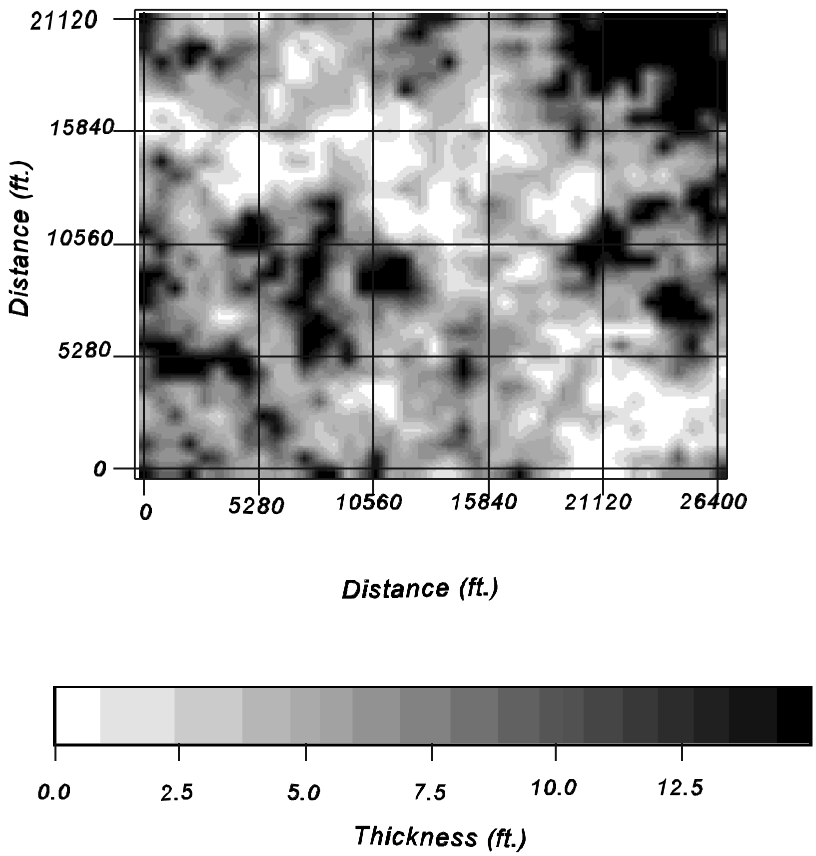

Figure 3.2. Thickness distribution of bed 18 in the 20-square-mile (51.8-km^2) area.

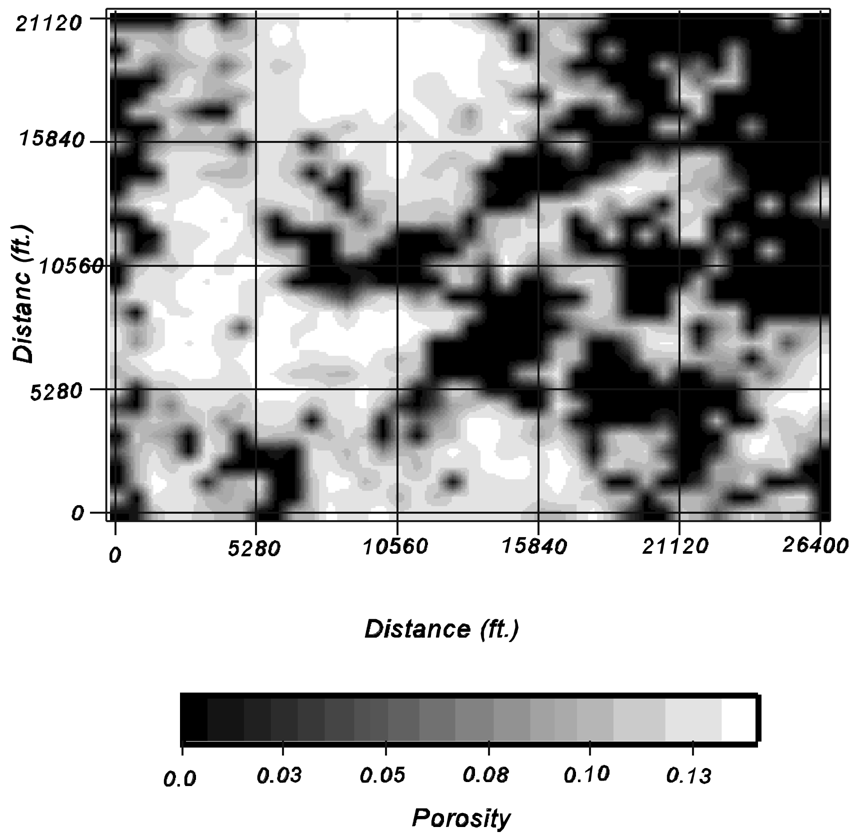

Figure 3.3. Porosity distribution of bed 18 in the 20-square-mile (51.8-km^2) area.

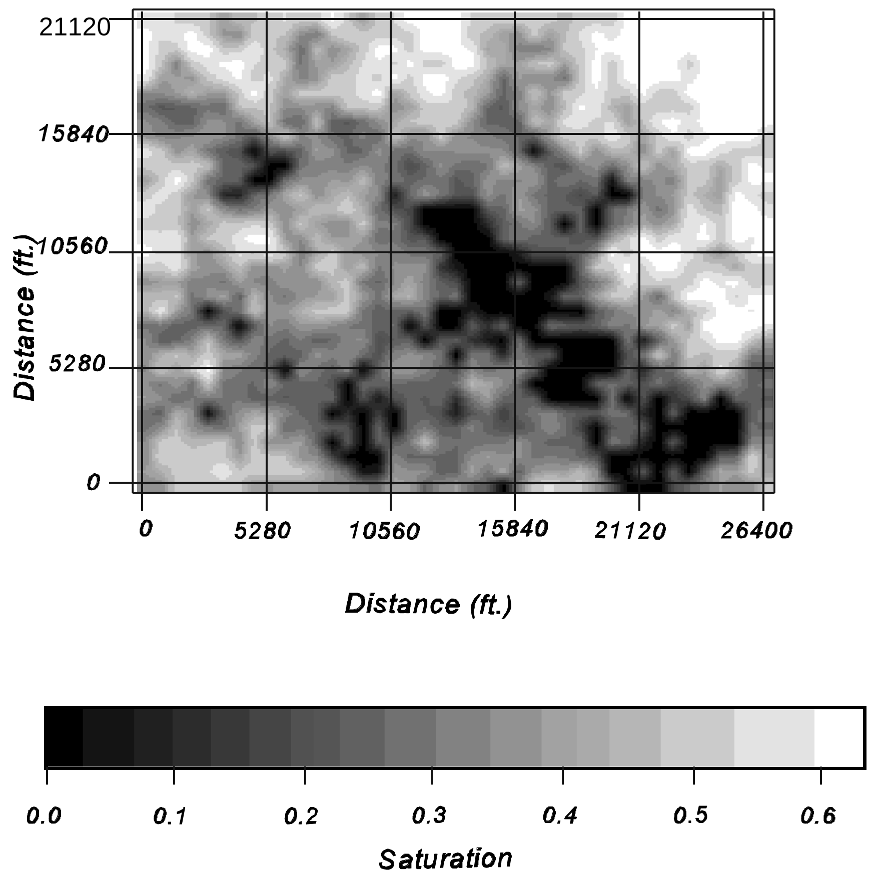

Figure 3.4. Water-saturation distribution of bed 18 in the 20-square-mile (51.8-km^2) area.

Table 3.1. Statistics of original-oil-in-place calculations. Sixty-four realizations were used for each bed.

Bed	Average (MMstb)	Minimum (MMstb)	Maximum (MMstb)	Standard Deviation (MMstb)
13	8.64	4.32	18.9	3.21
13a	8.16	4.15	20.9	3.72
13b	1.48	0.1	7.32	1.7
14	3.18	1.34	10.4	1.78
15	5.67	2.61	17.9	2.66
16	7.22	3.73	17.4	2.75
16 a	10.74	5.22	23.8	4.1
17	8.08	5.38	17.9	2.34
18	23.4	17.3	42.5	4.87
19	22.6	18.8	33.3	3.03

Bed	Average (MMstb)	Minimum (MMstb)	Maximum (MMstb)	Standard Deviation (MMstb)
19a	16.0	9.93	24.5	3.25
19b	6.0	3.6	11.1	1.8
19c	6.0	3.23	14.6	2.5
20	17.1	12.3	32.9	3.9
21	3.48	1.65	10.23	1.63
22	4.2	2.1	11.72	1.76
23	28.8	22.0	46.4	4.67
23a	3.46	1.17	12.3	2.35
23b	5.8	2.0	21.6	3.64
23c	9.51	4.47	19.4	3.22
24	2.2	0.63	9.02	1.55
24a	1.03	0.27	4.03	0.91
25	1.93	0.64	5.75	1.0
25a	2.7	0.98	9.54	1.68
26	5.5	3.47	11.9	1.67
26a	3.65	2.0	7.7	1.3
26b	4.24	1.91	12.3	2.1
26c	4.18	1.6	12.3	2.1
27	14.8	10.8	24.4	2.63
28	8.36	4.63	18.8	2.93
29	5.45	1.94	12.1	2.0
30	20.3	14.1	37.2	4.5
31	15.3	9.2	31.3	4.45
31a	6.8	3.7	13.2	2.0
32	10.3	6.3	24.2	3.6
33	6.3	3.1	19.3	3.1
34	8.8	4.5	22.1	3.6
35	1.98	0.42	7.6	1.5
36	8.95	5.1	22.7	3.4
37	7.9	4.1	18.8	3.2
37a	1.3	0.21	6.5	1.7
38	7.2	3.5	16.2	2.3
38a	1.9	0.46	5.0	1.0
39	9.88	5.7	21.1	3.3
40	3.05	1.42	11.3	1.73
41	4.1	1.5	13.0	2.3
41a	5.0	1.5	15.0	2.9
41b	5.9	2.8	17.9	2.9
41c	6.3	2.1	20.5	4.1
42	0.83	0.19	3.6	0.93
43	1.8	0.27	9.1	2.0
44	5.5	1.9	18.4	3.8

4. FRACTURED GEOSTATISTICAL MODELING AND RESERVOIR SIMULATIONS

Milind Deo and Rajesh Pawar
Department of Chemical and Fuels Engineering
University of Utah, Salt Lake City, Utah

4.1. Introduction

The non-fractured reservoir simulations and geostatistical models for a 20-square-mile (51.8-km^2) area in the Bluebell field are presented in Chapter 3 of this report. Fractures were incorporated into the database and the reservoir simulations and geostatistical models were run again to evaluate the effect that fracture porosity and permeability has on reservoir performance in the 20-square-mile (51.8-km^2) area.

4.2. Approach

The areal extent of the fractured model (20-square miles [51.8-km^2]) and the grid dimensions employed were the same as the non-fractured model. A block-centered grid was used with a uniform grid size of 660 feet (201.3 m). There were 41 grid blocks in the x-direction and 33 in the y-direction. The thicknesses of the beds that were simulated varied and were generated using the geostatistical model. As in the fractured model the five most promising beds were selected for flow simulations. In the base-fracture model, each block had three fractures at a 220-foot (67.1-m) spacing. The fractures were vertical and present in both the x-z and y-z planes. With the incorporation of fractures, it was necessary to use a dual-porosity, dual-permeability black-oil simulator (porosity and permeability of the matrix; porosity and permeability of fractures). The base matrix and fracture properties used in the flow simulations are presented in table 4.1.

4.3. Results and Discussions

4.3.1. Production Statistics

Sixty-four flow simulations were performed on each of the five beds. The mean oil and gas production for the entire 20-square-mile (51.8-km^2) area and the oil and gas production for the Michelle Ute and the Malnar Pike wells are shown in table 4.2. The table also lists production from the non-fractured model. The production in bed 18 tripled due to the presence of fractures; however, the gas production increased six times. The GOR for the fractured model increased from 945 scf/stb (standard cubic feet/stock tank barrel [3.5 m^3/MT]) to 1,660 scf/stb (6.5 m^3/MT). GOR values of about 1,000 scf/stb (3.9 m^3/MT) are more common in the Bluebell field than values around 1,500 scf/stb (5.9 m^3/MT). The Michelle Ute and the Malnar Pike wells appeared to be affected differently by the presence of fractures. The production in Michelle Ute increased by an order of magnitude while the production from Malnar Pike only doubled.

Because the fracture representation around the wells is uniform, the production must be related to petrophysical reservoir characteristics around the wells, such as bed thickness, porosity, and fluid saturation. The fractured model over-predicts production, leading to the following possibilities:

1. Most of the fractures are closed and for all practical purposes; the reservoir behaves as if it is non-fractured.

2. There are even fewer fractures than are represented in the fractured model.

3. There is extensive formation damage limiting the production potential of each well.

The standard deviations in both oil and gas production are significantly lower in the fractured model compared to the non-fractured model (table 4.2). Thus, introduction of a uniform fracture network reduces uncertainties in the simulated production compared to the use of equally probable reservoir images of the non-fractured reservoir. This is due to the fact that once the fractures are introduced into the model, they dominate production and reduce the importance of a more accurate representation of the petrophysical properties of the reservoir.

Production responses from beds 18, 19, and 23 are similar to each other. Oil production from these beds for the fractured model increases two to four times while the gas production is six to eight times greater. Thus, the effective GOR values for the fractured model are 1.5 to 3 times higher than the non-fractured models. Once again, production from Michelle Ute increases much more than production from Malnar Pike. This may be because the water saturation for Michelle Ute in bed 23 is 100 percent; in a non-fractured reservoir, there is no avenue for the drainage of oil that lies beyond the water saturated grid block. The fractures provide this drainage capability, resulting in an increase in the oil production in Michelle Ute for bed 23 of almost two orders of magnitude.

The quality of the reservoir around each of the wells also plays an important role in the production capability of the wells. The increase in oil and gas production from beds 30 and 31 shows the same trends in both the Michelle Ute and the Malnar Pike wells. The main reason for the matching trends is the similarity of the petrophysical properties of these beds in the near-well-bore regions of the two wells.

4.3.2. Effect of Fracture Spacing

The effect of fracture spacing on cumulative oil production from the 20-square-mile (51.8-km^2) area is shown in figures 4.1 and 4.2. As seen in figure 4.1, the oil production increases as the number of fractures increases. This increase in oil production is significant where the number of fractures increases from 1-in-10,560 feet (3,221 m) to 1-in-1,320 feet (403 m). However, as the number of fractures increase from 1-in-1,320 feet (403 m) to 1-in-110 feet (34 m), the increase in oil production is minor. The cumulative gas production however, follows an opposite trend. As the number of fractures increase, the gas production decreases (figure 4.2). As in the case of oil production, the decrease is minor when the number of fractures increases from 1-in-1,320 feet (403 m) to 1-in-110 feet (34 m).

4.3.3. Effect of Fracture Porosity

Fracture porosity is defined as the percentage of total reservoir volume occupied by fractures. The changes in cumulative oil and gas production with respect to fracture porosity are presented in figures 4.3 and 4.4. As the fracture porosity increases, the oil production increases. This increase is directly related to the initial oil in place. The gas production also increases but this increase is not directly related to the initial gas in place.

4.3.4. Effect of Fracture Permeability

The effect of fracture permeabilities on oil and gas production from the 20-square-mile (51.8-km^2) area is shown in figures 4.5 and 4.6. The gas production increases with fracture higher permeabilities. The oil production however, increases only to a point and then decreases due to increased gas production. At higher fracture permeabilities, the initial oil production increases but is rapidly inhibited by increasing gas production. This suggests that there is an optimum fracture-to-matrix permeability ratio which when exceeded, can actually cause lower oil production.

4.3.5. Effect of Fracture Properties on Production Rates

The effect of fracture spacing on oil- and gas-production rates is presented in figures 4.7 and 4.8. For each increase in fracture spacing, the oil-production rate declines, while the gas-production rate decreases initially, and then levels off. The oil production is related to pressure decline, while the gas production is tied more closely to the reservoir pressure approaching and then falling below, the oil bubble-point pressure. Once free gas appears in the reservoir, the gas-production rate increases rapidly. Consistent with observations regarding cumulative oil and gas production, the oil-production rate decreases as the number of fractures decreases and the gas-production rate increases as the number of fractures decreases.

As the fracture porosity increases, the oil-production rate also increases (figure 4.9). That is generally true for the gas-production rate until late in a well's history when the low-porosity reservoirs have higher gas-production rates (figure 4.10). In these reservoirs, free gas is formed later in the production history of the wells.

The oil- and gas-production rates, as functions of fracture permeabilities, are plotted in figures 4.11 and 4.12. The oil- and gas-production trends are similar to the cumulative oil- and gas-production trends. The initial rates are proportional to the fracture permeabilities; however, production rates from the high-permeability fractures decrease rapidly and after about three years of production, oil-production rates drop to near-zero. These trends highlight the danger of producing from high-permeability fractures in reservoirs with extremely low matrix permeabilities.

4.3.6. Effect of Fracture Properties on Production from Individual Wells

The effects of fracture spacing, porosity, and permeability on cumulative oil production from the Michelle Ute and the Malnar Pike wells are identical to those described for the cumulative oil production from the 20-square-mile (51.8-km^2) area. The same is true for cumulative gas production and oil- and gas-production rates for these two wells. Thus, the mechanisms that govern oil production for the 20-square-mile (51.8-km^2) area are also applicable at the single-well scale.

4.3.7. Fracture Properties and GOR

The effect of fractures on GORs in Michelle Ute well are plotted in figures 4.13 and 4.14. In the Michelle Ute well the GORs increase as the number of fractures decrease (figure 4.13). Initially, GORs are insensitive to fracture porosity, but late in the production life of the reservoir, the reservoirs with lower fracture porosities have higher GOR values. The GORs also increase rapidly as the fracture permeabilities increase. The GOR trends for Malnar Pike and the entire 20-square-mile (51.8-km^2) area are similar to those shown in figures 4.13 and 4.14 for the Michelle Ute well.

4.4. Conclusions

1. The overall variability in the flow simulations decreased as fractures were introduced into the reservoir model because fractures reduce the influence of variability in matrix characteristics.

2. Introduction of fractures into the reservoir model affected production from Michelle Ute considerably more than it did Malnar Pike production because of differences in petrophysical reservoir characteristics around the two wells, such as bed thickness, porosity, and fluid saturation.

3. Increasing the fracture spacing increased oil production but decreased gas production. As a result, the GORs decreased as fracture spacing increased.

4. Increasing fracture porosity increased oil and gas production and thus GORs remained practically unchanged; however, at late stages in reservoir development, production from reservoirs with lower fracture porosities had higher GOR values.

5. Fracture permeability had the most significant and unexpected result on production. As the fracture permeability increased, the oil production increased, up to a point. At permeabilities higher than this optimum, the oil production was dwarfed by gas production and the oil-production rates declined precipitously. Thus, for each fractured reservoir with a given matrix permeability there is an optimum fracture permeability (about three to five times the matrix permeability) beyond which oil production decreases rapidly.

Table 4.1. Matrix and fracture properties used in the flow simulations

Grid	41 x 33 x 1
Grid-Block Dimensions (x and y)	660 ft x 660 ft
Fracture Spacing	1/220 ft
Thickness	0 ft to 16 ft
Matrix Porosity	0.0 to 0.13
Fracture Porosity	0.005
Matrix Permeability	0.5 mD
Fracture Permeability	1.5 mD
Initial Pressure Gradient	0.5 psi/ft
Initial Matrix Oil Saturation	0.06 to 1.0
Initial Fracture Oil Saturation	1.0
Initial Bubble-Point Pressure	3,900 psi

Table 4.2. Summary of production from the five most significant beds.

statistics	20-square-mile area			Michelle Ute			Malnar Pike		
bed 18 (non - fractured)									
	Oil (Mstb)	Gas (MMscf)	Water (Mstb)	Oil (Mstb)	Gas (MMscf)	Water (Mstb)	Oil (Mstb)	Gas (MMscf)	Water (Mstb)
average	785.38	742.24	42.45	20.48	16.73	11.92	35.33	36.84	0.06
minimum	681.07	680.4	41.06	18.48	11.72	10.84	13.58	19.56	0.0
maximum	897.95	809.67	43.66	22.44	19.07	18.10	49.33	44.65	0.21
standard deviation	60.83	37.58	0.86	1.35	2.11	2.20	12.47	8.99	0.08
bed 18 (fractured)									
	Oil (Mstb)	Gas (MMscf)	Water (Mstb)	Oil (Mstb)	Gas (MMscf)	Water (Mstb)	Oil (Mstb)	Gas (MMscf)	Water (Mstb)
average	2547.40	4228.2	19.41	231.06	260.57	7.43	89.95	136.82	0.001
minimum	2321.7	3925.6	16.3	194.21	242.04	6.53	64.06	89.6	0.0
maximum	2994.5	4497.6	23.23	263.25	289	8.98	132.56	173.24	.009
standard deviation	136.4	150.07	1.42	21.53	11.98	0.51	20.09	22.37	0.002
bed 19 (non - fractured)									
	Oil (Mstb)	Gas (MMscf)	Water (Mstb)	Oil (Mstb)	Gas (MMscf)	Water (Mstb)	Oil (Mstb)	Gas (MMscf)	Water (Mstb)
average	967.11	898.94	39.44	96.25	80.27	7.41	29.11	26.66	0.88
minimum	894.44	874.15	38.58	82.98	70.49	7.11	17.34	16.51	0.62
maximum	1003.0	912.6	40.65	110.01	90.88	7.67	38.23	33.29	1.02
standard deviation	31.65	13.38	0.66	8.66	6.43	0.18	7.17	5.43	0.13
bed 19 (fractured)									
	Oil (Mstb)	Gas (MMscf)	Water (Mstb)	Oil (Mstb)	Gas (MMscf)	Water (Mstb)	Oil (Mstb)	Gas (MMscf)	Water (Mstb)
average	2850.31	5401.7	12.92	345.31	508.86	3.0	78.19	152.18	0.15
minimum	2699.4	5123.2	11.18	315.56	469.93	2.6	59.72	99.9	0.0
maximum	3043.7	5756.1	14.81	373.11	553.13	3.43	105.93	191.22	0.35
standard deviation	101.13	173.15	0.89	16.42	14.70	0.29	14.04	24.77	0.11

bed 23 (non - fractured)

statistics	20-square-mile area			Michelle Ute			Malnar Pike		
	Oil (Mstb)	Gas (MMscf)	Water (Mstb)	Oil (Mstb)	Gas (MMscf)	Water (Mstb)	Oil (Mstb)	Gas (Mscf)	Water (Mstb)
average	993.23	846.47	274.84	1.71	1.51	73.01	18.24	15.31	8.27
minimum	877.36	754.64	221.01	0.0	0.0	0.0	11.81	9.91	4.87
maximum	1106.7	944.67	349.62	8.55	7.49	129.63	31.99	26.50	11.86
standard deviation	77.28	65.16	35.28	3.44	3.05	46.87	6.85	5.61	2.32

bed 23 (fractured)

statistics	20-square-mile area			Michelle Ute			Malnar Pike		
	Oil (Mstb)	Gas (MMscf)	Water (Mstb)	Oil (Mstb)	Gas (MMscf)	Water (Mstb)	Oil (Mstb)	Gas (Mscf)	Water (Mstb)
average	4441.68	8156.44	179.04	161.28	215.33	44.85	132.76	228.94	7.49
minimum	4228.9	7689	121.23	146.39	197.75	18.97	108.82	200.45	2.15
maximum	4799.4	8508.5	279	185.17	237.91	63.7	171.71	280.4	14.73
standard deviation	140.99	172.50	42.91	9.62	9.47	15.71	19.09	18.96	3.98

bed 30 (non - fractured)

statistics	20-square-mile area			Michelle Ute			Malnar Pike		
	Oil (Mstb)	Gas (MMscf)	Water (Mstb)	Oil (Mstb)	Gas (MMscf)	Water (Mstb)	Oil (Mstb)	Gas (Mscf)	Water (Mstb)
average	431.80	370.78	268.57	21.73	18.45	29.96	15.71	13.25	22.97
minimum	351.28	301.11	217.24	12.41	10.55	23.58	7.58	6.37	19.99
maximum	496.39	422.1	374.22	28.29	24.05	42.06	27.79	23.59	26.45
standard deviation	46.85	39.99	47.77	6.13	5.20	6.12	6.66	5.68	2.14

bed 30 (fractured)

statistics	20-square-mile area			Michelle Ute			Malnar Pike		
	Oil (Mstb)	Gas (MMscf)	Water (Mstb)	Oil (Mstb)	Gas (MMscf)	Water (Mstb)	Oil (MMstb)	Gas (Mscf)	Water (Mstb)
average	3492.84	6255.07	214.93	340.49	505.51	31.34	235.06	432.78	22.93
minimum	3142	5771	146.97	305.1	446.66	15.9	186.72	361.05	15.48
maximum	3819.2	6710	312.66	377.43	576.28	52.19	313.14	519.57	32.91
standard deviation	202.35	243.60	41.60	16.52	26.82	9.22	35.28	38.74	4.45

bed 31 (non - fractured)

statistics	20-square-mile area			Michelle Ute			Malnar Pike		
	Oil (Mstb)	Gas (MMscf)	Water (Mstb)	Oil (Mstb)	Gas (MMscf)	Water (Mstb)	Oil (Mstb)	Gas (Mscf)	Water (Mstb)
average	298.07	256.42	263.89	28.43	24.16	22.08	36.67	29.40	20.77
minimum	243.00	212.91	223.4	17.89	15.21	15.58	23.96	19.07	16.24
maximum	370.97	314.43	330.56	43.91	37.32	31.70	62.51	51.64	27.66
standard deviation	48.39	38.03	30.72	8.65	7.35	5.51	12.96	11.21	4.69

bed 31 (fractured)

statistics	20-square-mile area			Michelle Ute			Malnar Pike		
	Oil (Mstb)	Gas (MMscf)	Water (Mstb)	Oil (Mstb)	Gas (MMscf)	Water (Mstb)	Oil (Mstb)	Gas (Mscf)	Water (Mstb)
average	2824.33	4720.75	208.43	342.69	425.56	24.51	324.28	576.83	19.06
minimum	2546.1	4346.9	126.38	309.51	388.35	12.35	276.58	494.88	13.28
maximum	3222.2	5090.3	324.02	372.2	473.41	33.94	425.48	691.76	27.98
standard deviation	192.73	183.56	41.43	18.33	22.28	7.0	39.21	45.58	3.57

M = thousand
stb = stock tank barrel
scf = standard cubic feet

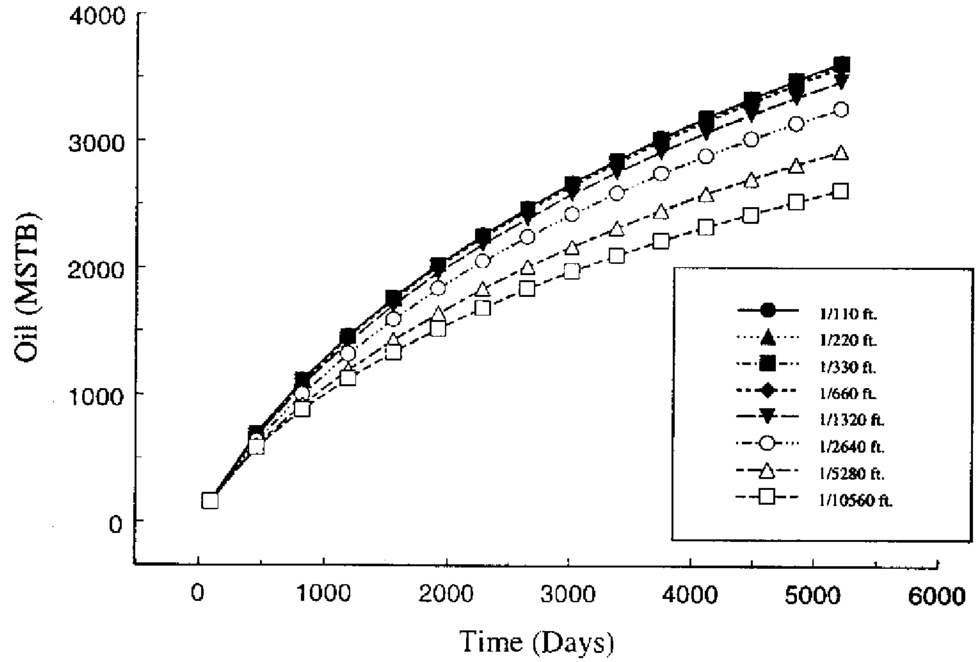

Figure 4.1. Effect of fracture spacing on cumulative oil production in the 20-square-mile (51.8-km^2) area.

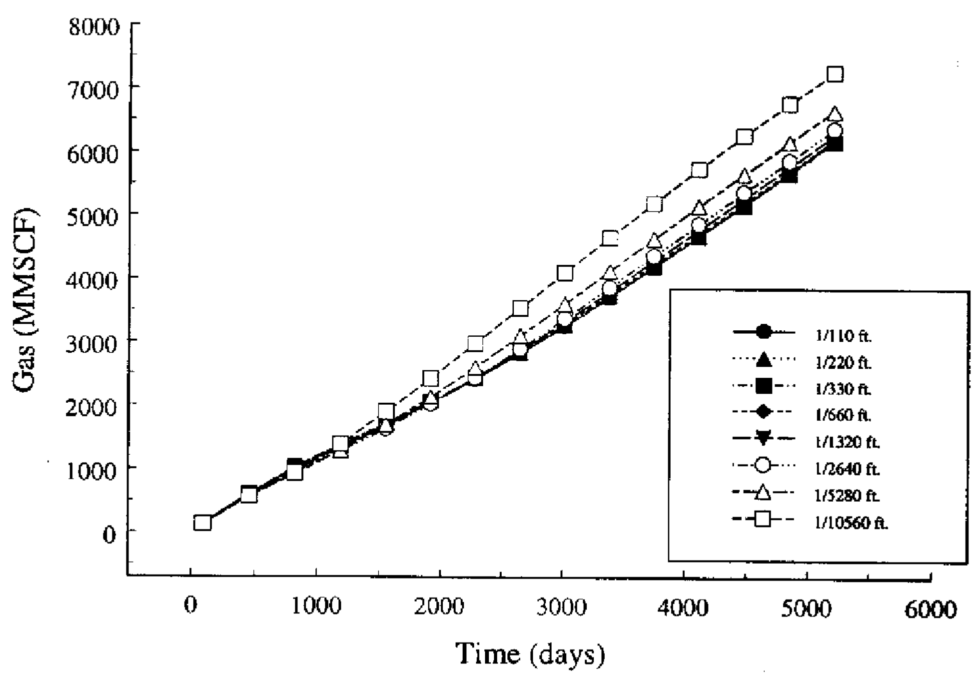

Figure 4.2. Effect of fracture spacing on cumulative gas production in the 20-square-mile (51.8-km^2) area.

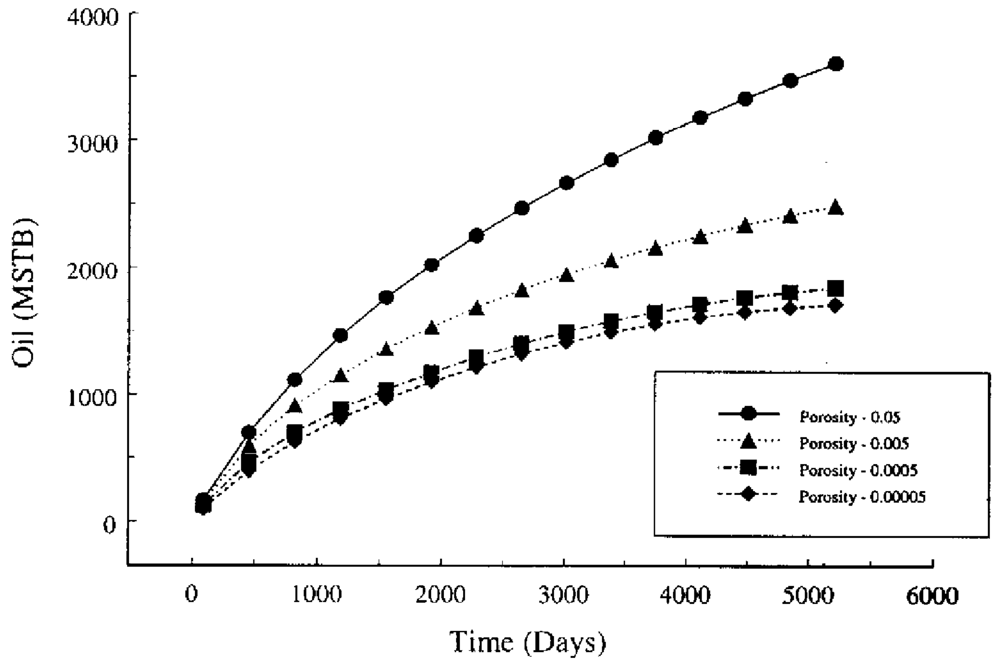

Figure 4.3. Effect of fracture porosity on cumulative oil production in the 20-square-mile (51.8-km^2) area.

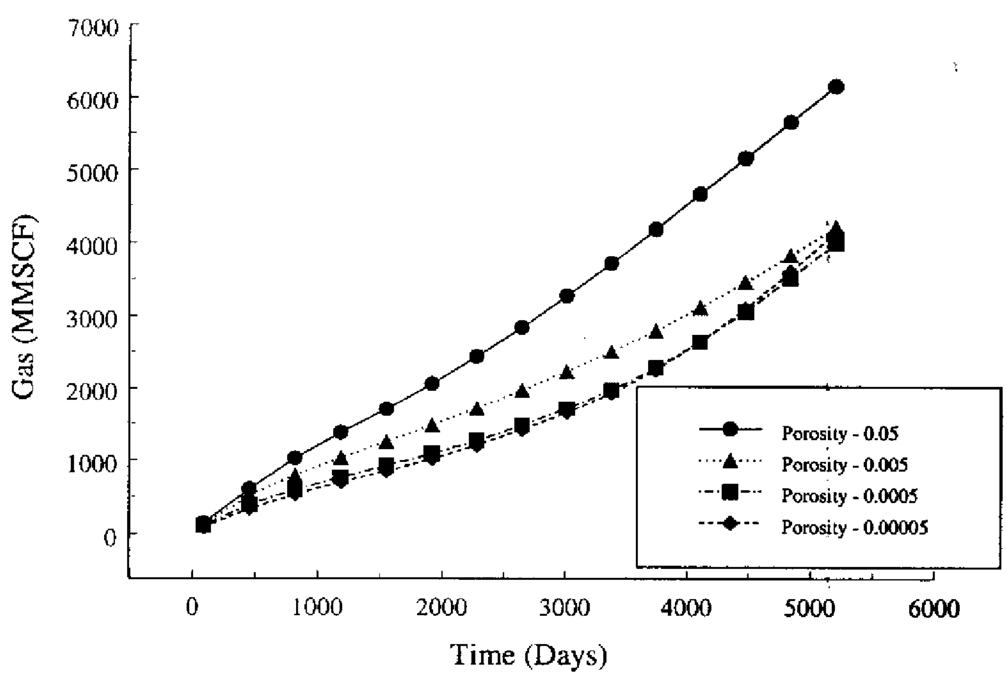

Figure 4.4. Effect of fracture porosity on cumulative gas production in the 20-square-mile (51.8-km^2) area.

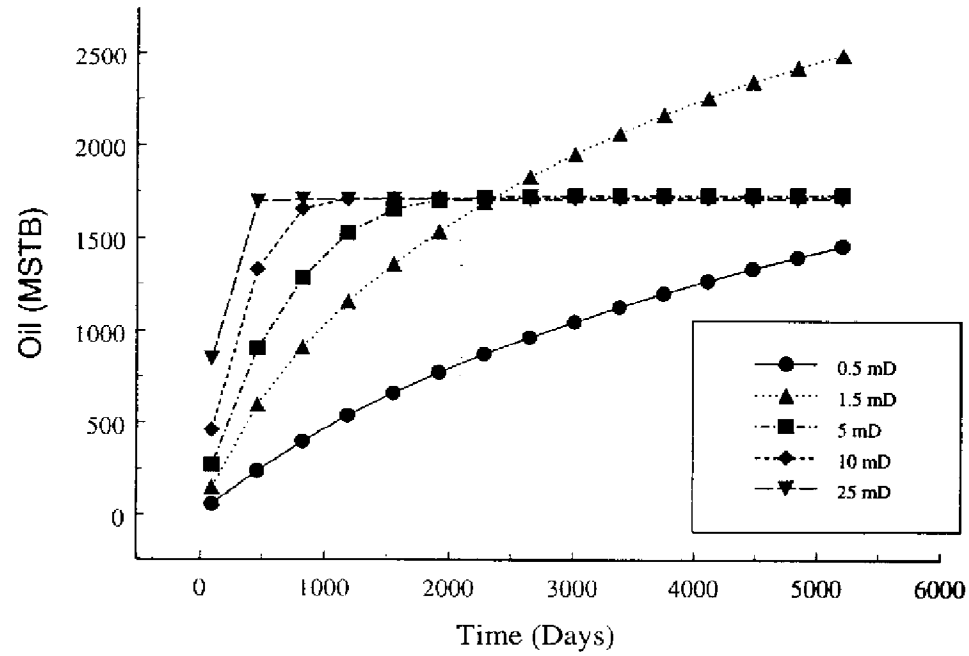

Figure 4.5. Effect of fracture permeability on cumulative oil production in the 20-square-mile (51.8-km^2) area (matrix permeability = 0.5 mD).

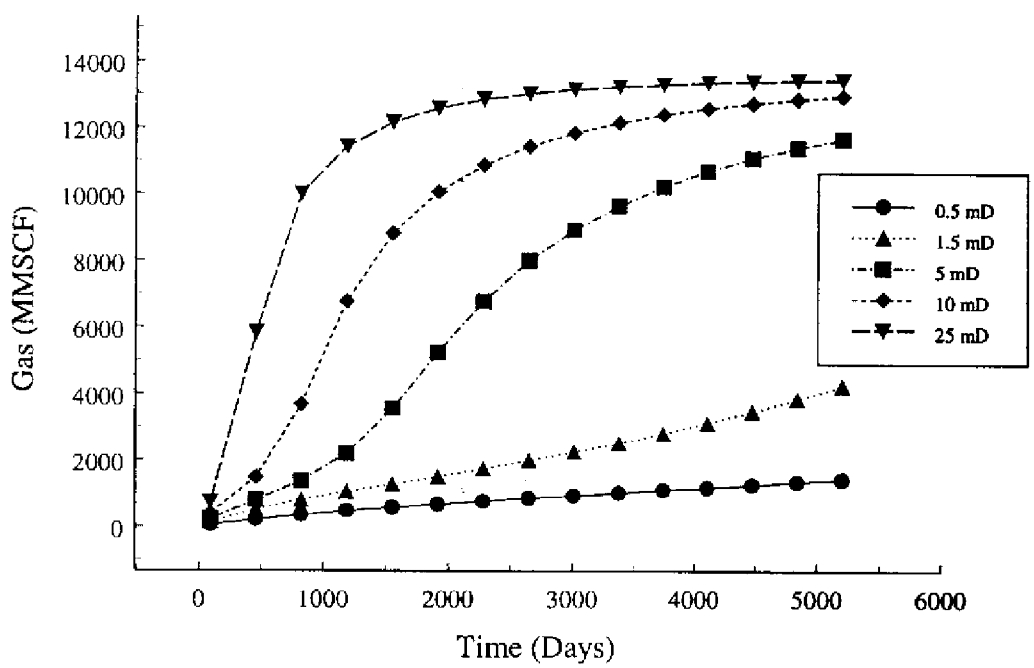

Figure 4.6. Effect of fracture permeability on cumulative gas production in the 20-square-mile (51.8-km^2) area (matrix permeability = 0.5 mD).

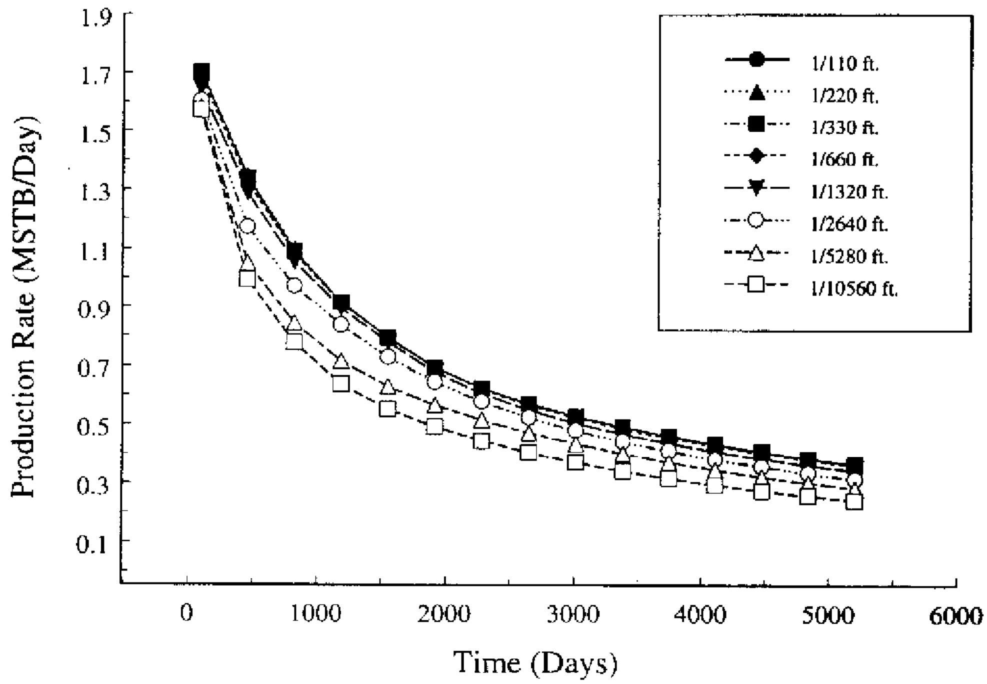

Figure 4.7. Effect of fracture frequency on oil-production rate in the 20-square-mile (51.8-km^2) area.

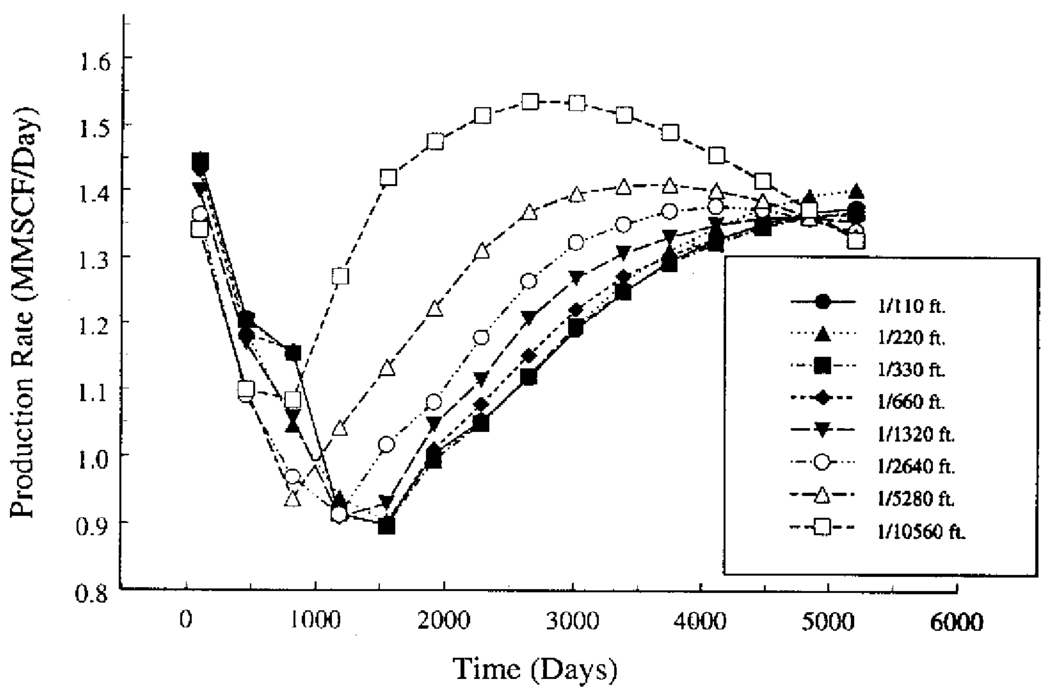

Figure 4.8. Effect of fracture frequency on gas-production rate in the 20-square-mile (51.8-km^2) area.

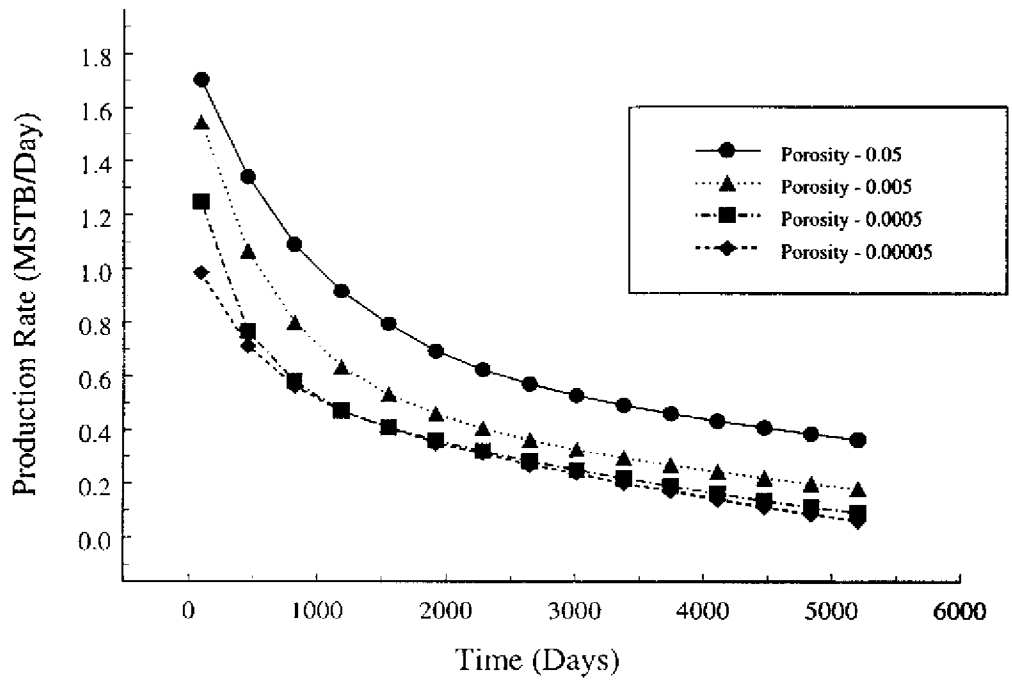

Figure 4.9. Effect of fracture porosity on oil-production rate in the 20-square-mile (51.8-km^2) area.

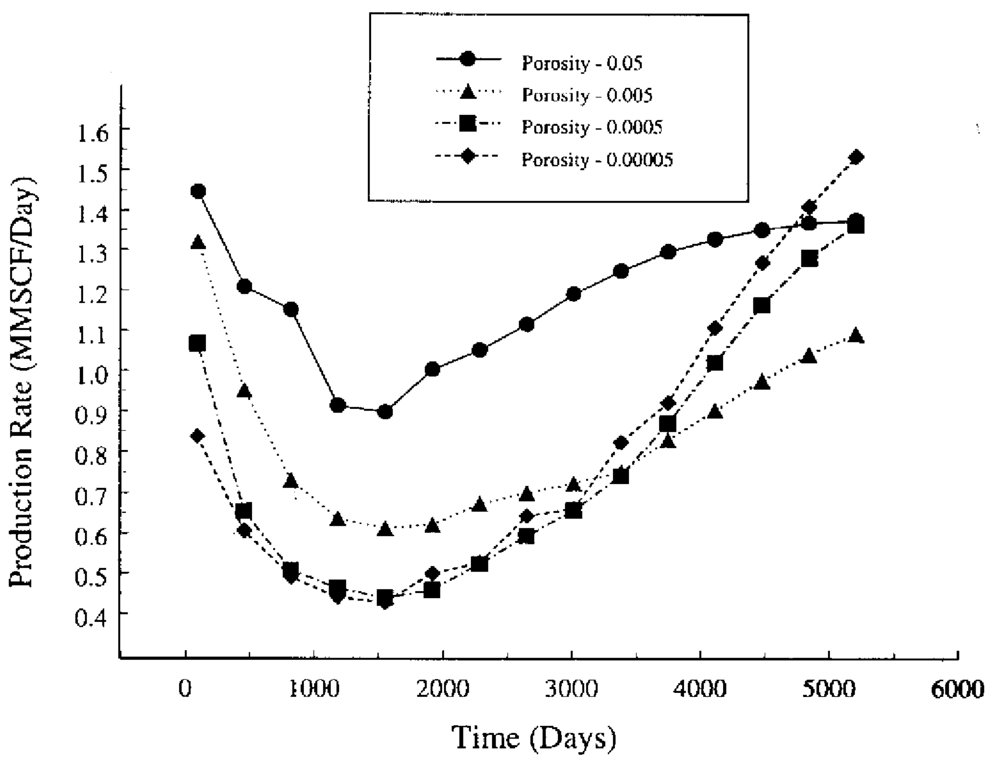

Figure 4.10. Effect of fracture porosity on gas-production rate in the 20-square-mile (51.8-km^2) area.

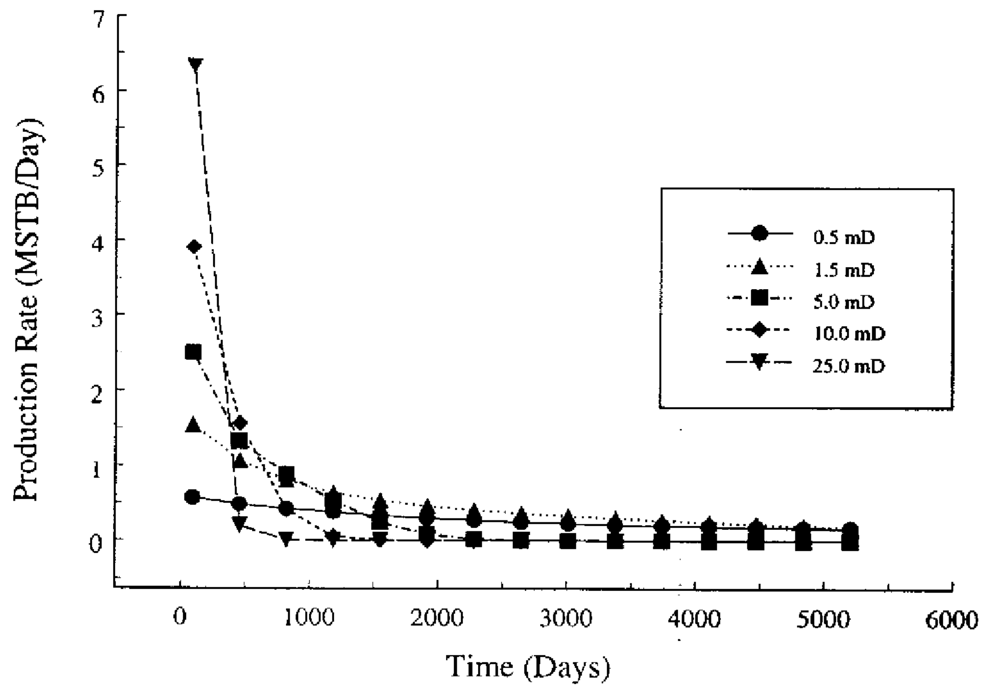

Figure 4.11. Effect of fracture permeability on oil-production rate in the 20-square-mile (51.8-km^2) area (matrix permeability - 0.5 mD).

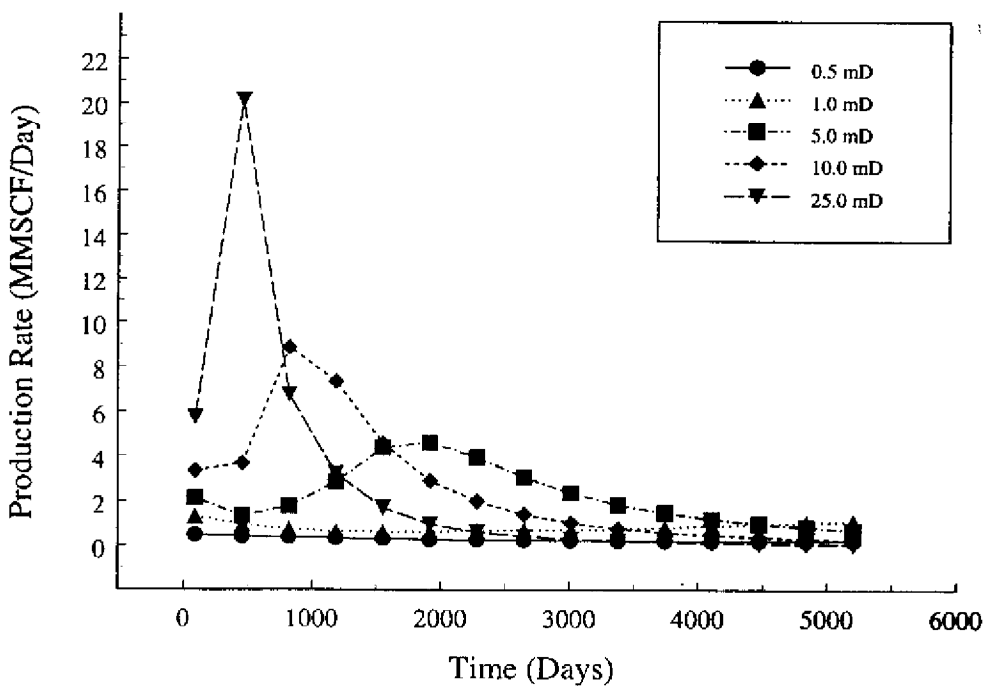

Figure 4.12. Effect of fracture permeability on gas-production rate in the 20-square-mile (51.8-km^2) area (matrix permeability - 0.5 mD).

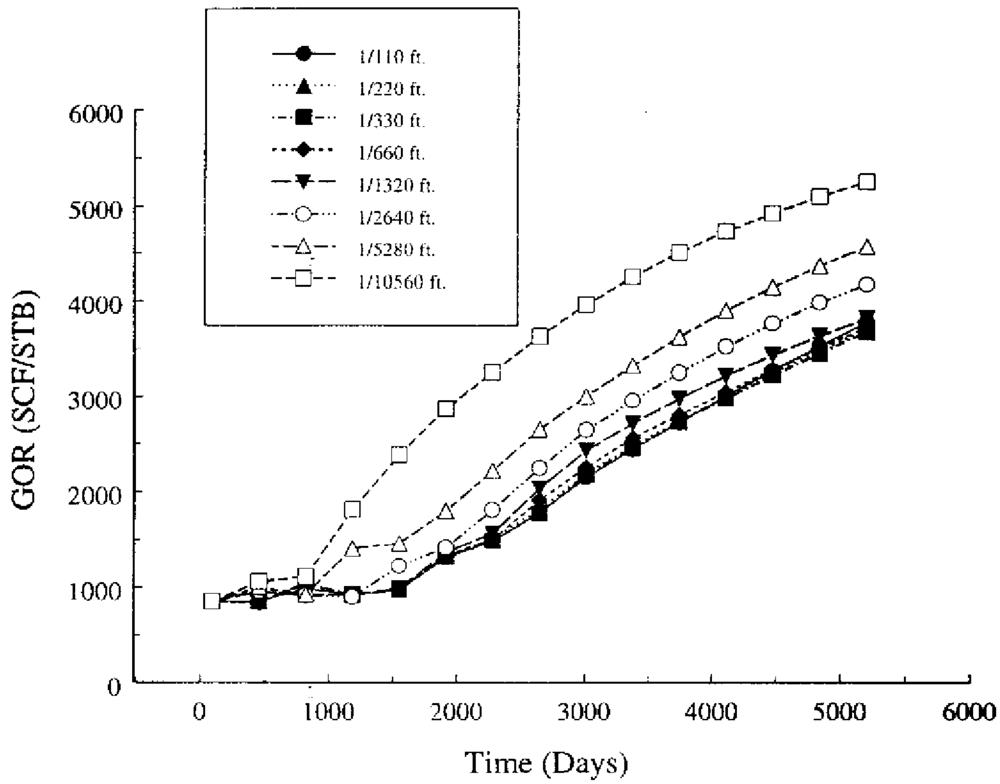

Figure 4.13. Effect of fracture frequency on GORs for Michelle Ute well.

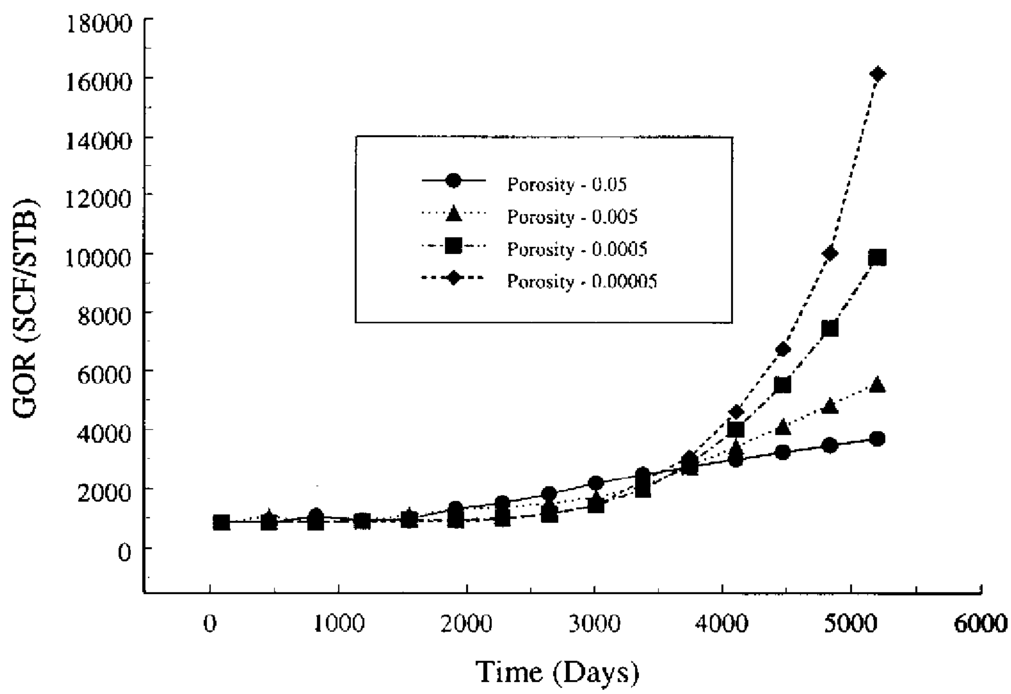

Figure 4.14. Effect of fracture porosity on GORs for Michelle Ute well.

5. TECHNOLOGY TRANSFER

Roger L. Bon
Utah Geological Survey
Salt Lake City, Utah

5.1. Introduction

Technology transfer activities for the year include information exhibits at one regional and one national petroleum industry meeting, a local petroleum-related event, one published article, two Masters theses, establishment of a project home page on the Internet, and articles published in Utah Geological Survey (UGS) *Petroleum News*, and presentations made to local professional organizations.

5.2. Information Exhibits

Petroleum Days, local petroleum industry event, May 1996, Vernal, UT.

American Association of Petroleum Geologists, Annual Meeting and Exhibition, May 1996, San Diego, CA.

American Association of Petroleum Geologists, Rocky Mountain Section Meeting, July 1996, Billings, MT.

Geology and Resources of the Paradox Basin, September 1996, Durango, CO.

5.3. Publications

Garner, Ann, 1996, *Outcrop study of the Lower Green River Formation for the purpose of reservoir characterization and hydrocarbon production enhancement in the Altamont-Bluebell field, Uinta Basin, Utah*: Provo, Brigham Young University M.S. thesis, 192 p.

Garner, Ann, and Morris, T. H., 1996, *Outcrop study of the Lower Green River Formation for reservoir characterization and hydrocarbon production enhancement in the Altamont-Bluebell field, Uinta Basin, Utah*: Utah Geological Survey Miscellaneous Publication 96-2, 61 p.

Wegner, MaryBeth, 1996, *Core analysis and description as an aid to hydrocarbon production enhancement - lower Green River and Wasatch Formations, Bluebell field, Uinta Basin, Utah:* Provo, Brigham Young University M.S. thesis, 233 p.

5.4. Petroleum News

Petroleum News is a newsletter published semi-annually by the Utah Geological Survey. The newsletter keeps petroleum companies, researchers, and other parties involved in exploring and developing Utah's energy resources informed of the progress on various energy-related projects of the Utah Geological Survey. The newsletter is free to anyone interested and is currently sent to roughly 750 individuals and organizations. One issue (July 1996) was published in the past twelve months.

5.5. Internet

The Utah Geological Survey has established a Bluebell home page on the Internet containing the following data: (1) a description of the project, (2) a list of project participants including addresses, (3) each of the Quarterly Technical Progress Reports, (4) a description of planned field demonstration work, (5) portions of the First and Second Annual Technical Reports with information on where to obtain complete reports, (6) a reference list of all publications that are a direct result of the project, and (7) an extensive selected reference list for the Uinta Basin and lacustrine deposits worldwide. The address is **http://utstdpwww.state.ut.us/~ugs/bluebell.htm**

REFERENCES

Allison, M.L., 1995, Increased oil production and reserves from improved completion techniques in the Bluebell field, Uinta Basin, Utah-annual report for the period September 30, 1993 to September 30, 1994: U.S. Department of Energy Report DOE/BC/14953-10, (DE95000171), 123 p.

Allison, M.L., and Morgan, C.D., 1996, Increased oil production and reserves from improved completion techniques in the Bluebell field, Uinta Basin, Utah-annual report for the period October 1, 1994 to September 30, 1995: U.S. Department of Energy Report DOE/BC/14953-14, (DE96001227), 118 p.

Bruhn, R.L., Picard, M.D., and Beck, S.L., 1983, Mesozoic and early Tertiary structure and sedimentology of the central Wasatch Mountains, Uinta Mountains and Uinta Basin: Utah Geological and Mineral Survey Special Studies 59, p. 63-105.

Castle, J.W., 1991, Sedimentation in Eocene Lake Uinta (lower Green River Formation), northeastern Uinta Basin, Utah, *in* Katz, B.J., editor, Lacustrine basin exploration-case studies and modern analogs: American Association of Petroleum Geologists Memoir 50, p. 243-263.

Fouch, T.D., 1975, Lithofacies and related hydrocarbon accumulation in Tertiary strata of the western and central Uinta Basin, Utah, *in* Bolyard, D.W., editor, Symposium on deep drilling frontiers of the central Rocky Mountains: Rocky Mountain Association of Geologists, p. 163-173.

---1976, Revision of the lower part of the Tertiary system in the central and western Uinta Basin, Utah: U.S. Geological Survey Bulletin 1405-c, 7 p.

---1981, Distribution of rock types, lithologic groups, and interpreted depositional environments for some lower Tertiary and Upper Cretaceous rocks from outcrops at Willow Creek - Indian Canyon through the subsurface of Duchesne and Altamont oil fields, southeast to north-central parts of the Uinta Basin, Utah: U.S. Geological Survey Oil and Gas Investigations Map, Chart OC-81, 2 sheets.

Fouch, T.D., Nuccio, V.F., and Chidsey, T.C., Jr., editors, 1992, Hydrocarbon and mineral resources of the Uinta Basin, Utah and Colorado: Utah Geological Association Guidebook 20, 366 p.

Fouch, T.D., and Pitman, J.K., 1991, Tectonic and climate changes expressed as sedimentary cycles and stratigraphic sequences in the Paleogene Lake Uinta system, central Rocky Mountains, Utah and Colorado [abs]: American Association of Petroleum Geologists Bulletin, v. 75, no. 3, p. 575.

---1992, Tectonic and climate changes expressed as sedimentary and geochemical cycles - Paleogene Lake systems, Utah and Colorado - implications for petroleum source and reservoir rocks, *in* Carter, L.J., editor, U.S. Geological Survey research on energy resources, 1992 McKelvey forum program and abstracts [abs]: U.S. Geological Survey Circular 1074, p. 29-30.

Fouch, T.D., Pitman, J.K., Wesley, J.B., Szantay, Adam, and Ethridge, F.G., 1990, Sedimentology, diagenesis, and reservoir character of Paleogene fluvial and lacustrine rocks, Uinta Basin, Utah - evidence from the Altamont and Red Wash fields, *in* Carter, L.M., editor, Sixth V. E. McKelvey forum on mineral and energy resources, U.S. Geological Survey research on energy resources - 1990 - program and abstracts: U.S. Geological Survey Circular 1060, p. 31-32.

Franczyk, K.J., Fouch, T.D., Johnson, R.C., Molenaar, C.M., and Cobban, W.A., 1992, Cretaceous and Tertiary paleogeographic reconstructions for the Uinta-Piceance Basin study area, Colorado and Utah: U. S. Geological Survey Bulletin 1787-Q, 37 p.

Pitman, J.K., Anders, D.E., Fouch, T.D., and Nichols, D.J., 1986, Hydrocarbon potential of nonmarine Upper Cretaceous and Lower Tertiary rocks, eastern Uinta Basin, Utah, *in* Spencer, C.W., and Mast, R.F., editors, Geology of tight gas reservoirs: American Association of Petroleum Geologists Studies in Geology 24, p. 235-252.

Pitman, J.K., Fouch, T.D., and Goldaber, M.B., 1982, Depositional setting and diagenetic evolution of some Tertiary unconventional reservoir rocks, Uinta Basin, Utah: American Association of Petroleum Geologists Bulletin, v. 66, no. 10, p. 1,581-1,596.

Ryder, R.T., Fouch, T.D., and Elison, J.H., 1976, Early Tertiary sedimentation in the western Uinta Basin, Utah: Geological Society of America Bulletin, v. 87, p. 496-512.

Stokes, W.L., 1986, Geology of Utah: Utah Geological Survey Miscellaneous Publication S, 317 p.

APPENDIX

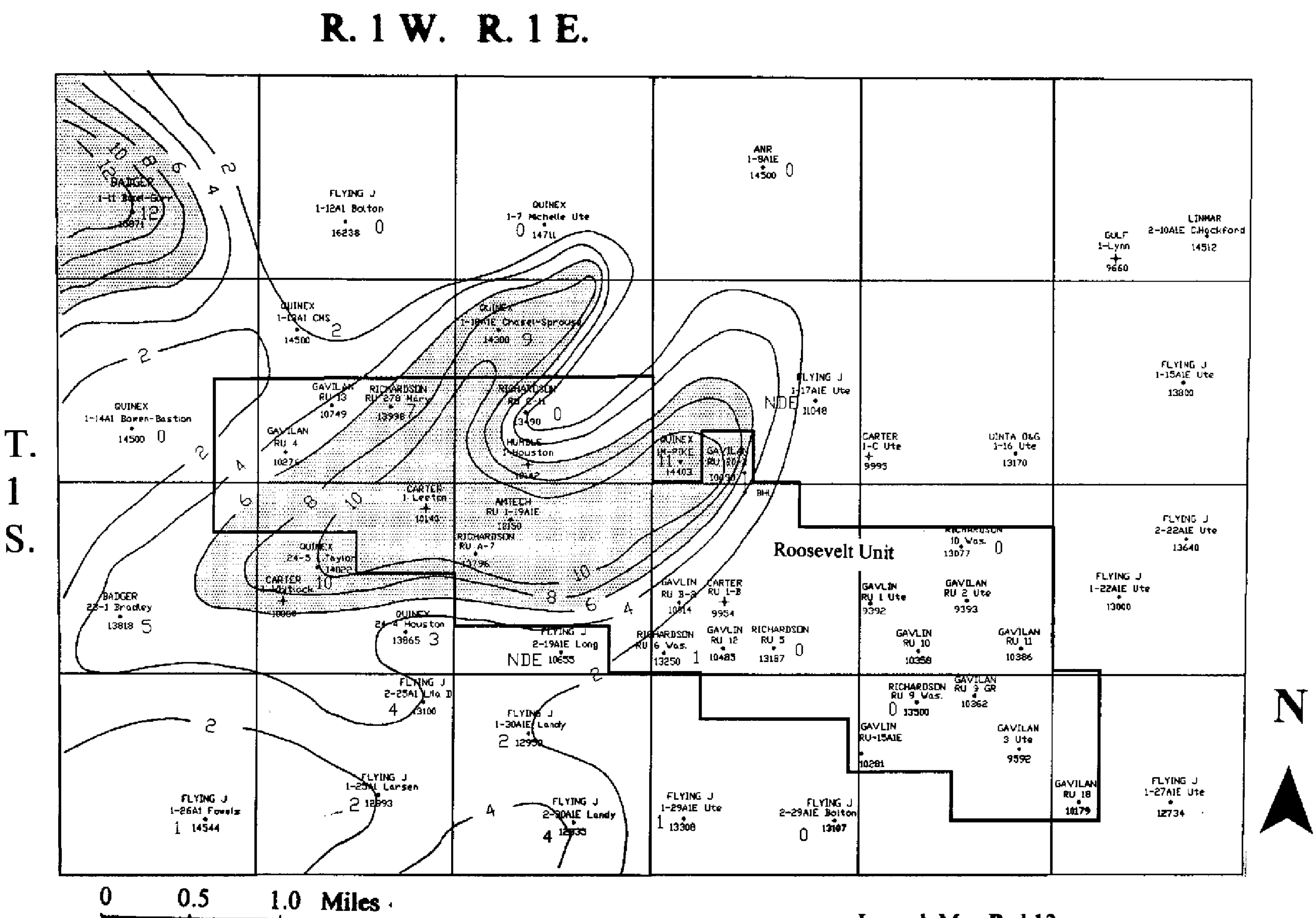

Contour interval 2 feet
Shaded areas are 6 feet or thicker
Bed thickness is defined by
gamma-ray count of 60 API or less

Isopach Map Bed 13
Eastern Bluebell Field
Uintah County, Utah

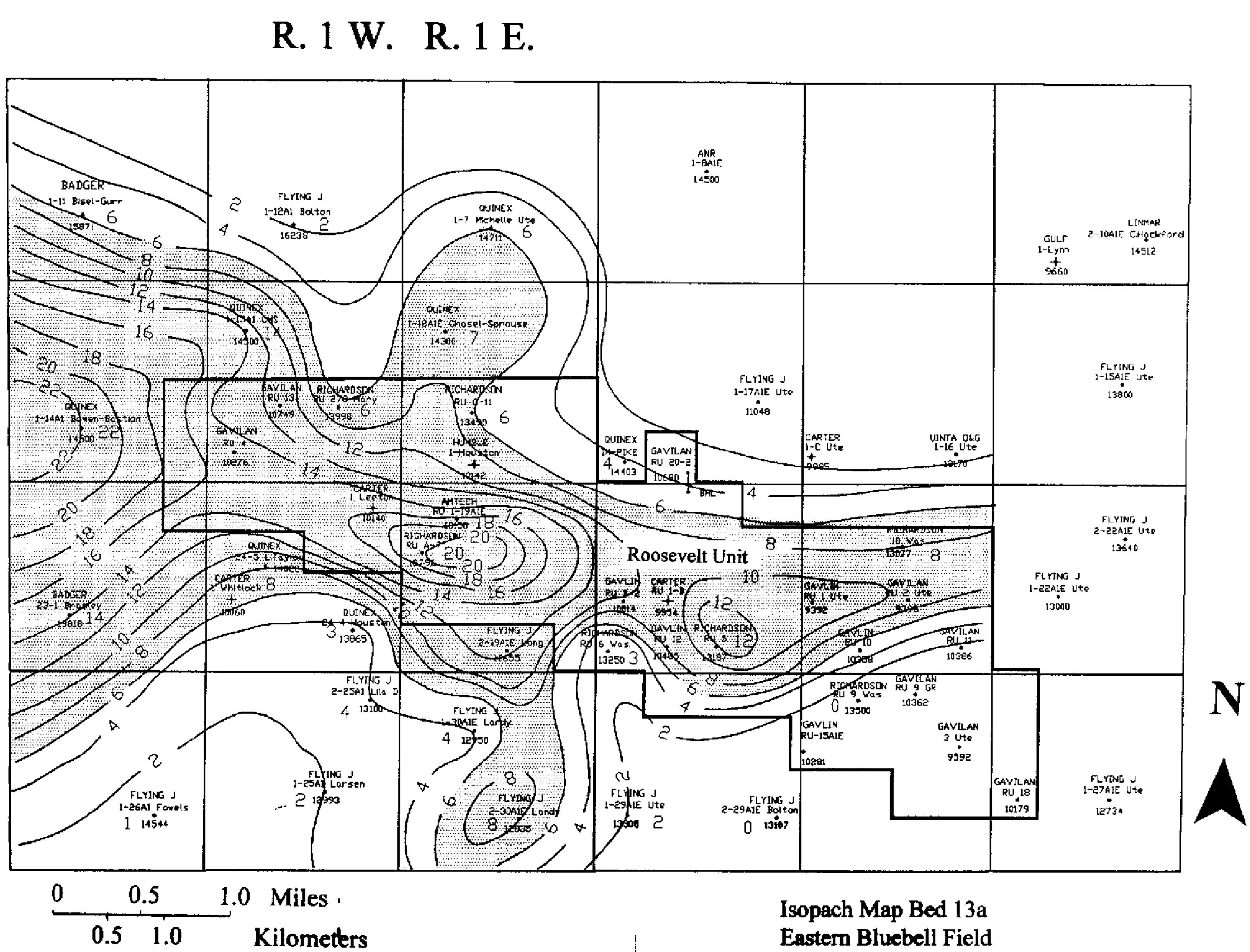

Contour interval 2 feet
Shaded areas are 6 feet or thicker
Bed thickness is defined by gamma-ray count of 60 API or less

Isopach Map Bed 13a
Eastern Bluebell Field
Uintah County, Utah

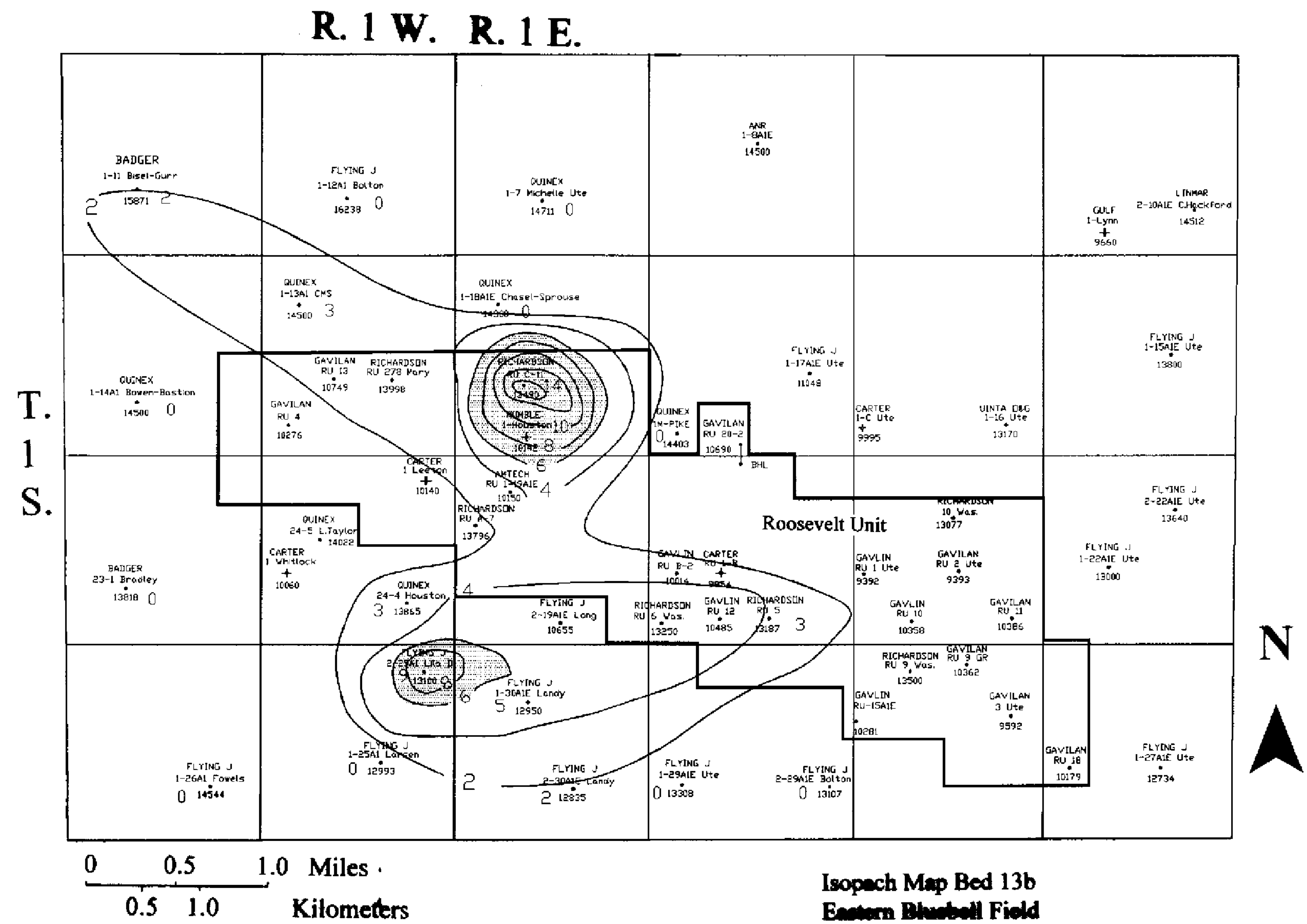

Isopach Map Bed 13b
Eastern Bluebell Field
Uintah County, Utah

Contour interval 2 feet
Shaded areas are 6 feet or thicker
Bed thickness is defined by
gamma-ray count of 60 API or less

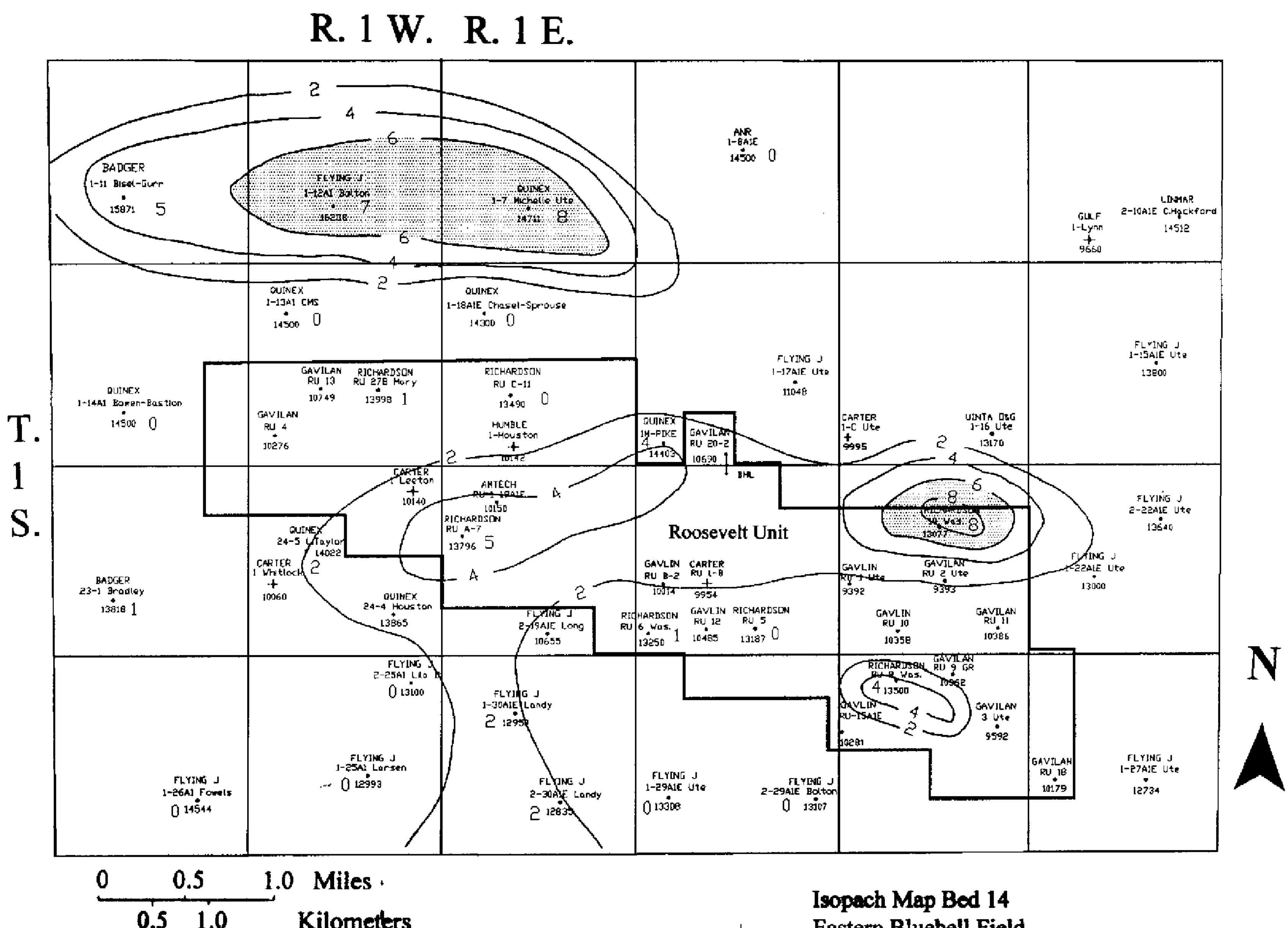

Contour interval 2 feet
Shaded areas are 6 feet or thicker
Bed thickness is defined by
gamma-ray count of 60 API or less

Isopach Map Bed 14
Eastern Bluebell Field
Uintah County, Utah

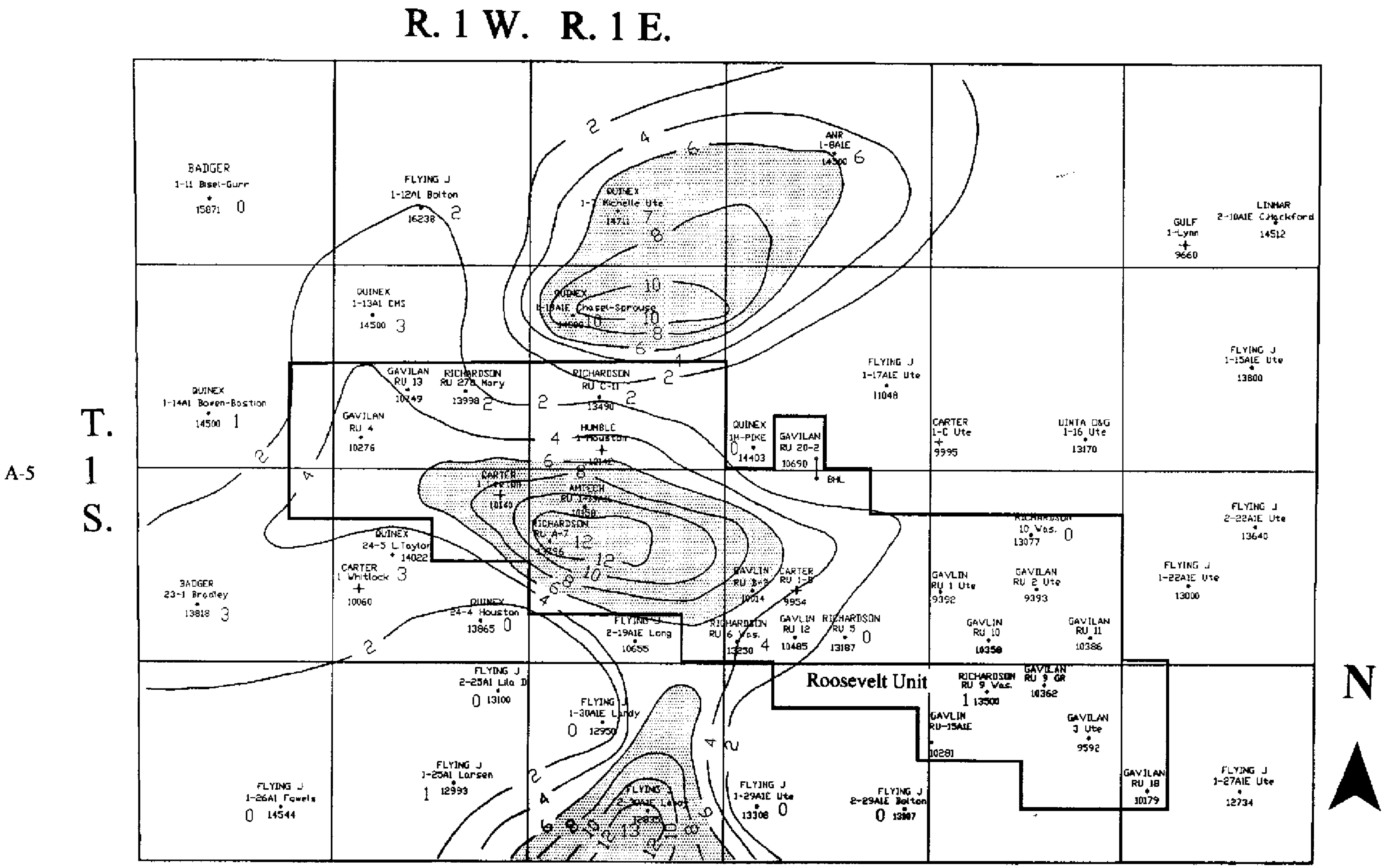

0 0.5 1.0 Miles

0.5 1.0 Kilometers

Contour interval 2 feet
Shaded areas are 6 feet or thicker
Bed thickness is defined by
gamma-ray count of 60 API or less

Isopach Map Bed 15
Eastern Bluebell Field
Uintah County, Utah

R. 1 W.   R. 1 E.

T. 1 S.

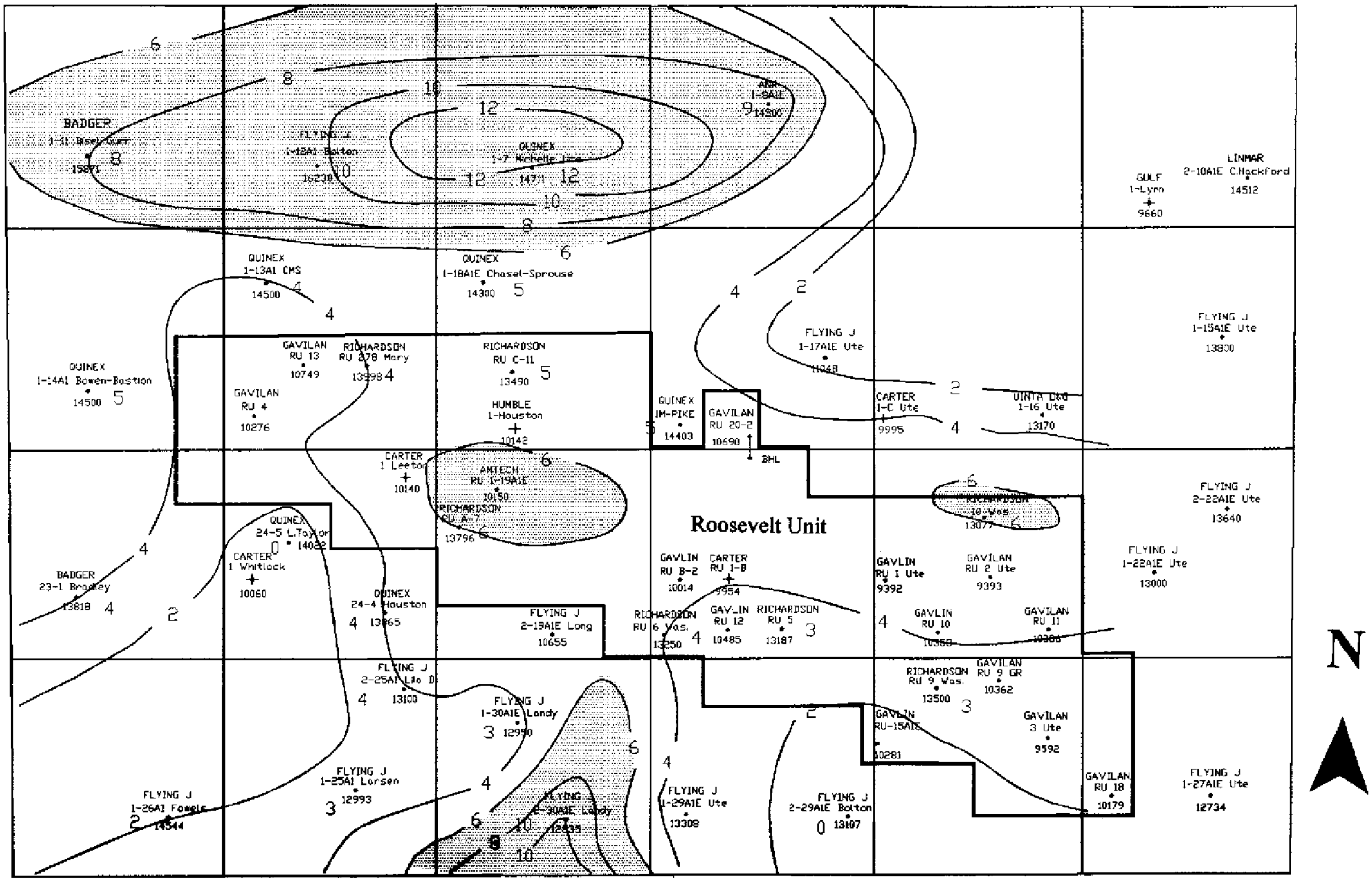

0 0.5 1.0 Miles

0.5 1.0 Kilometers

Contour interval 2 feet
Shaded areas are 6 feet or thicker
Bed thickness is defined by

Isopach Map Bed 16
Eastern Bluebell Field
Uintah County, Utah

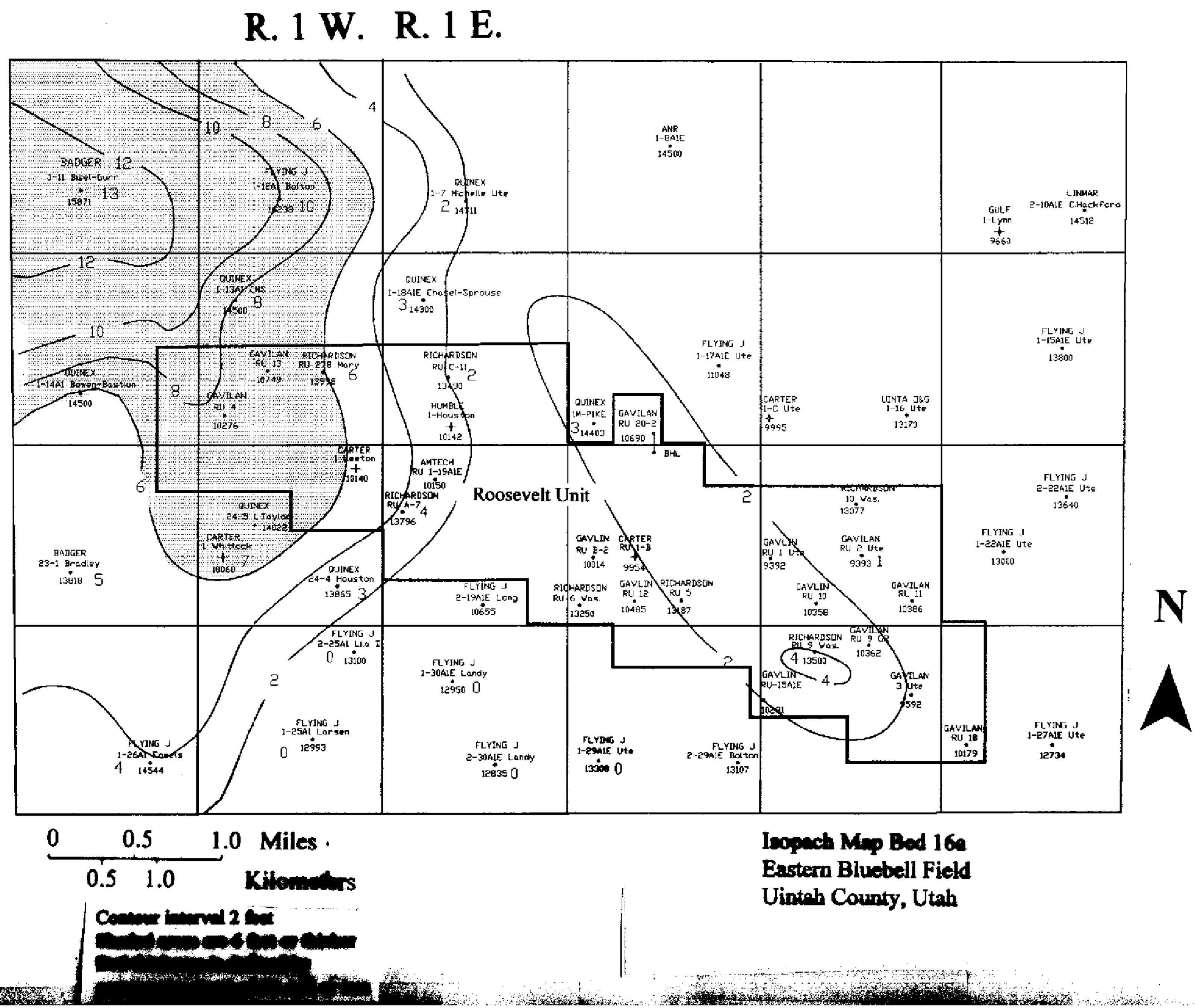

Isopach Map Bed 16a
Eastern Bluebell Field
Uintah County, Utah

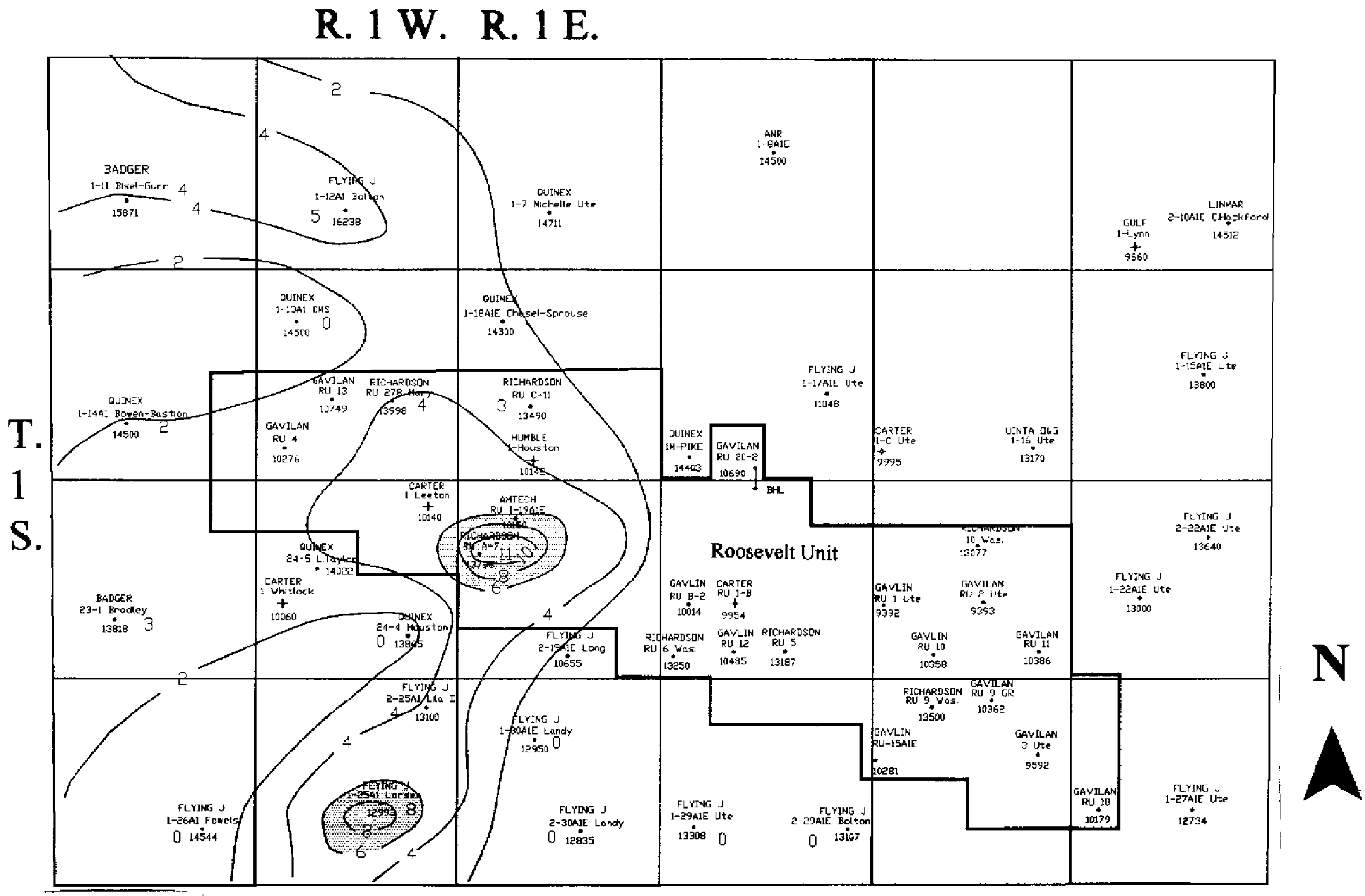

Contour interval 2 feet

Shaded areas are 6 feet or thicker

Isopach Map Bed 16b
Eastern Bluebell Field
Uintah County, Utah

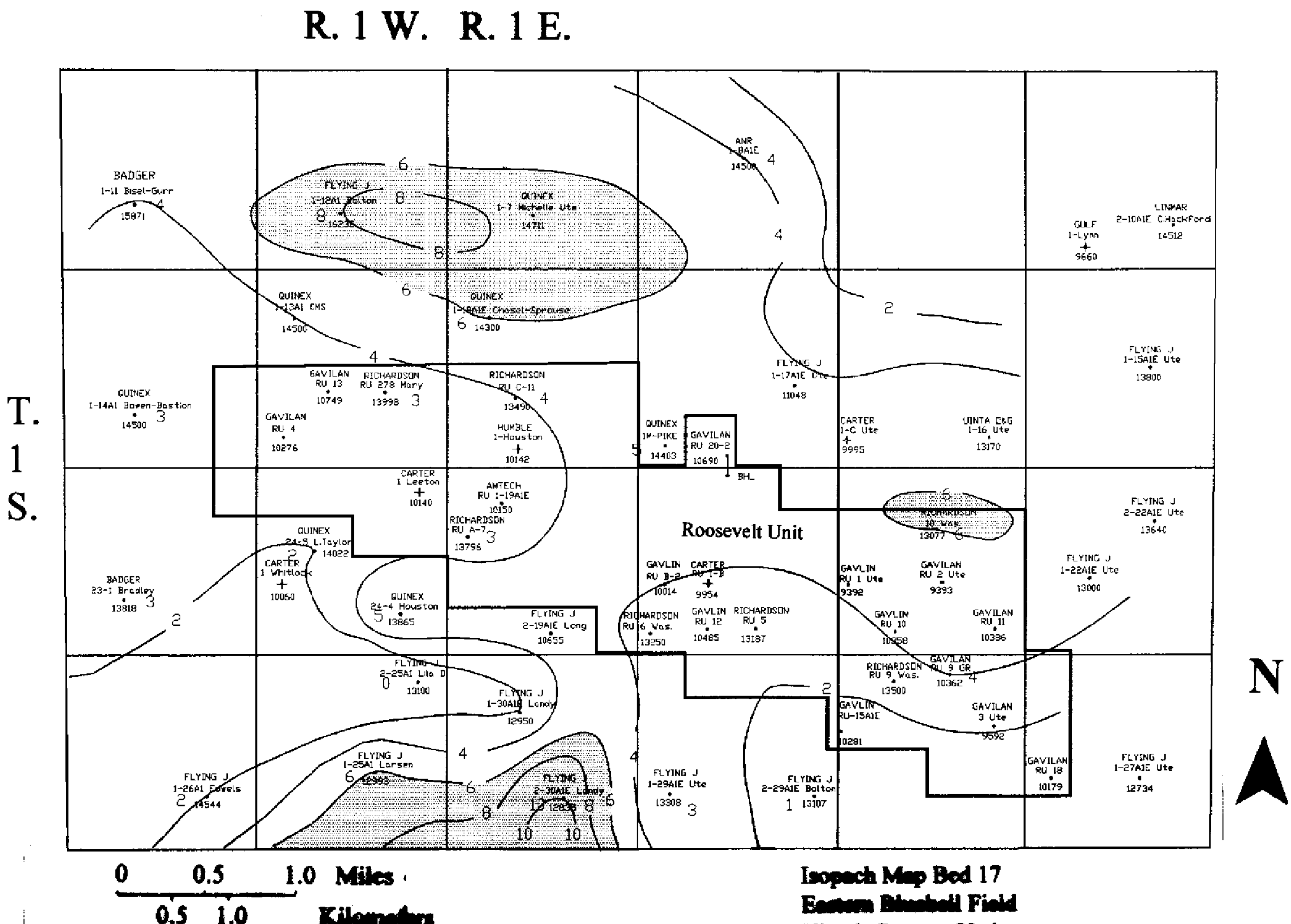

Contour interval 2 feet

Isopach Map Bed 17
Eastern Bluebell Field
Uintah County, Utah

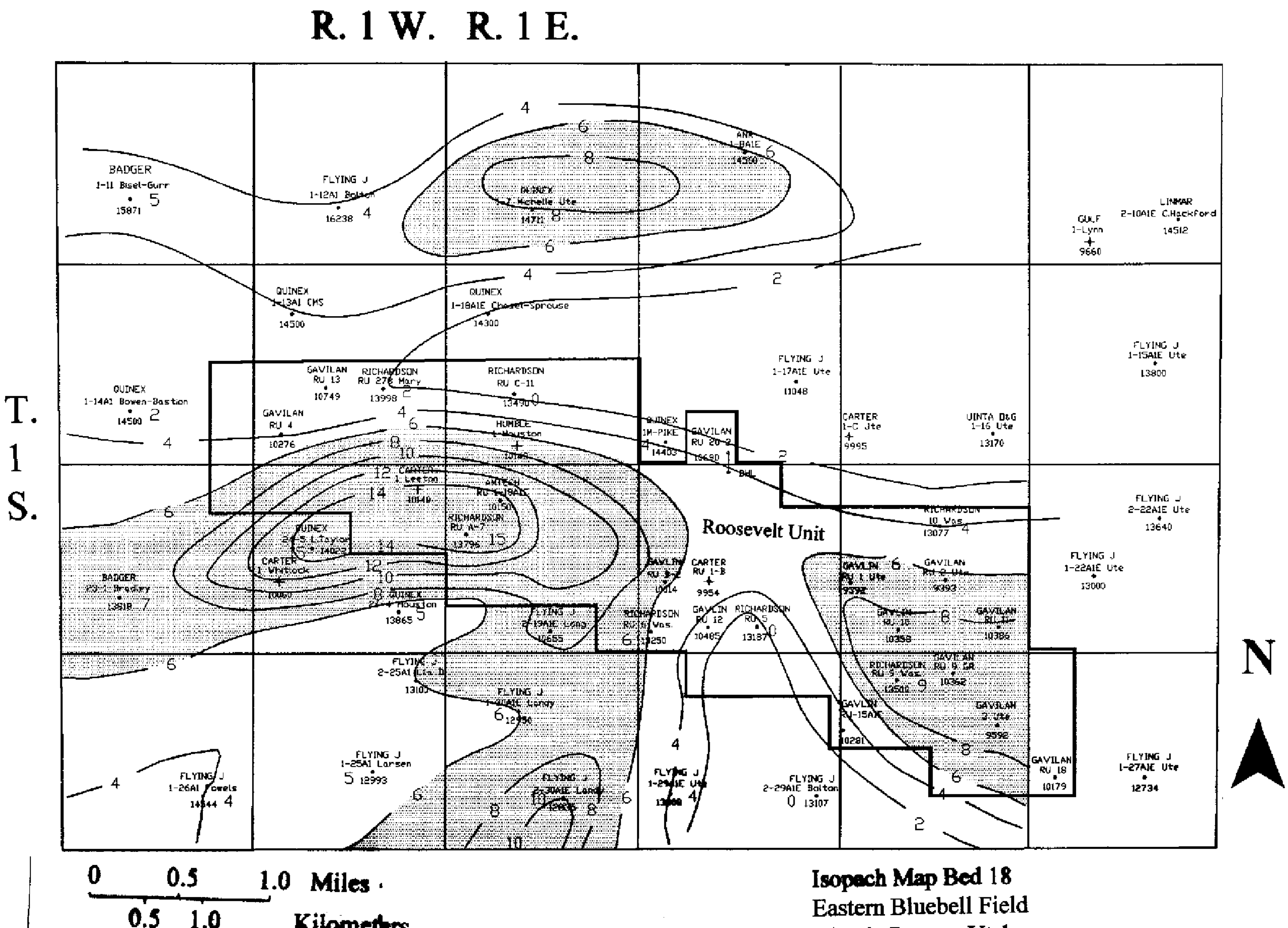

Isopach Map Bed 18
Eastern Bluebell Field
Uintah County, Utah

Contour interval 2 feet
Shaded areas are 6 feet or thicker
Bed thickness is defined by
gamma-ray cutoff of 60 API units.

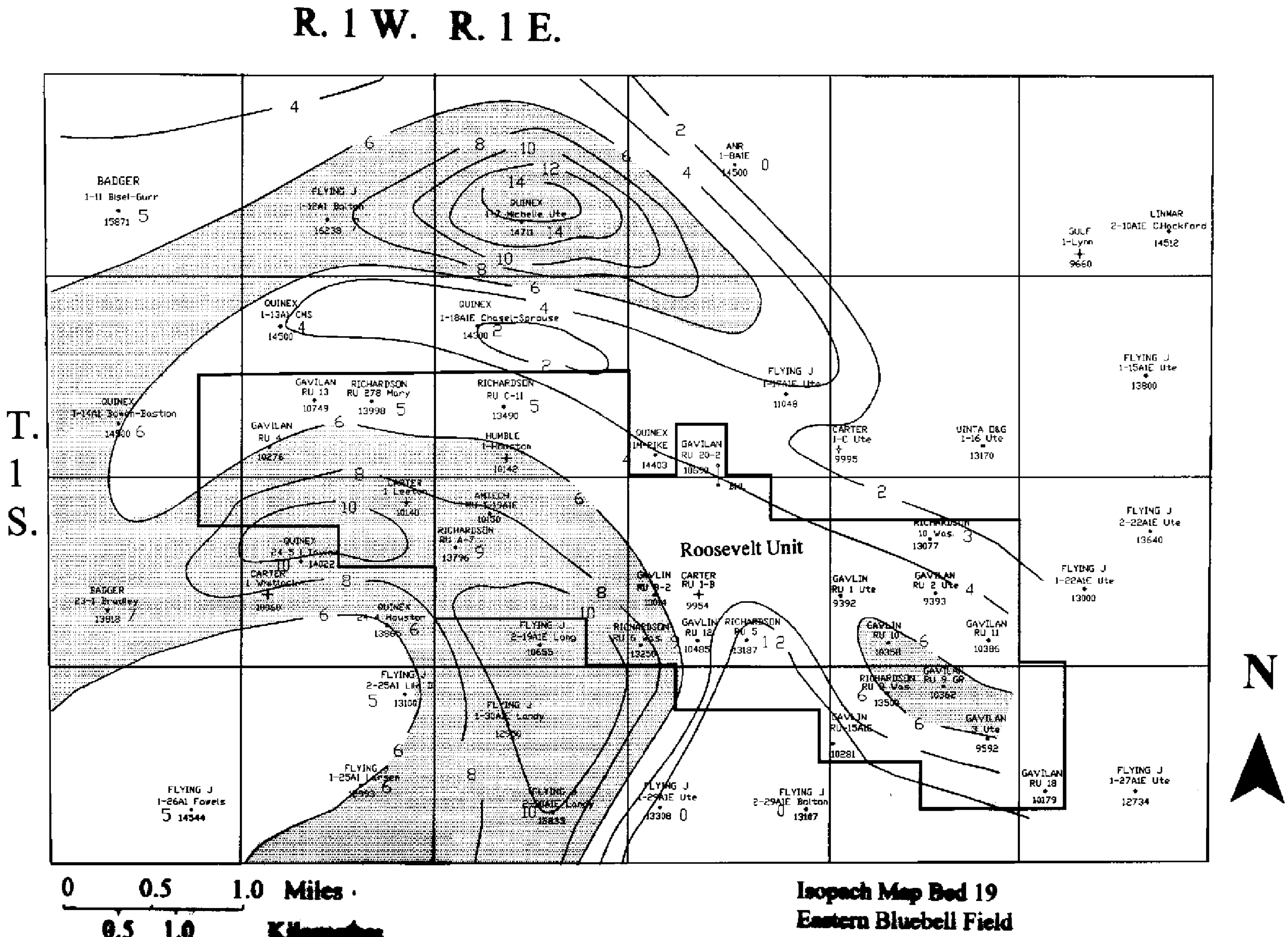

Isopach Map Bed 19
Eastern Bluebell Field
Uintah County, Utah

Contour interval 2 feet
Shaded areas are 6 feet or thicker

A-11

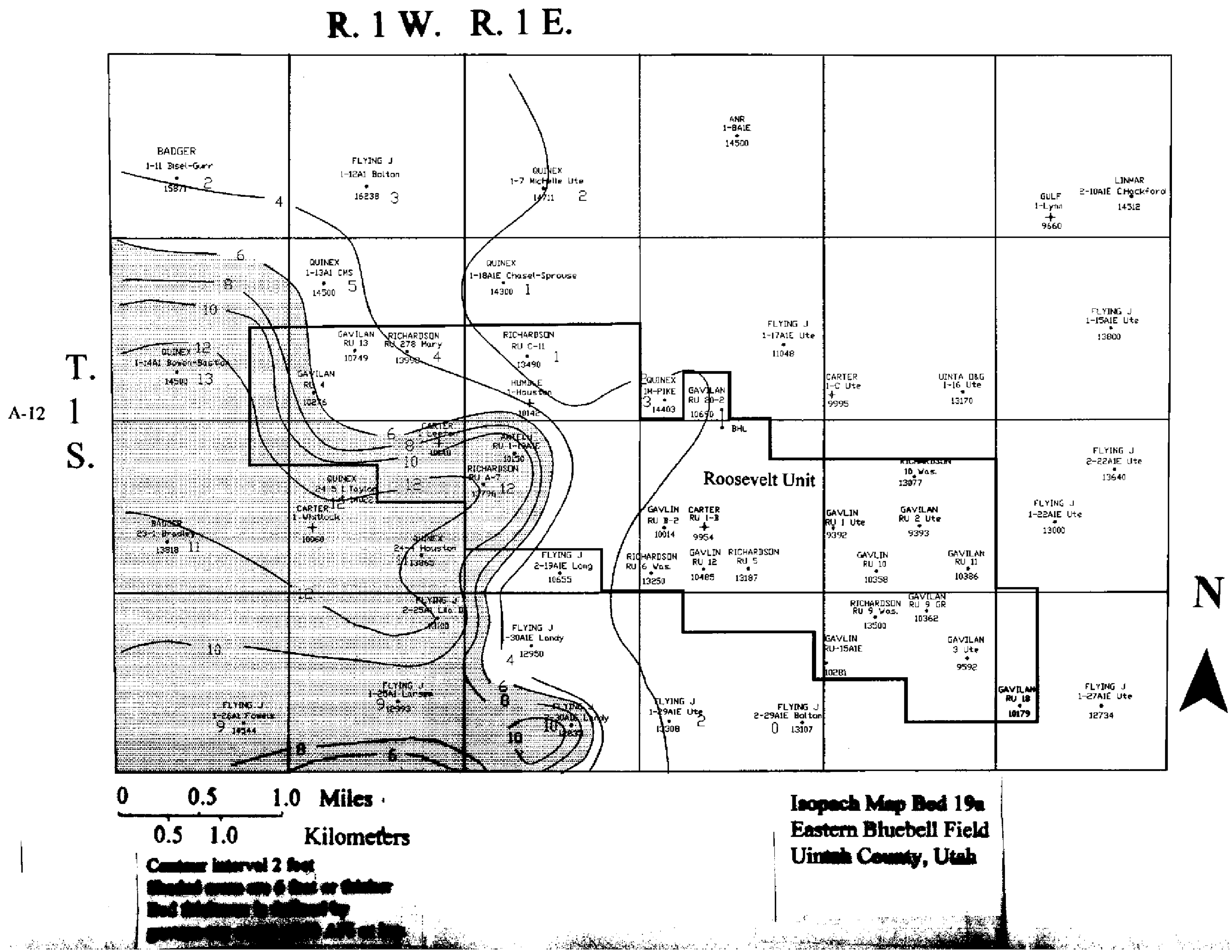

R. 1 W. R. 1 E.
T. 1 S.
BADGER 1-11 Bisel-Gurr 15871
FLYING J 1-12A1 Bolton 16238
QUINEX 1-7 Michelle Ute 14711
ANR 1-8A1E 14500
GULF 1-Lynn 9660
LINMAR 2-10A1E C.Hackford 14512
QUINEX 1-13A1 CMS 14500
QUINEX 1-18A1E Chasel-Sprouse 14300
FLYING J 1-17A1E Ute 11048
FLYING J 1-15A1E Ute 13800
GAVILAN RU 13 10749
RICHARDSON RU 278 Mary 13998
RICHARDSON RU C-11 13490
QUINEX 1-14A1 Bowen-Bastian 14500
GAVILAN RU 4 10276
HUMBLE 1-Houston 10142
QUINEX 1M-PIKE 14403
GAVILAN RU 80-2 10650
BHL
CARTER 1-C Ute 9995
UINTA O&G 1-16 Ute 13170
Roosevelt Unit
RICHARDSON RU A-7 13796
QUINEX 24-5 L Taylor
CARTER 1-Whitlock 10060
BADGER 29-1 Bradley 13818
QUINEX 24-4 Houston 13865
FLYING J 2-19A1E Long 10655
GAVLIN RU B-2 10014
CARTER RU 1-B 9954
GAVLIN RU 12 10485
RICHARDSON RU 5 13187
RICHARDSON RU 6 Vas. 13250
RICHARDSON 10 Vas. 13077
GAVLIN RU 1 Ute 9392
GAVILAN RU 2 Ute 9393
GAVLIN RU 10 10358
GAVILAN RU 11 10386
FLYING J 2-22A1E Ute 13640
FLYING J 1-22A1E Ute 13000
RICHARDSON RU 9 Vas. 13500
GAVILAN RU 9 GR 10362
GAVLIN RU-15A1E 10281
GAVILAN 3 Ute 9592
GAVILAN RU 18 10179
FLYING J 1-27A1E Ute 12734
FLYING J 2-25A1 Lar. D 10180
FLYING J 1-30A1E Landy 12950
FLYING J 1-26A1 Fowles 14544
FLYING J 1-25A1 Larsen 12593
FLYING J 2-30A1E Landy
FLYING J 1-29A1E Ute 13308
FLYING J 2-29A1E Bolton 13107
N
0 0.5 1.0 Miles
0.5 1.0 Kilometers
Contour interval 2 feet
Isopach Map Bed 19a
Eastern Bluebell Field
Uintah County, Utah

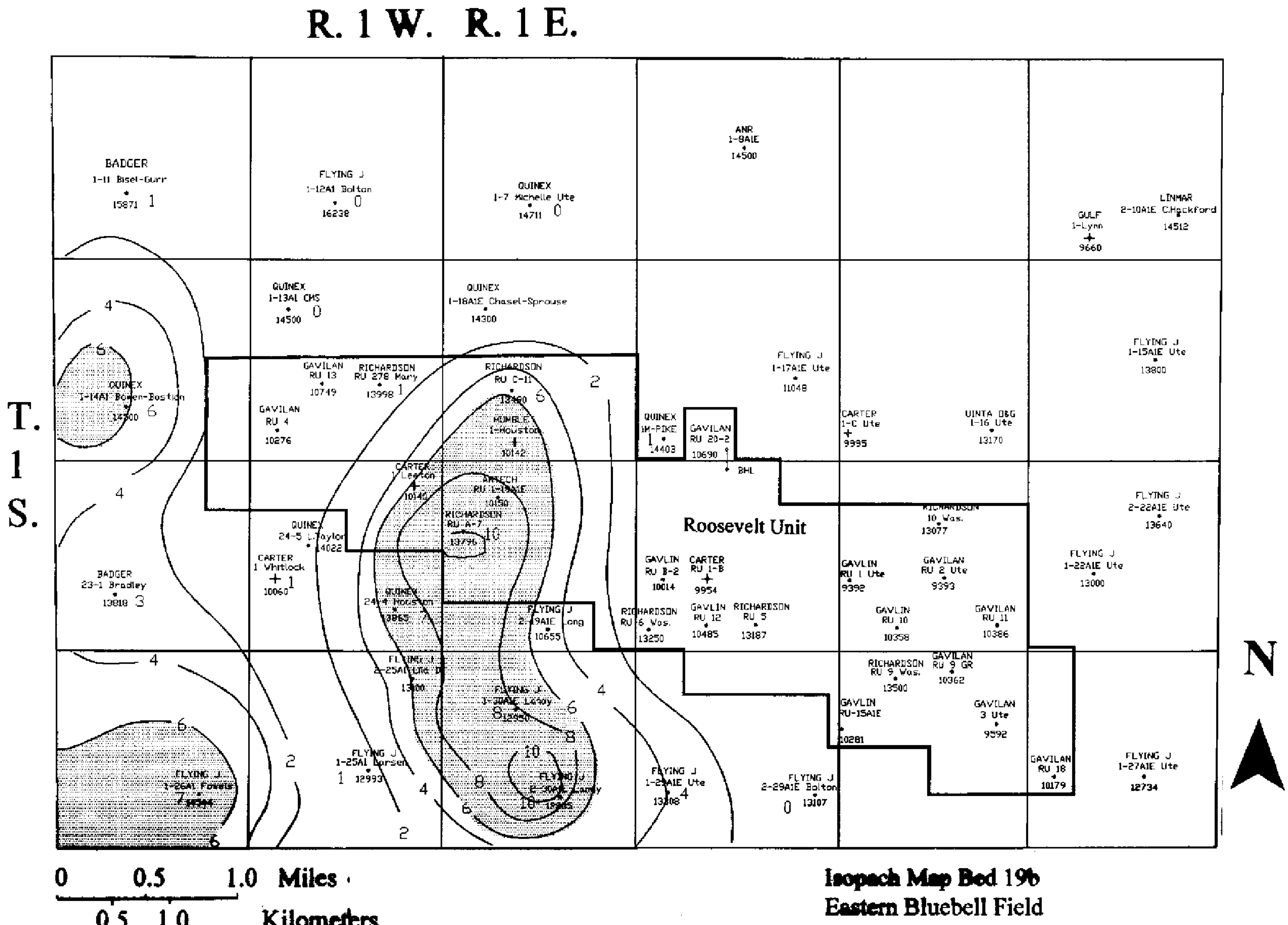

Isopach Map Bed 19b
Eastern Bluebell Field
Uintah County, Utah

Contour interval 2 feet
Shaded areas are 6 feet or thicker
Bed thickness is defined by

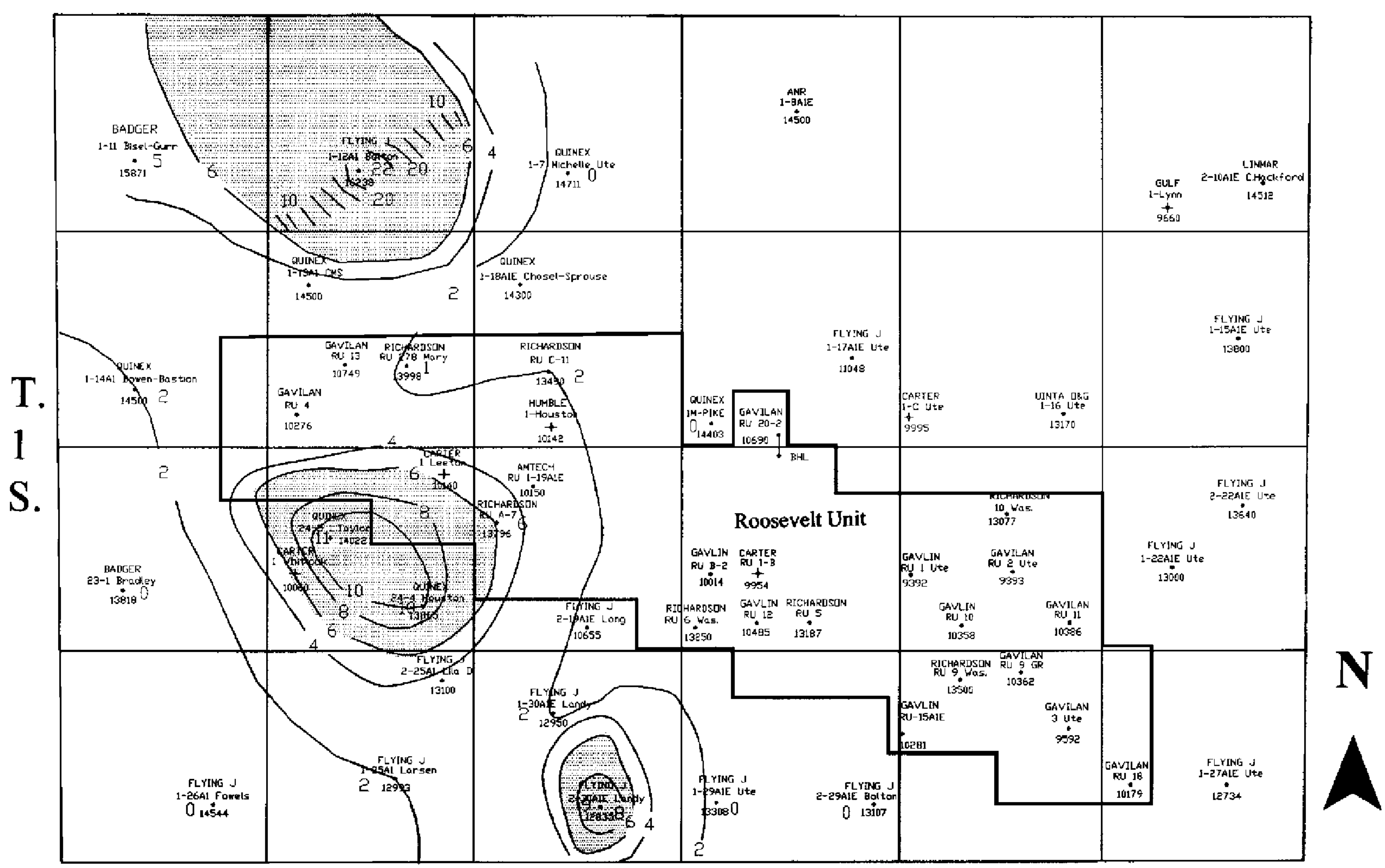

0 0.5 1.0 Miles

0.5 1.0 Kilometers

Isopach Map Bed 19c
Eastern Bluebell Field
Uintah County, Utah

Contour interval 2 feet

R. 1 W. R. 1 E.

T. 1 S.

A-15

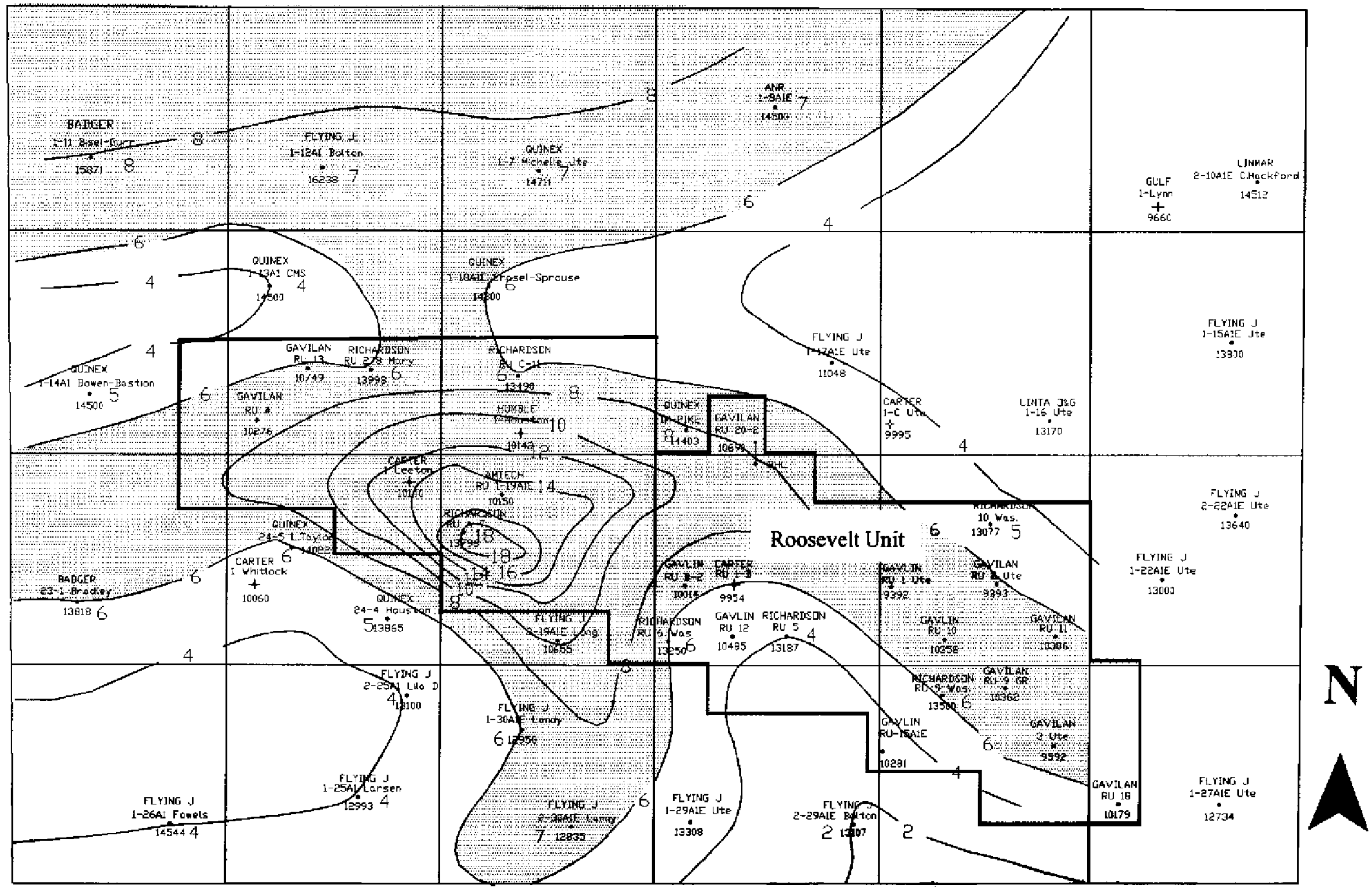

0 0.5 1.0 Miles

0.5 1.0 Kilometers

Contour interval 2 feet
Shaded areas are 6 feet or thicker
Bed thickness is defined by
[illegible]

Isopach Map Bed 20
Eastern Bluebell Field
Uintah County, Utah

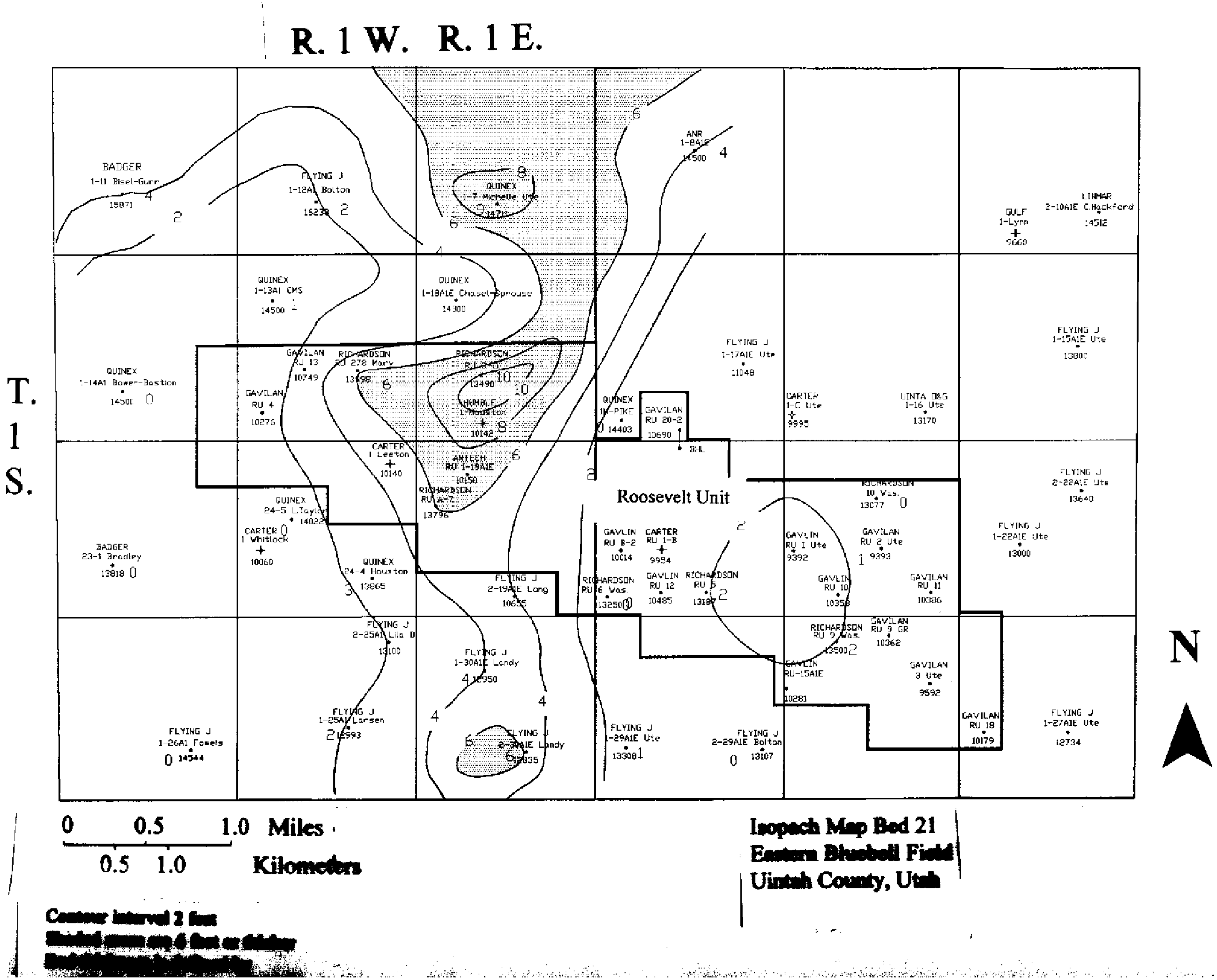

Isopach Map Bed 21
Eastern Bluebell Field
Uintah County, Utah

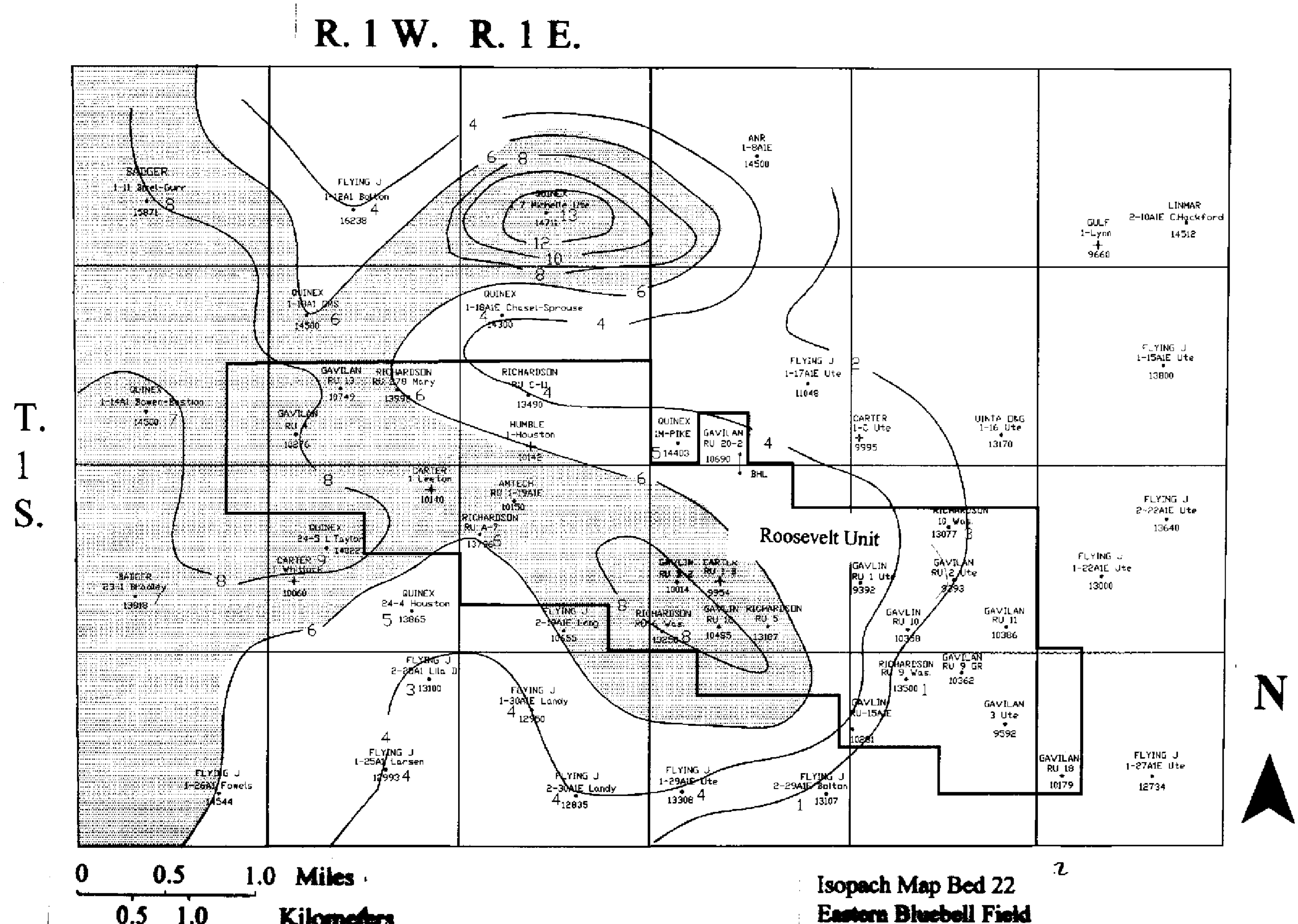

Isopach Map Bed 22
Eastern Bluebell Field
Uintah County, Utah

Contour interval 2 feet
Shaded areas are 6 feet or thicker
Bed thickness is defined by

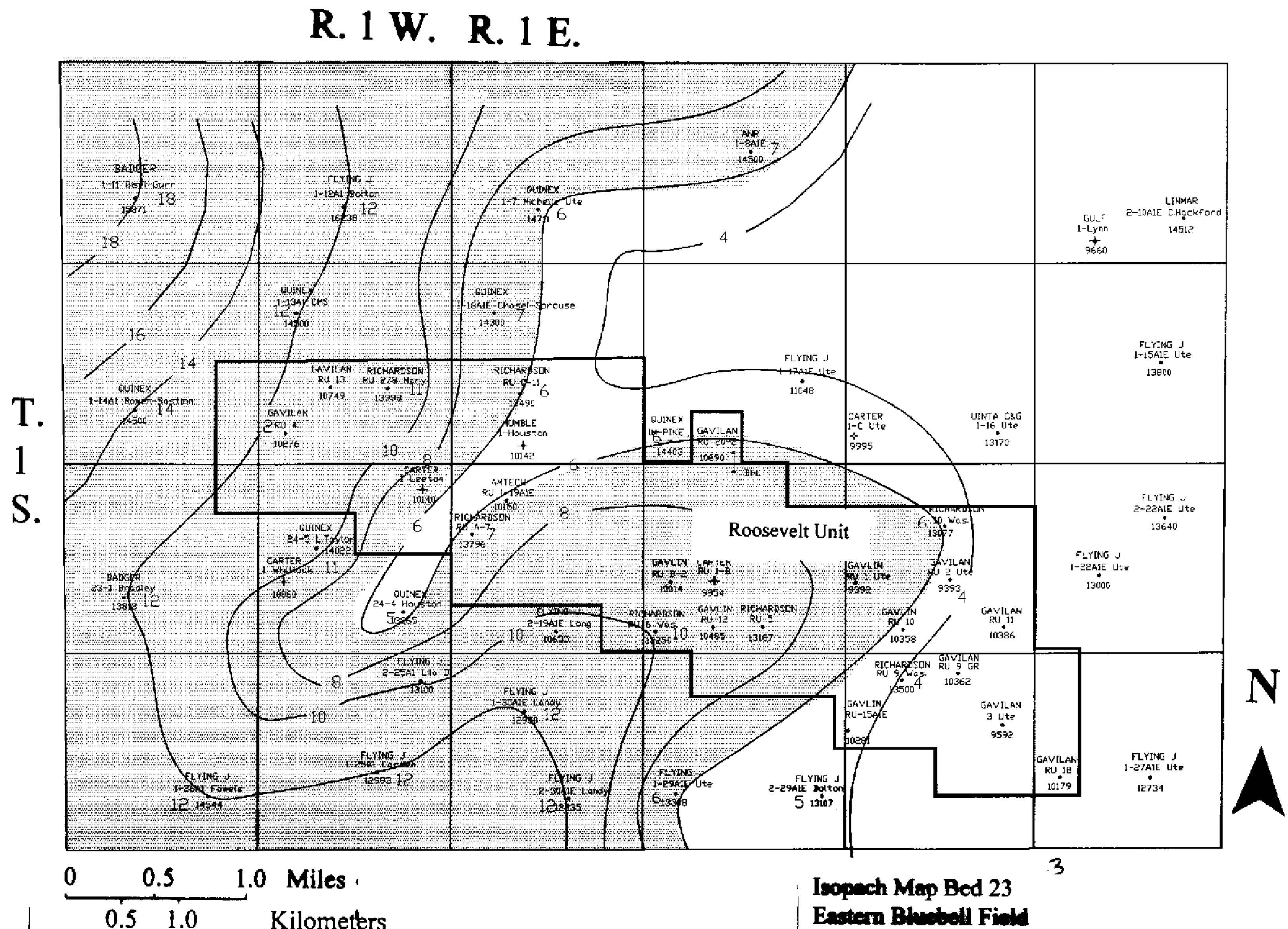

Isopach Map Bed 23
Eastern Bluebell Field
Uintah County, Utah

Contour interval 2 feet
Shaded areas are 6 feet or thicker
Bed thickness is defined by

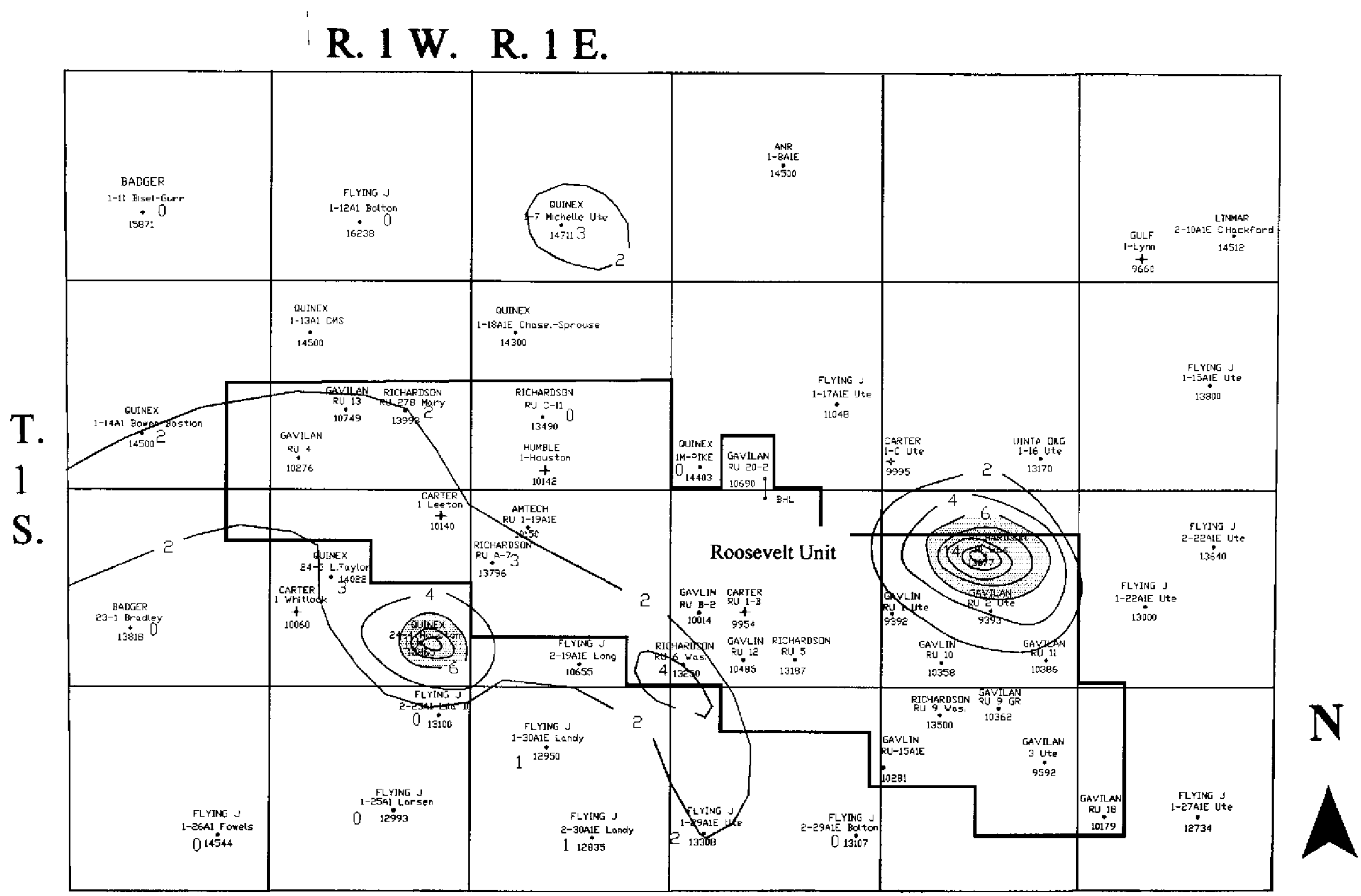

Isopach Map Bed 23a
Eastern Bluebell Field
Uintah County, Utah

Contour interval 2 feet
Shaded areas are 6 feet or thicker
Bed thickness is defined by

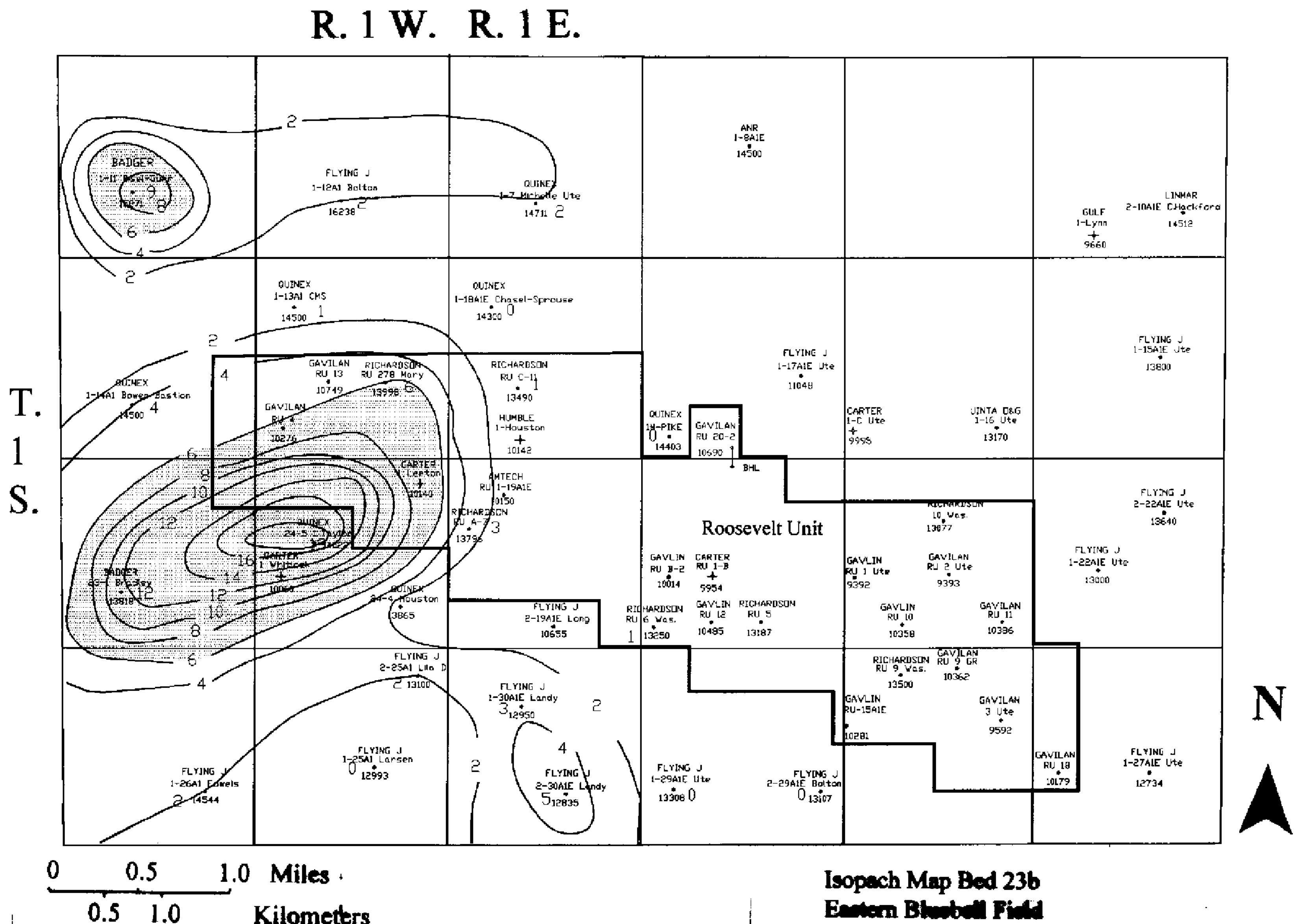

Isopach Map Bed 23b
Eastern Bluebell Field
Uintah County, Utah

Contour interval 2 feet

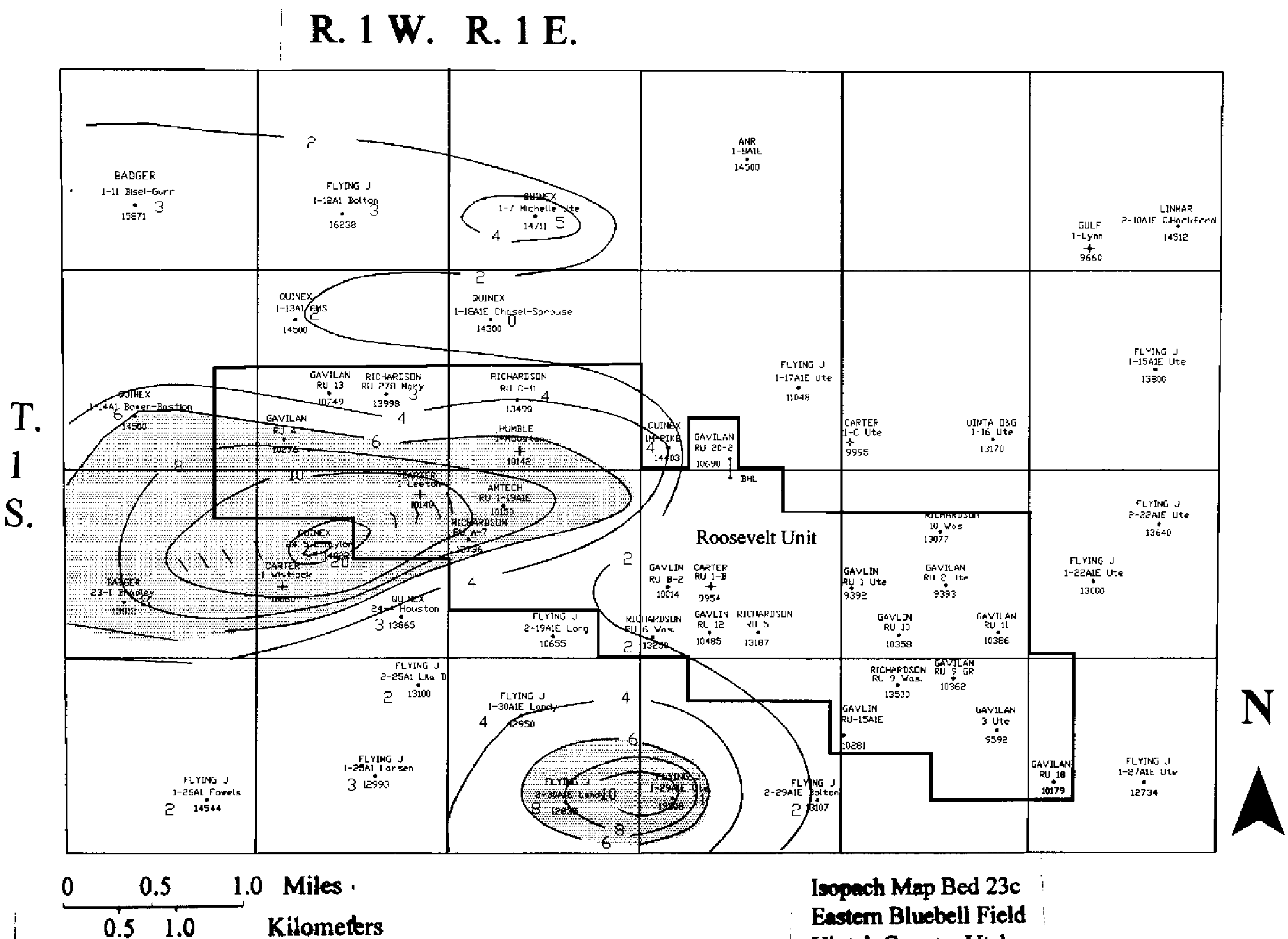

Isopach Map Bed 23c
Eastern Bluebell Field
Uintah County, Utah

Contour Interval 2 feet

R. 1 W. R. 1 E.

T. 1 S.

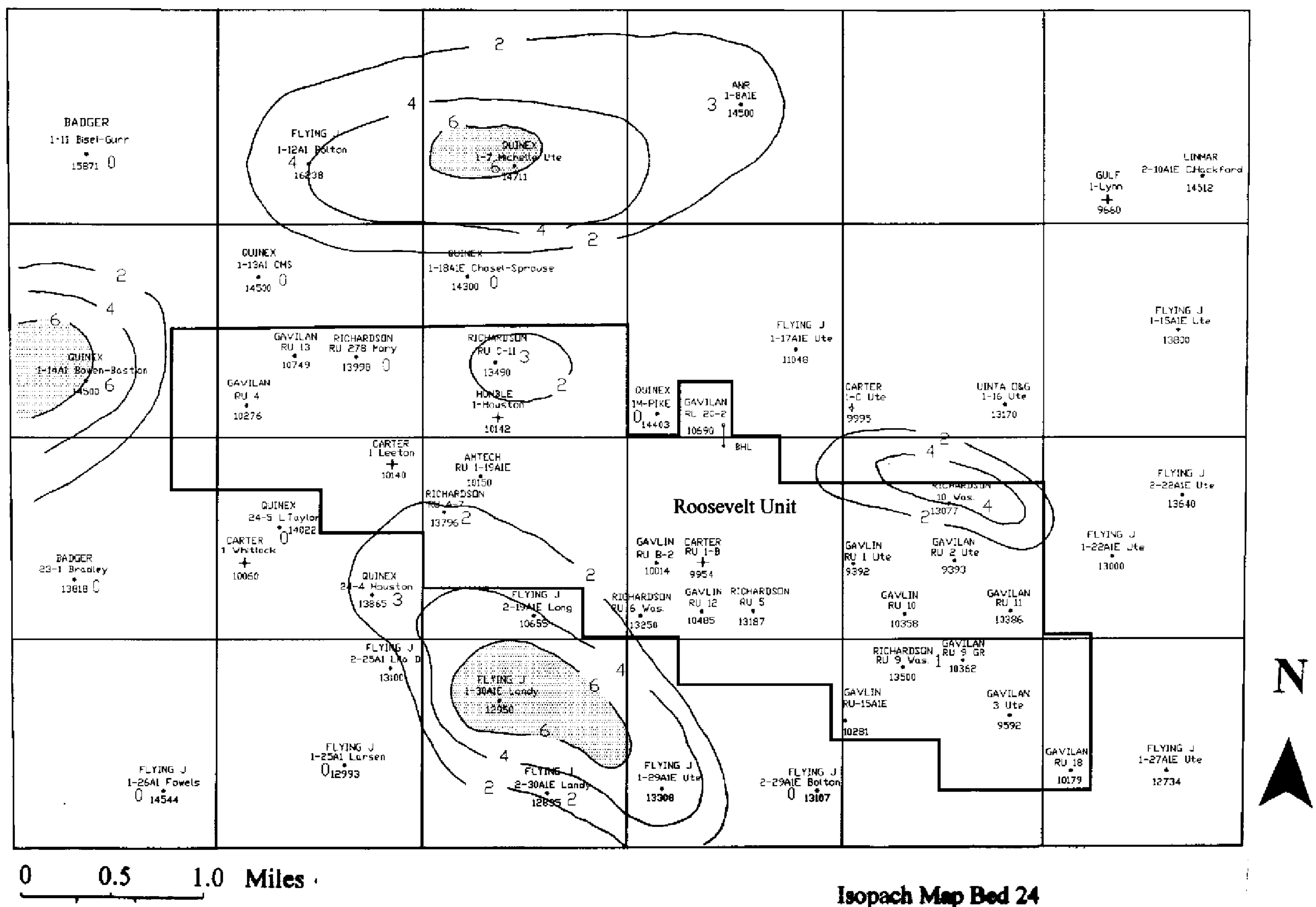

Contour interval 2 feet

Isopach Map Bed 24
Eastern Bluebell Field
Uintah County, Utah

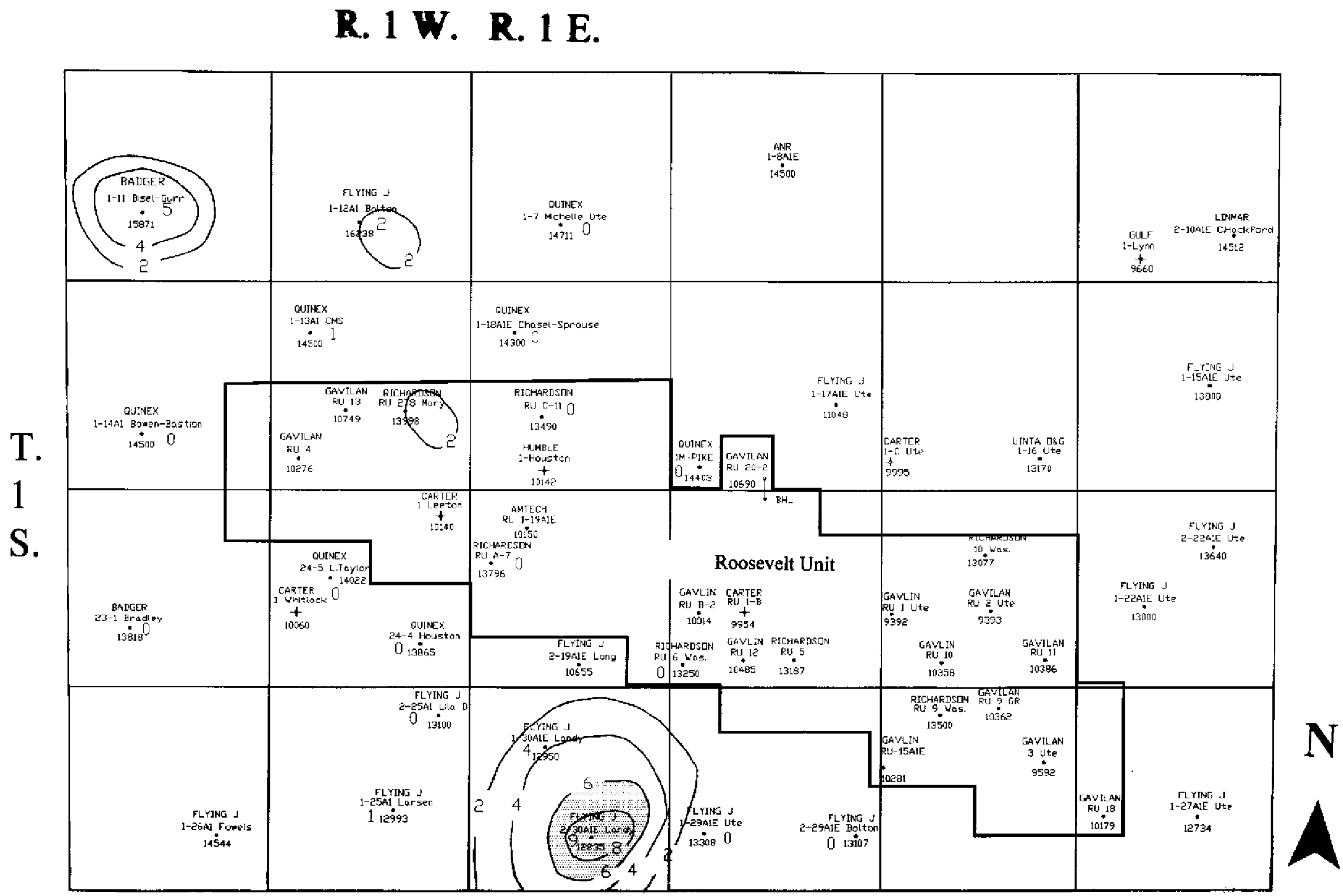

0 0.5 1.0 Miles

0.5 1.0 Kilometers

Contour interval 2 feet

Isopach Map Bed 24a
Eastern Bluebell Field
Uintah County, Utah

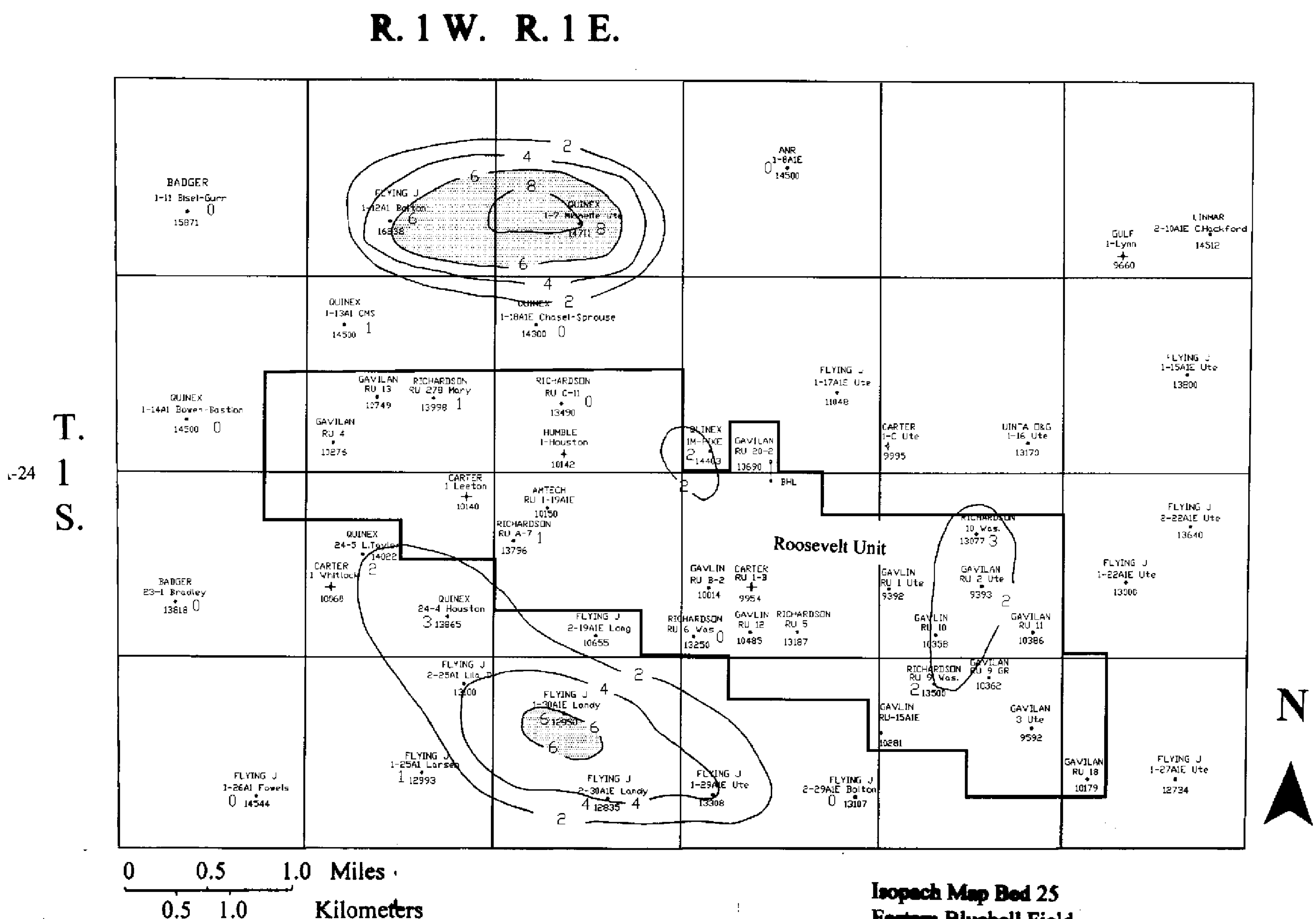

Contour interval 2 feet
Shaded areas are 6 feet or thicker
Bed thickness is defined by

Isopach Map Bed 25
Eastern Bluebell Field
Uintah County, Utah

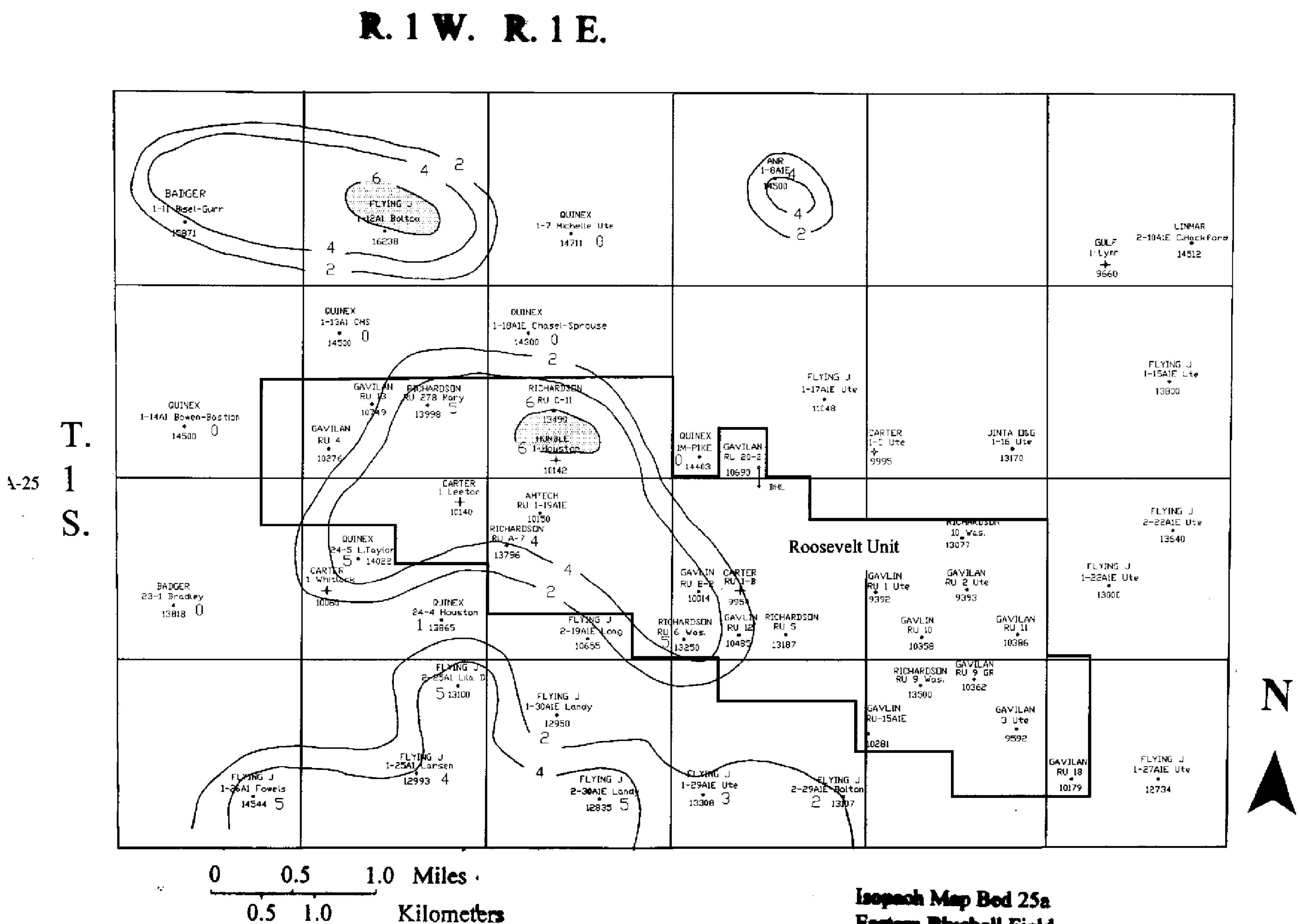

Isopach Map Bed 25a
Eastern Bluebell Field
Uintah County, Utah

Contour interval 2 feet
Shaded areas are 6 feet or thicker
Bed thickness is defined by
[illegible]

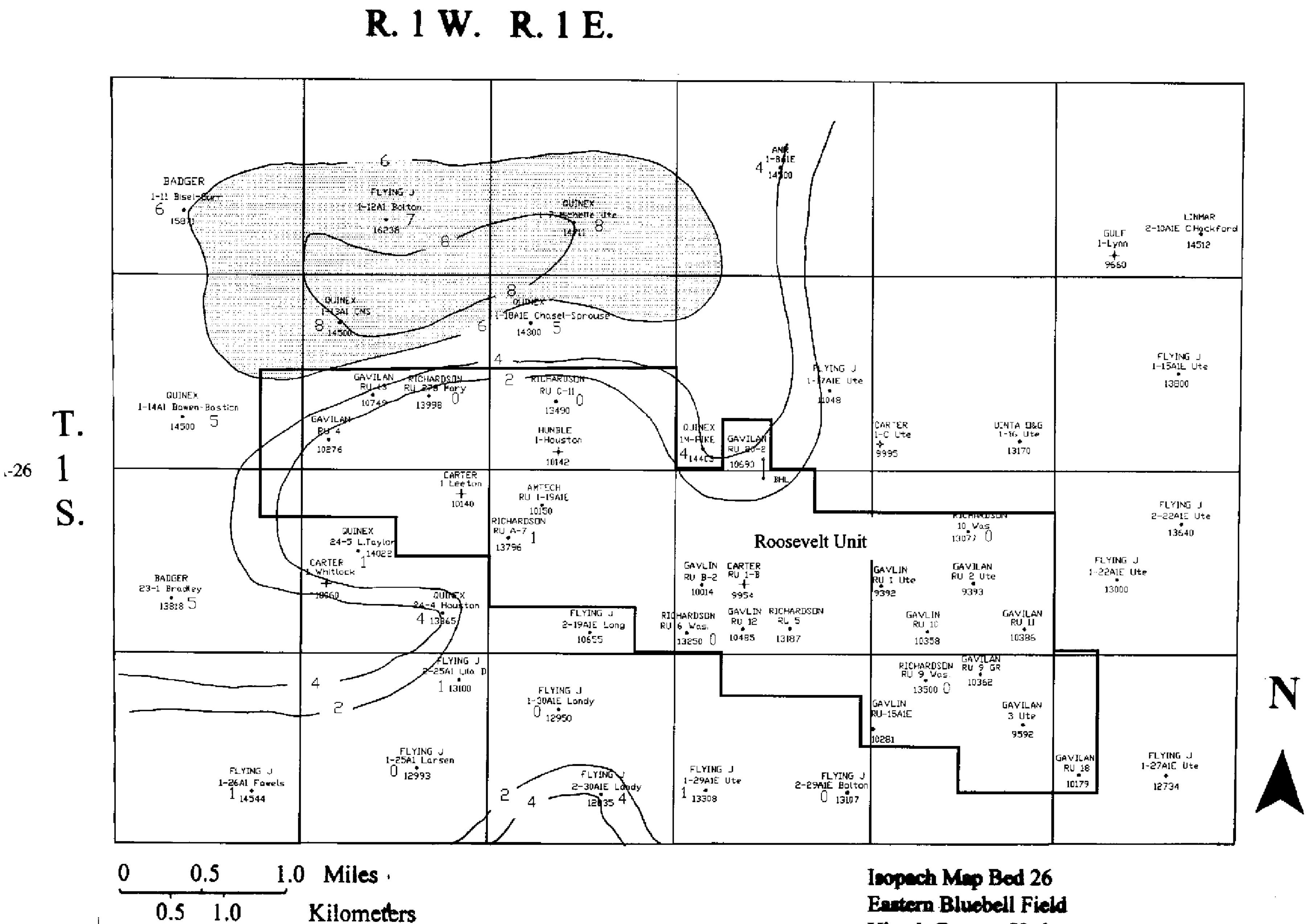

Isopach Map Bed 26
Eastern Bluebell Field
Uintah County, Utah

Contour interval 2 feet
Shaded areas are 6 feet or thicker
Bed thickness is defined by

R. 1 W. R. 1 E.

T. 1 S.

A-27

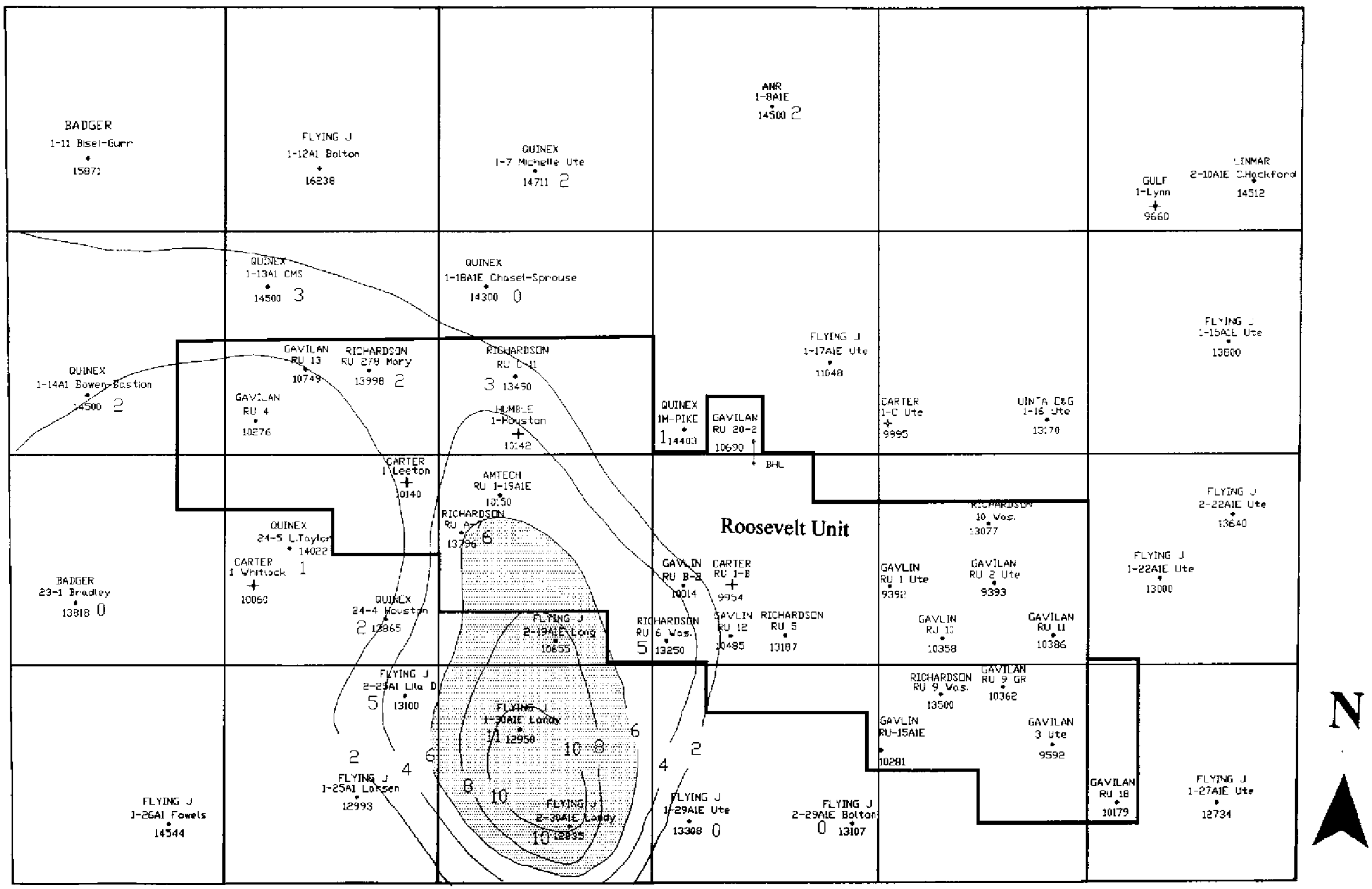

0 0.5 1.0 Miles

0.5 1.0 Kilometers

Contour interval 2 feet
Shaded areas are 6 feet or thicker
Bed thickness is defined by
[illegible]

Isopach Map Bed 26a
Eastern Bluebell Field -
Uintah County, Utah

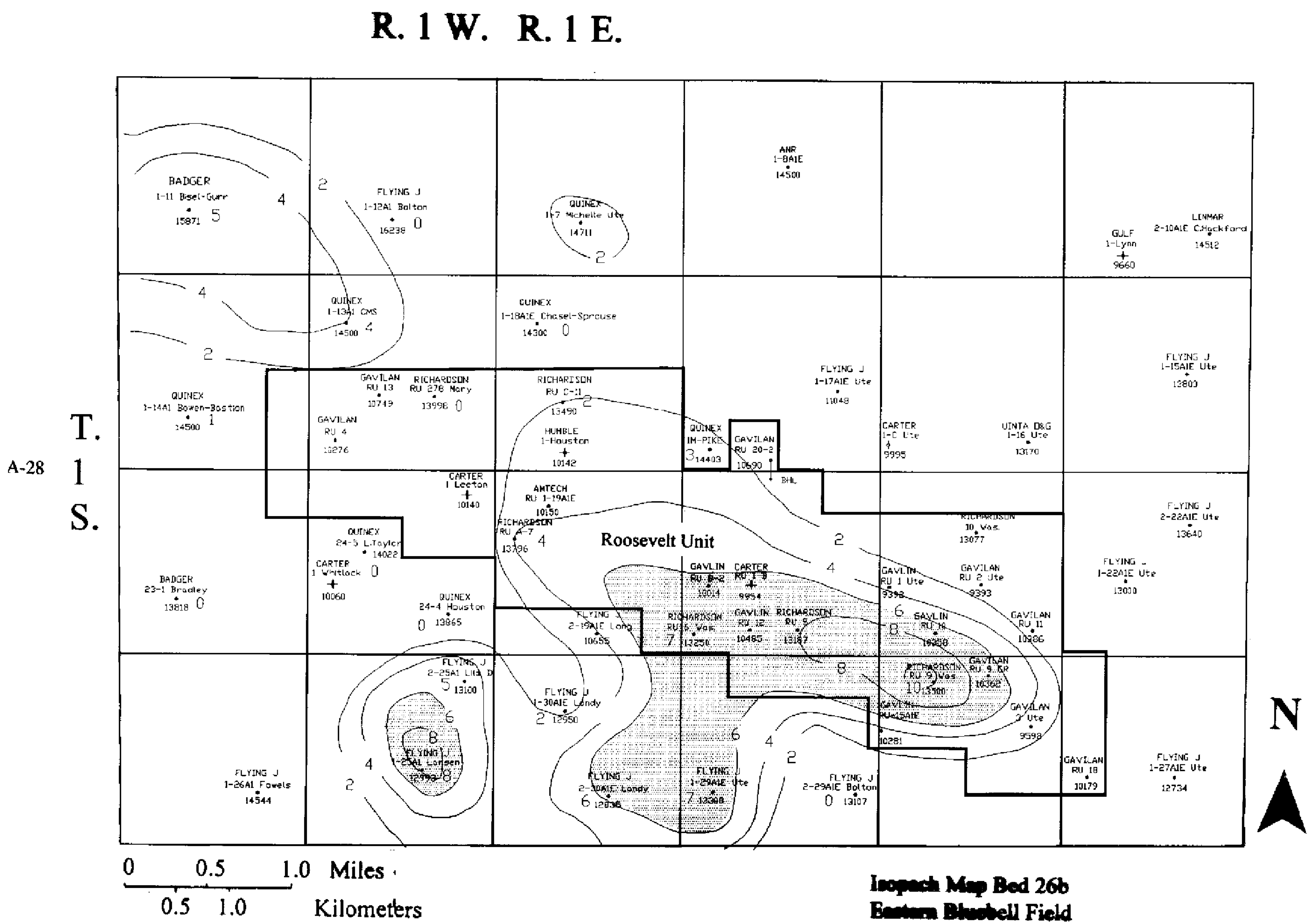

Isopach Map Bed 26b
Eastern Bluebell Field
Uintah County, Utah

Contour interval 2 feet

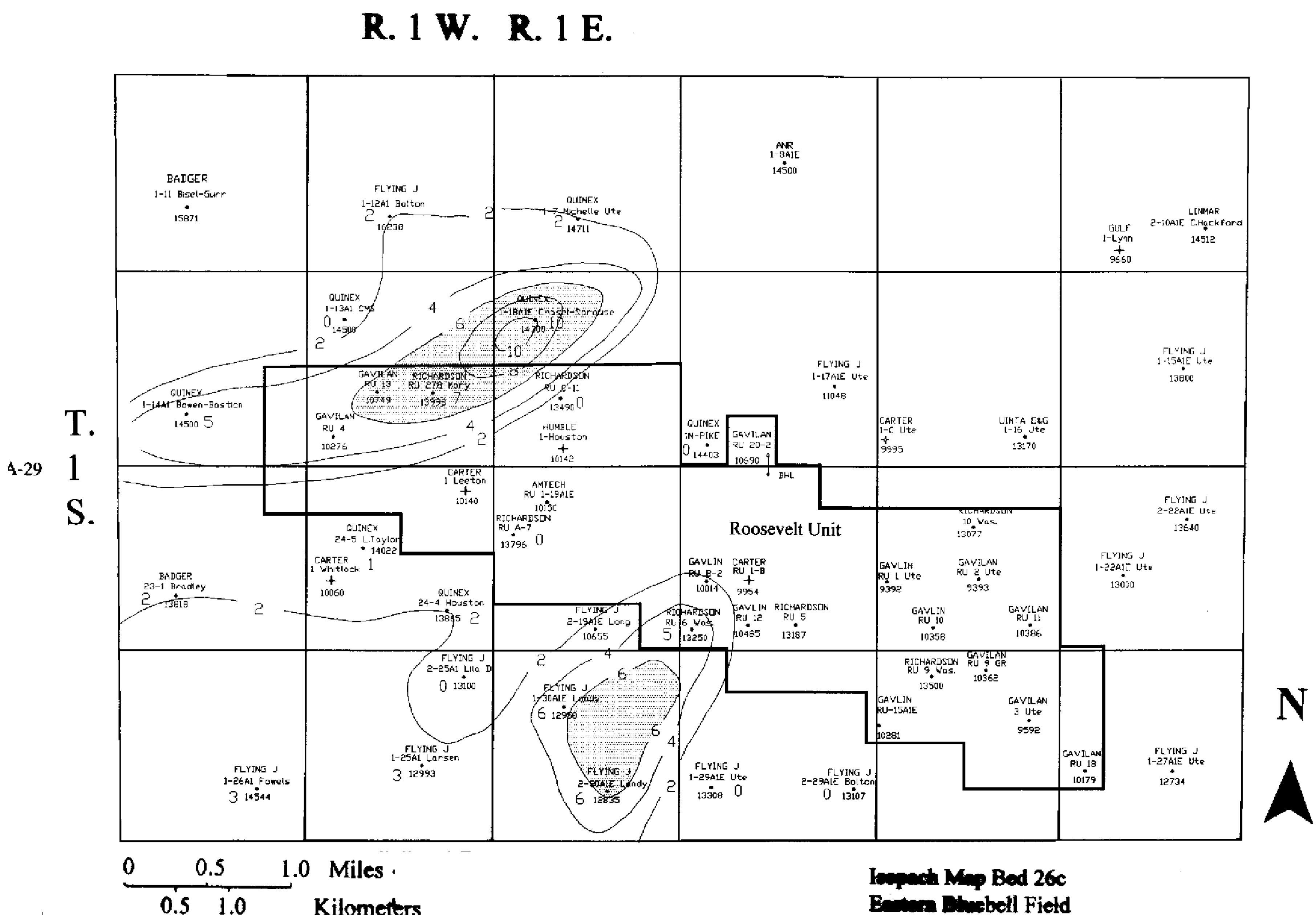

Isopach Map Bed 26c
Eastern Bluebell Field
Uintah County, Utah

Contour interval 2 feet
Shaded areas are 6 feet or thicker
Bed thickness is defined by
[illegible]

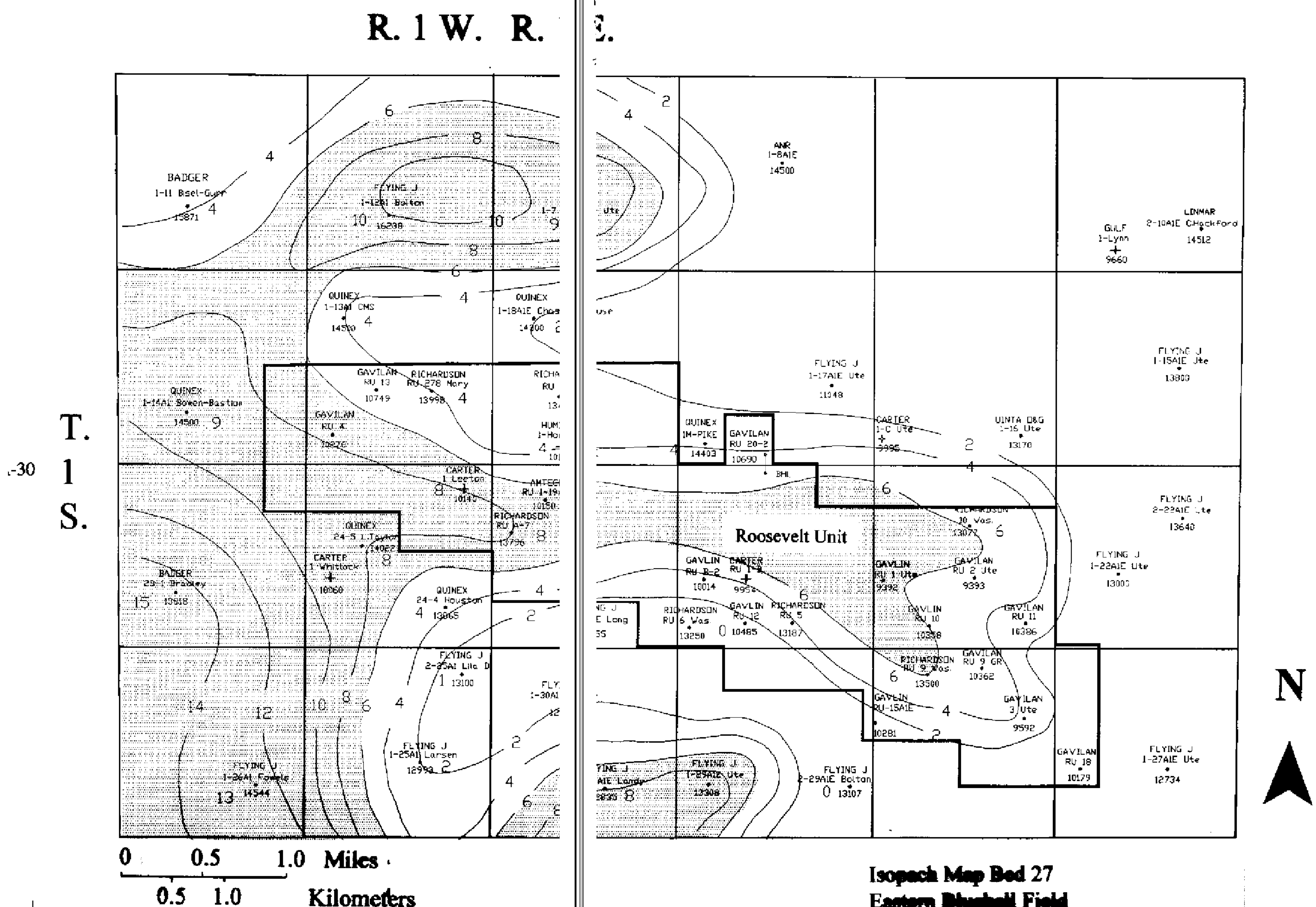

Contour interval 2 feet
Shaded areas are 6 feet or thicker
Bed thickness is defined by
gamma-ray count of 60 API or less

Isopach Map Bed 27
Eastern Bluebell Field
Uintah County, Utah

-30

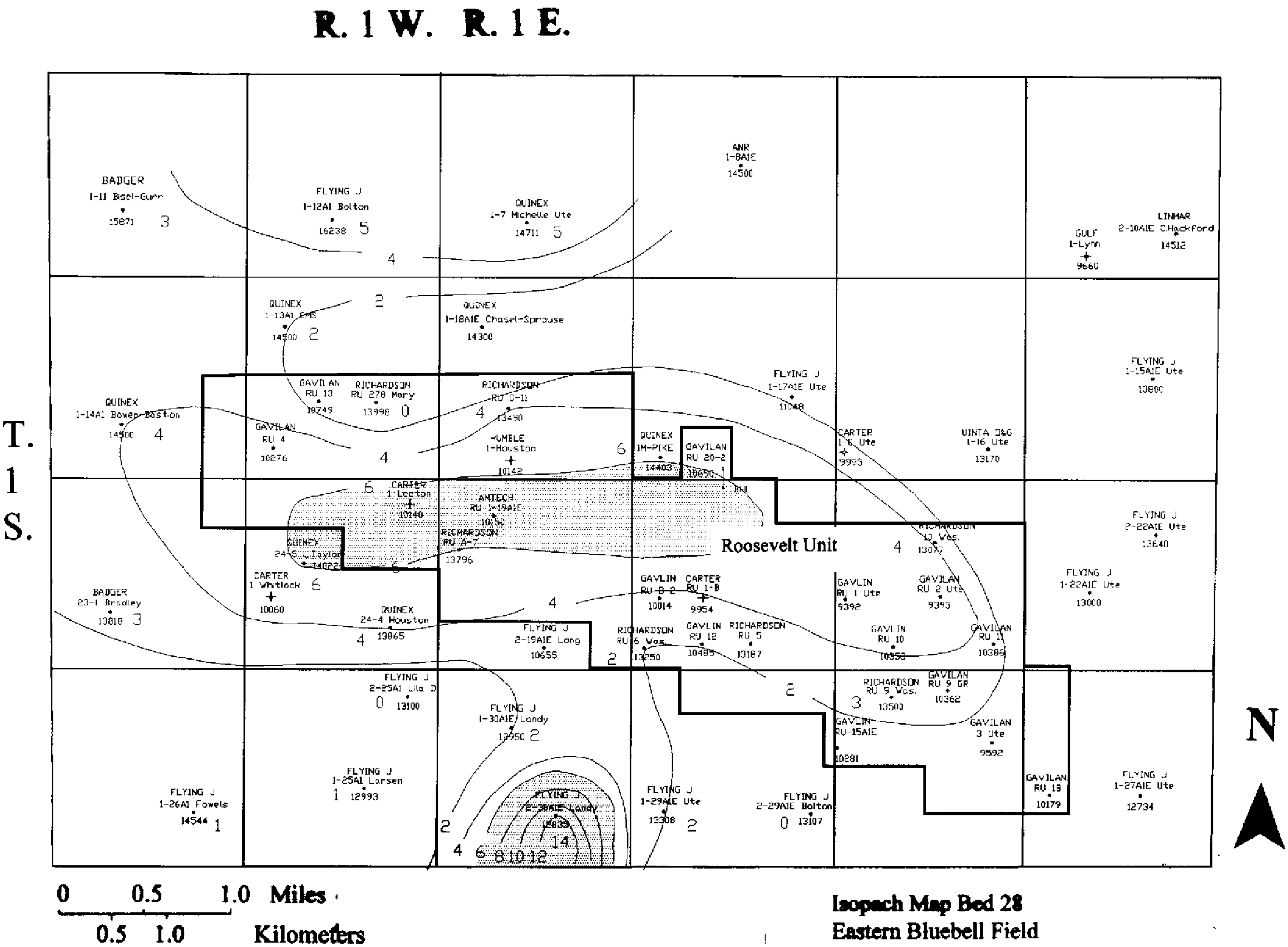

Isopach Map Bed 28
Eastern Bluebell Field
Uintah County, Utah

Contour interval 2 feet
Shaded areas are 6 feet or thicker
Bed thickness is defined by
[illegible]

R. 1 W. R. 1 E.

T. 1 S.

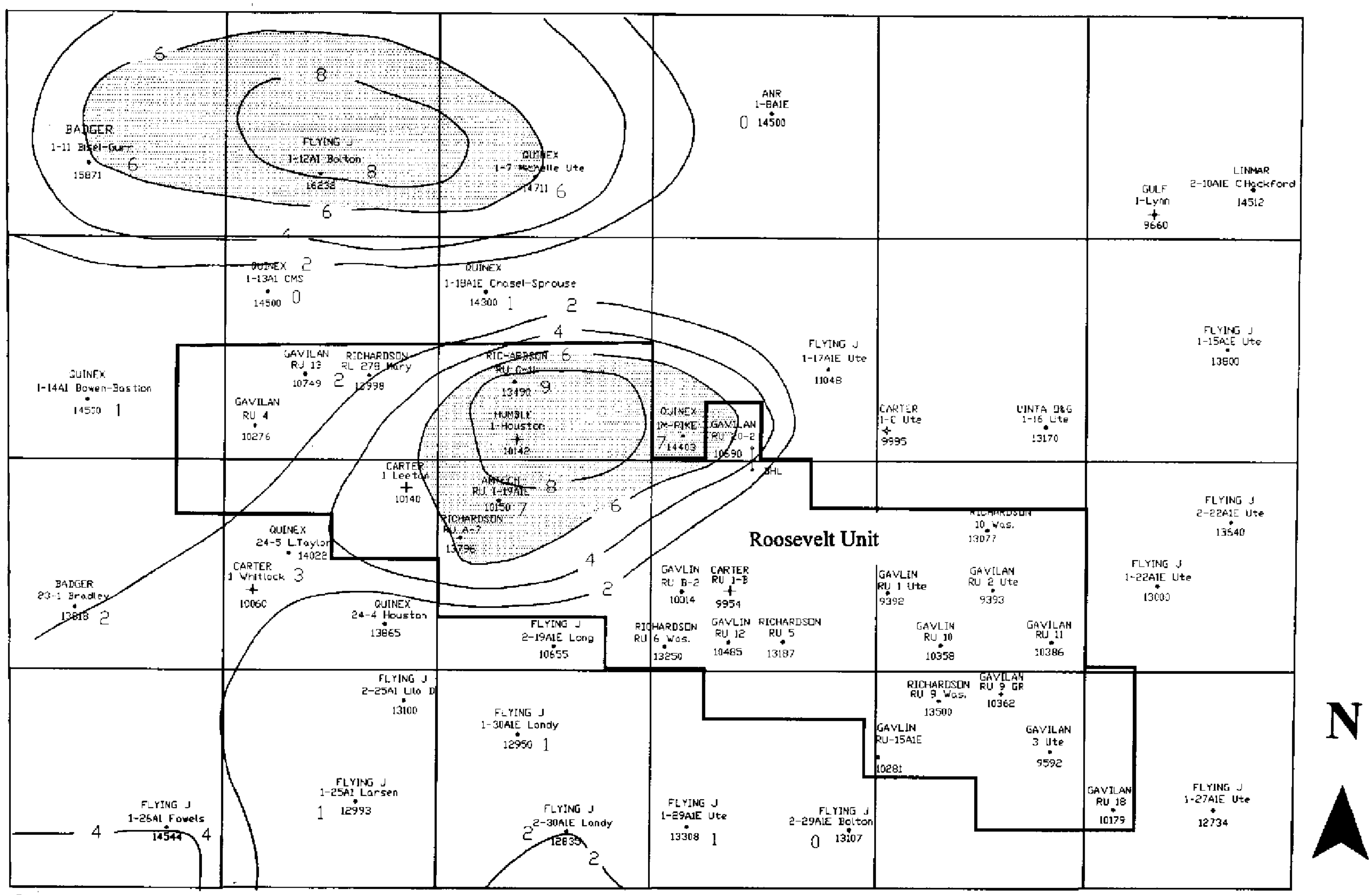

0 0.5 1.0 Miles

0.5 1.0 Kilometers

Contour interval 2 feet
Shaded areas are 6 feet or thicker
Bed thickness is defined by
gamma-ray count of 60 API or less

Isopach Map Bed 29
Eastern Bluebell Field
Uintah County, Utah

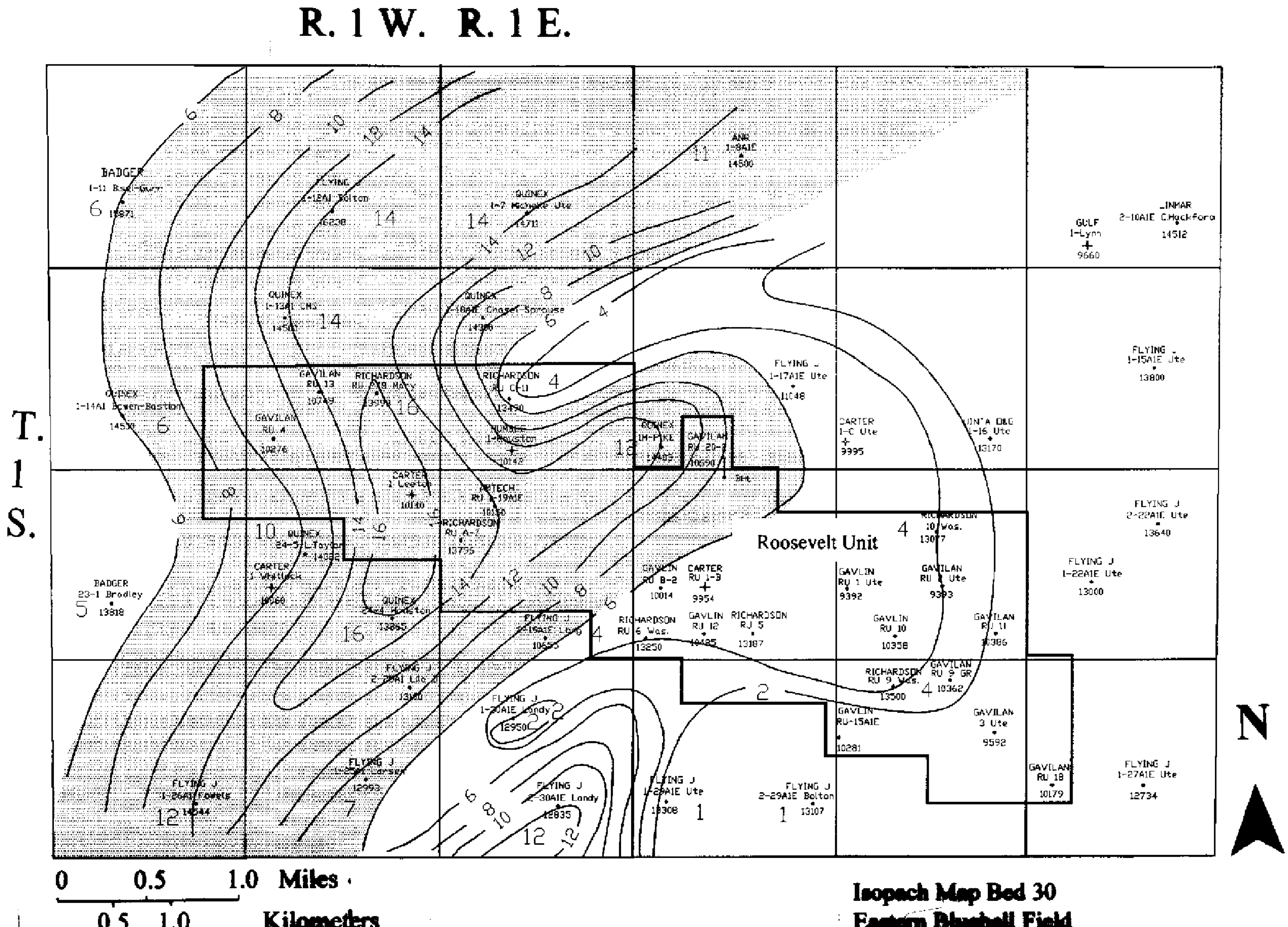

Isopach Map Bed 30
Eastern Bluebell Field
Uintah County, Utah

Contour interval 2 feet
Shaded areas are 6 feet or thicker
Bed thickness is defined by

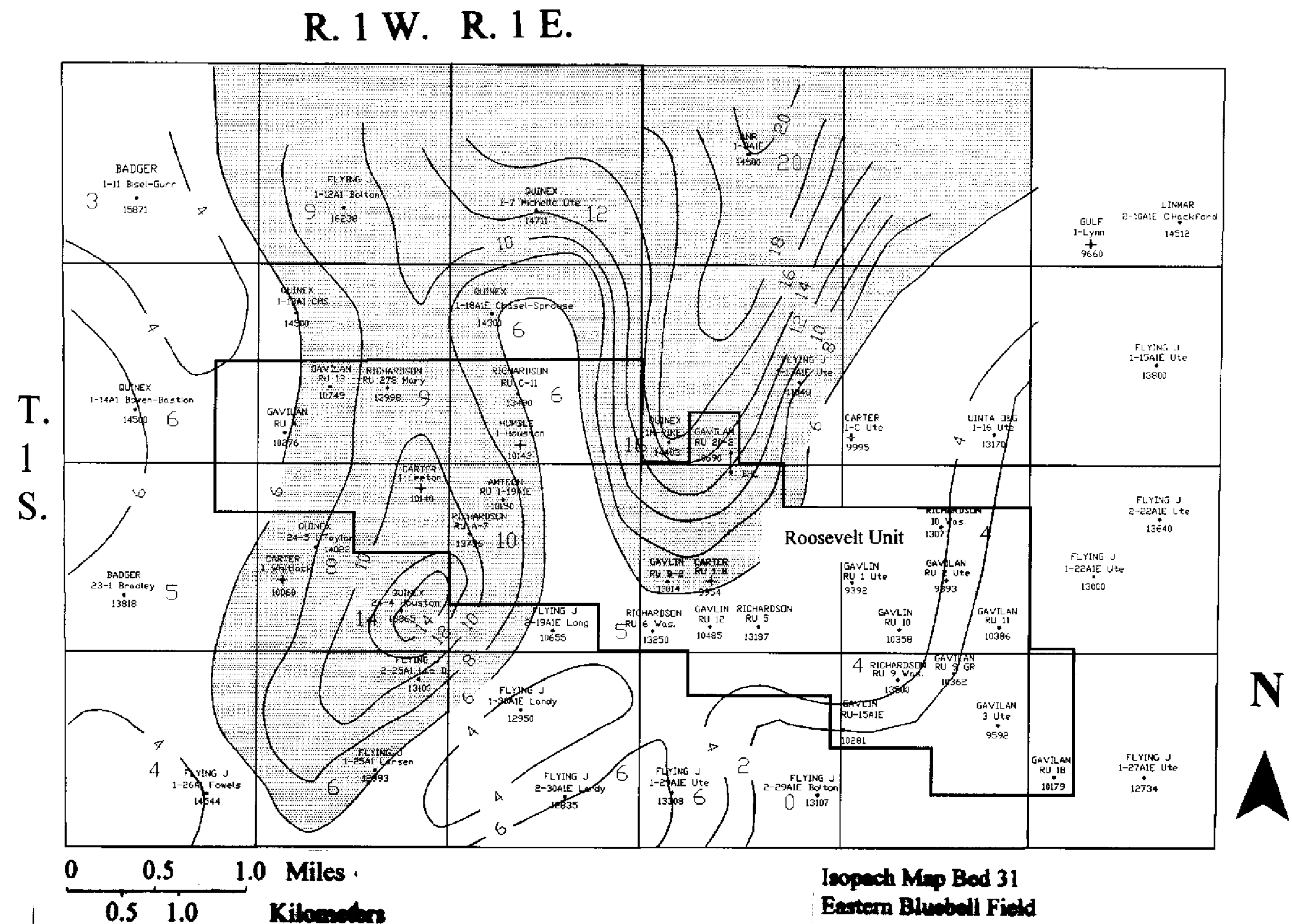

Isopach Map Bed 31
Eastern Bluebell Field
Uintah County, Utah

Contour interval 2 feet
Shaded areas are 6 feet or thicker
Bed thickness is defined by

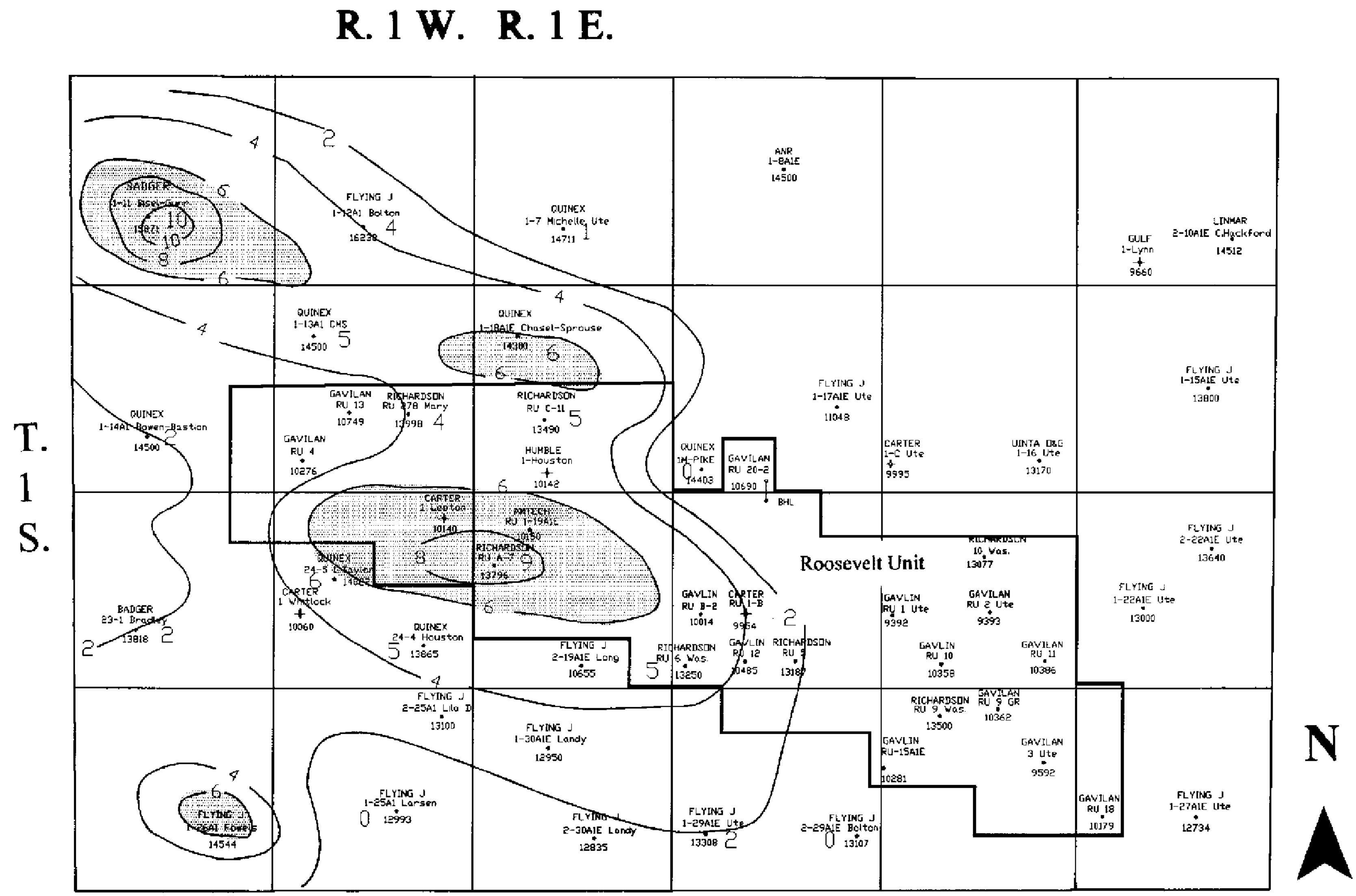

0 0.5 1.0 Miles

0.5 1.0 Kilometers

Isopach Map Bed 31a
Eastern Bluebell Field
Uintah County, Utah

Contour interval 2 feet
Shaded areas are 6 feet or thicker
Bed thickness is defined by

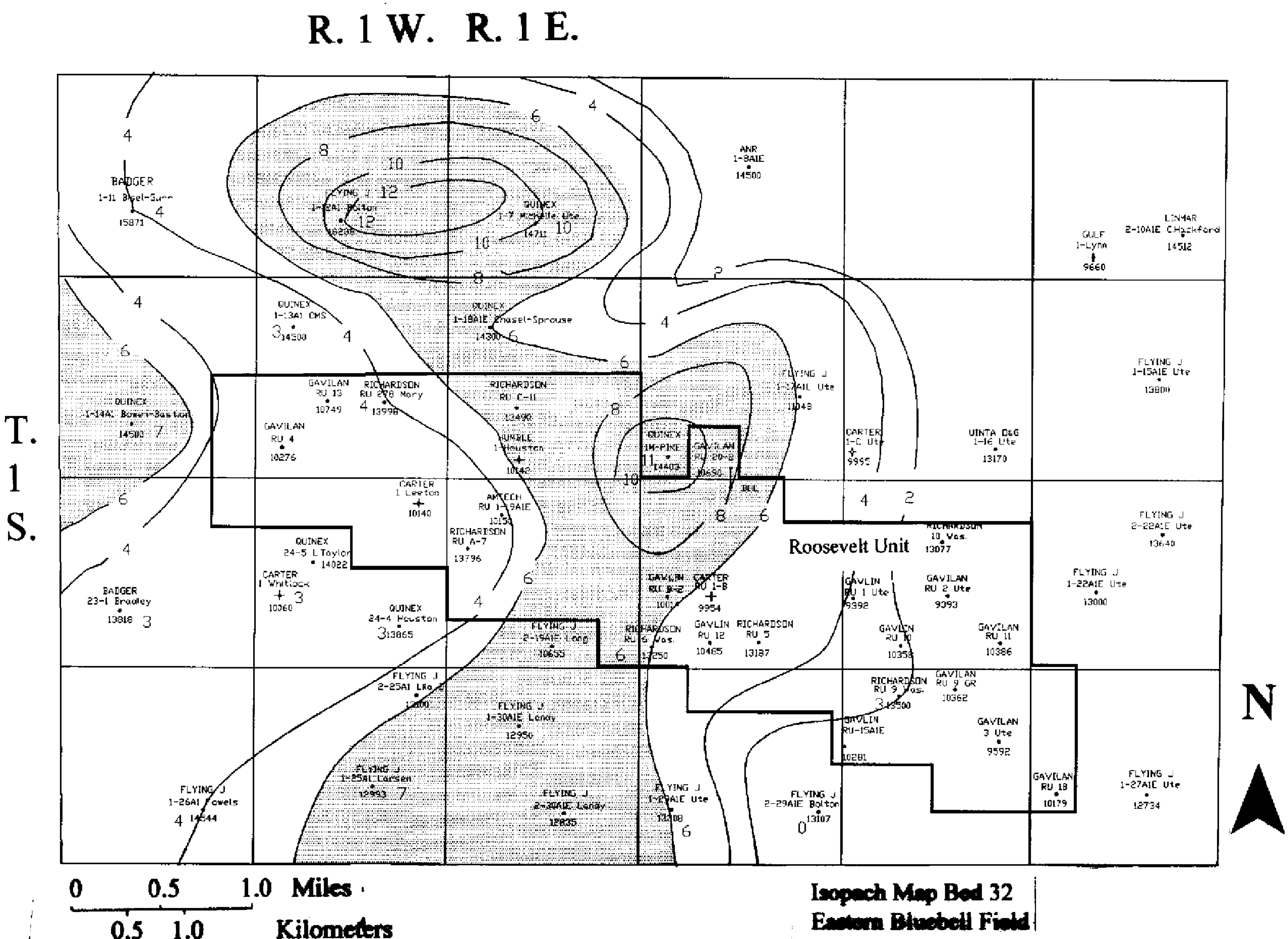

Isopach Map Bed 32
Eastern Bluebell Field
Uintah County, Utah

Contour interval 2 feet
Shaded areas are 6 feet or thicker
Bed thickness is defined by

A-36

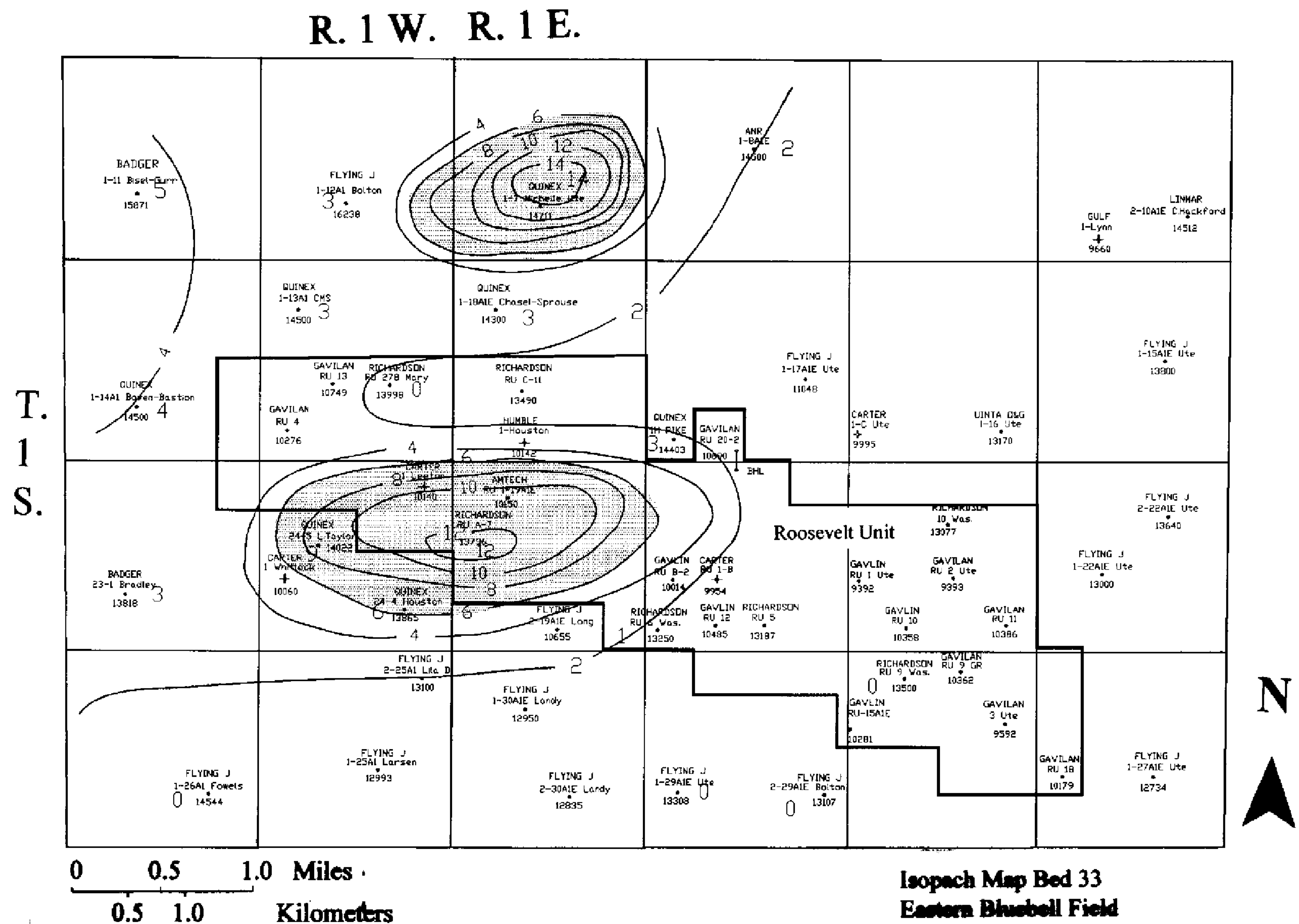

Isopach Map Bed 33
Eastern Bluebell Field
Uintah County, Utah

Contour interval 2 feet
Shaded areas are 6 feet or thicker

A-38

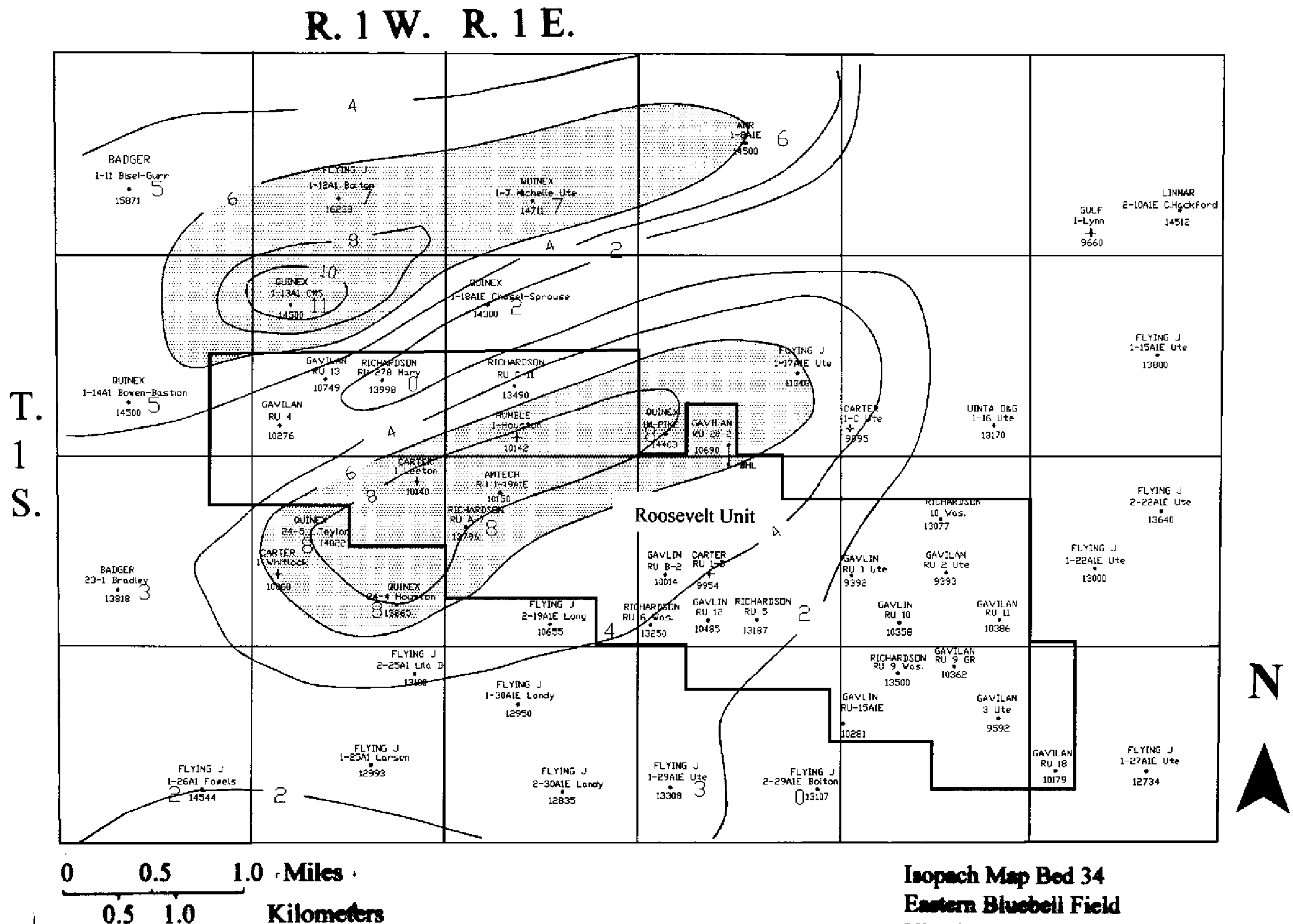

Isopach Map Bed 34
Eastern Bluebell Field
Uintah County, Utah

Contour interval 2 feet
Shaded areas are 6 feet or thicker
Bed thickness is defined by

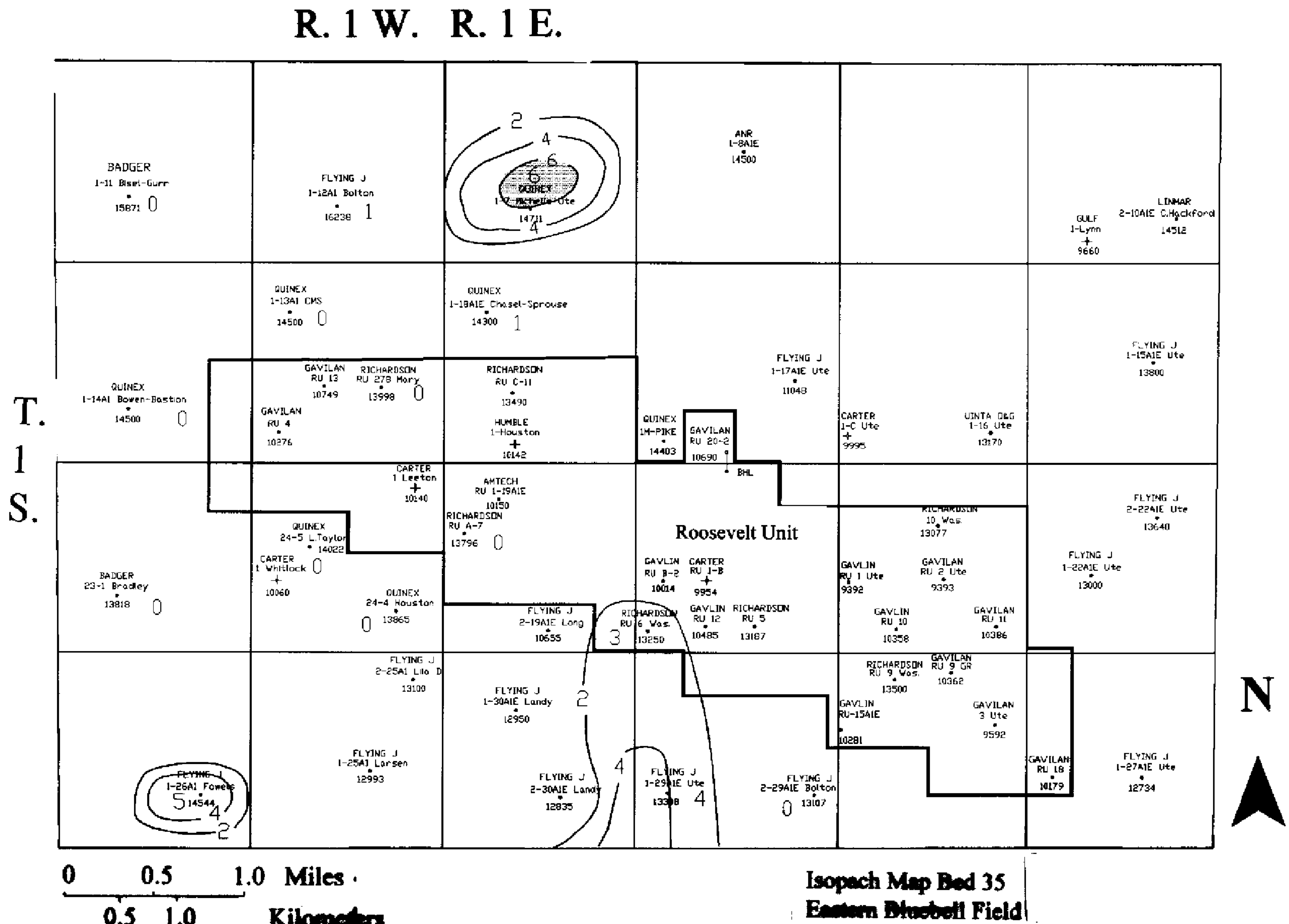

Isopach Map Bed 35
Eastern Bluebell Field
Uintah County, Utah

Contour interval 2 feet
Shaded areas are 6 feet or thicker

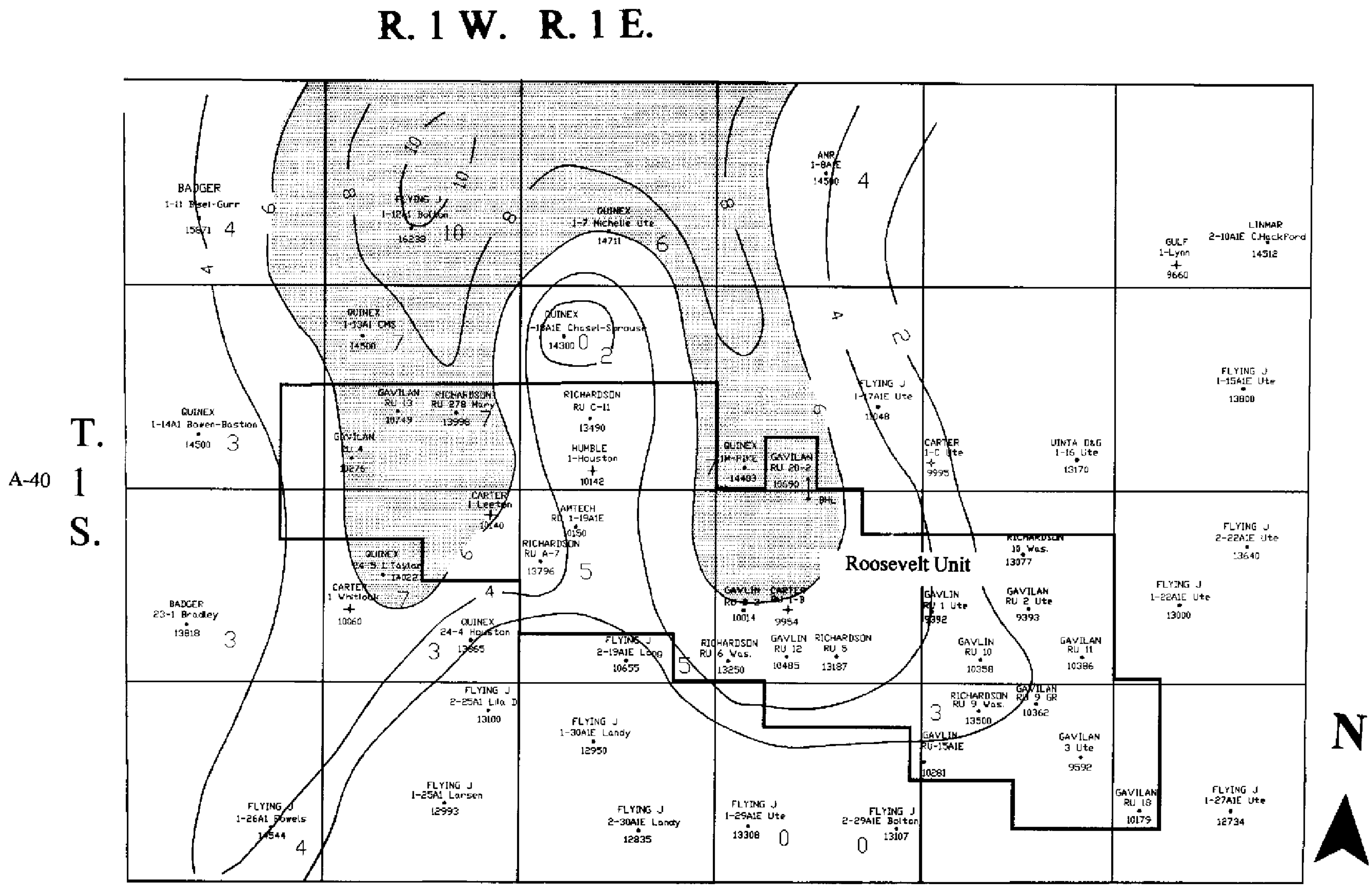

A-40

Isopach Map Bed 36
Eastern Bluebell Field
Uintah County, Utah

Contour interval 2 feet
Shaded areas are 6 feet or thicker
Bed thickness is defined by

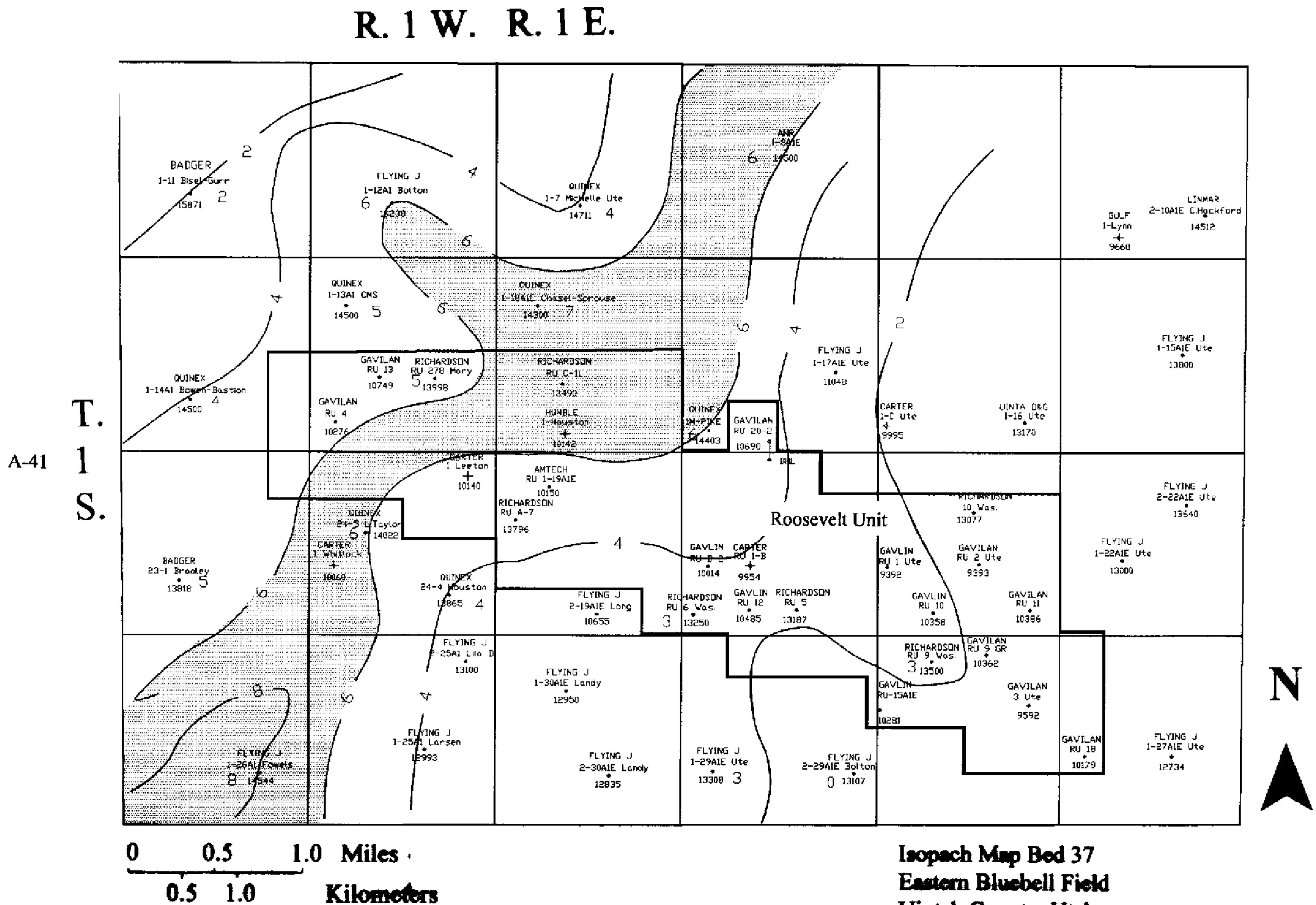

Isopach Map Bed 37
Eastern Bluebell Field
Uintah County, Utah

Contour interval 2 feet
Shaded areas are 6 feet or thicker
Bed thickness is defined by

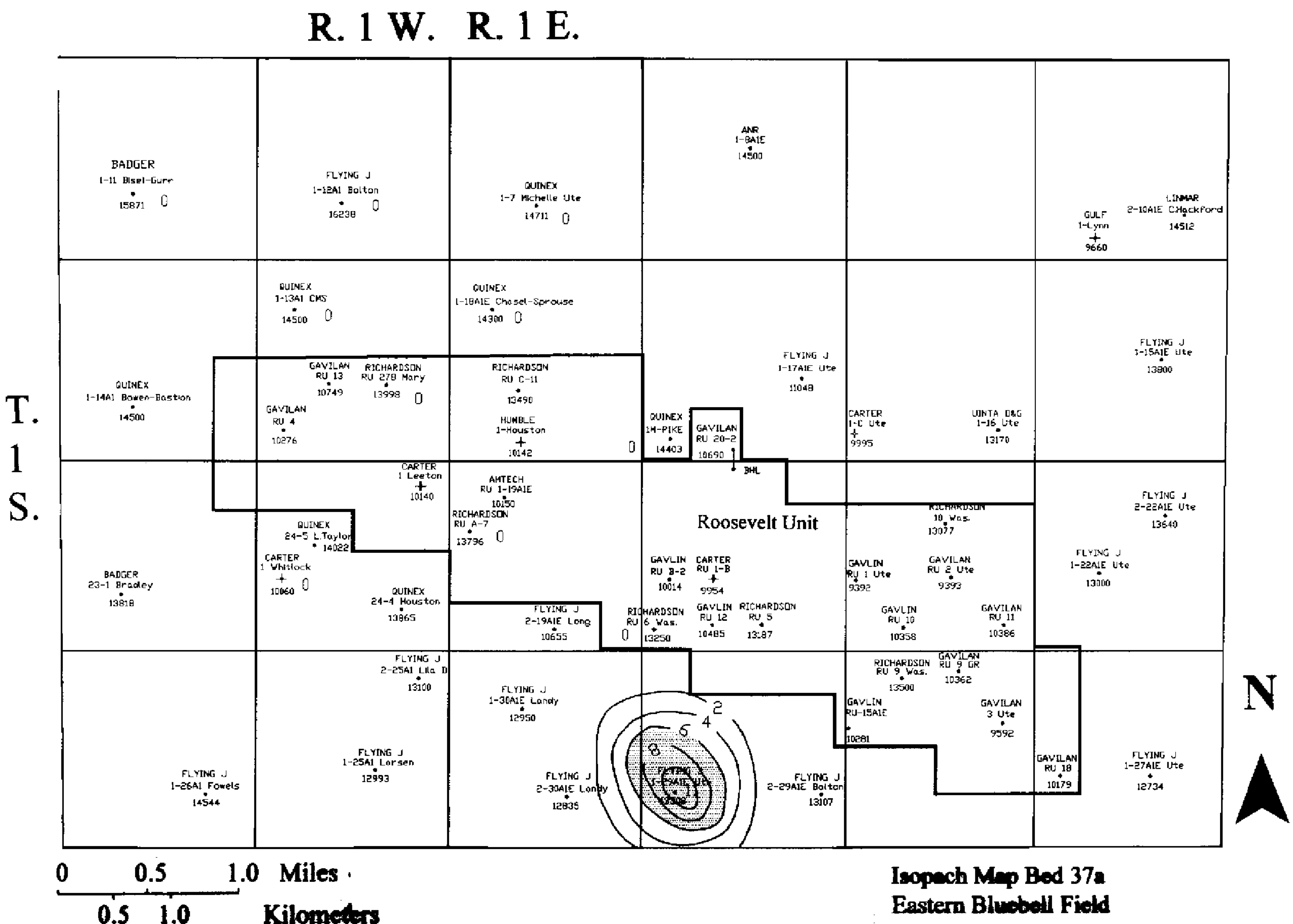

Isopach Map Bed 37a
Eastern Bluebell Field
Uintah County, Utah

Contour interval 2 feet
Shaded areas are 6 feet or thicker
Bed thickness is defined by

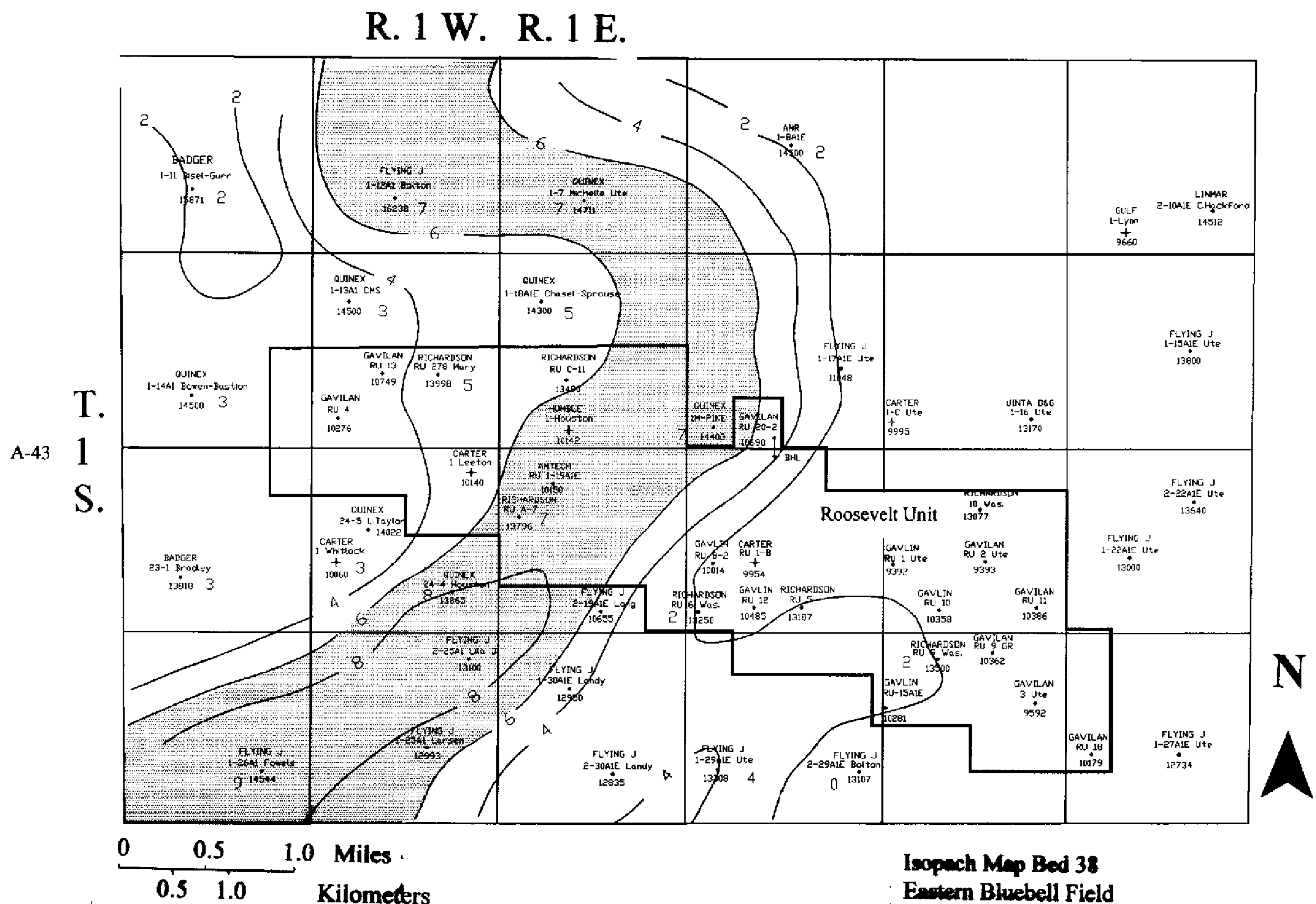

A-43

Isopach Map Bed 38
Eastern Bluebell Field
Uintah County, Utah

Contour interval 2 feet
Shaded areas are 6 feet or thicker
Bed thickness is defined by

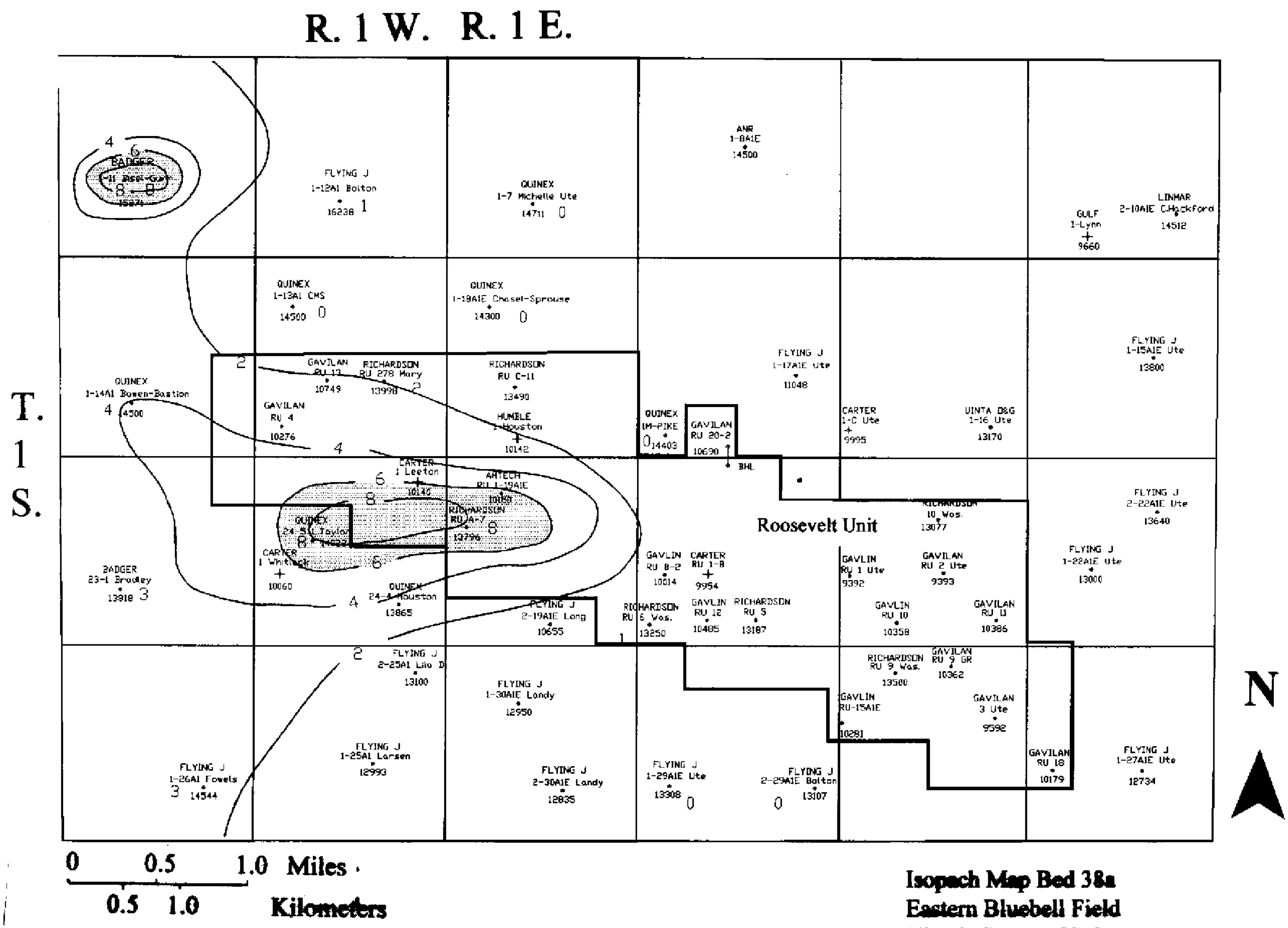

Isopach Map Bed 38a
Eastern Bluebell Field
Uintah County, Utah

Contour interval 2 feet
Shaded areas are 6 feet or thicker
Bed thickness is defined by

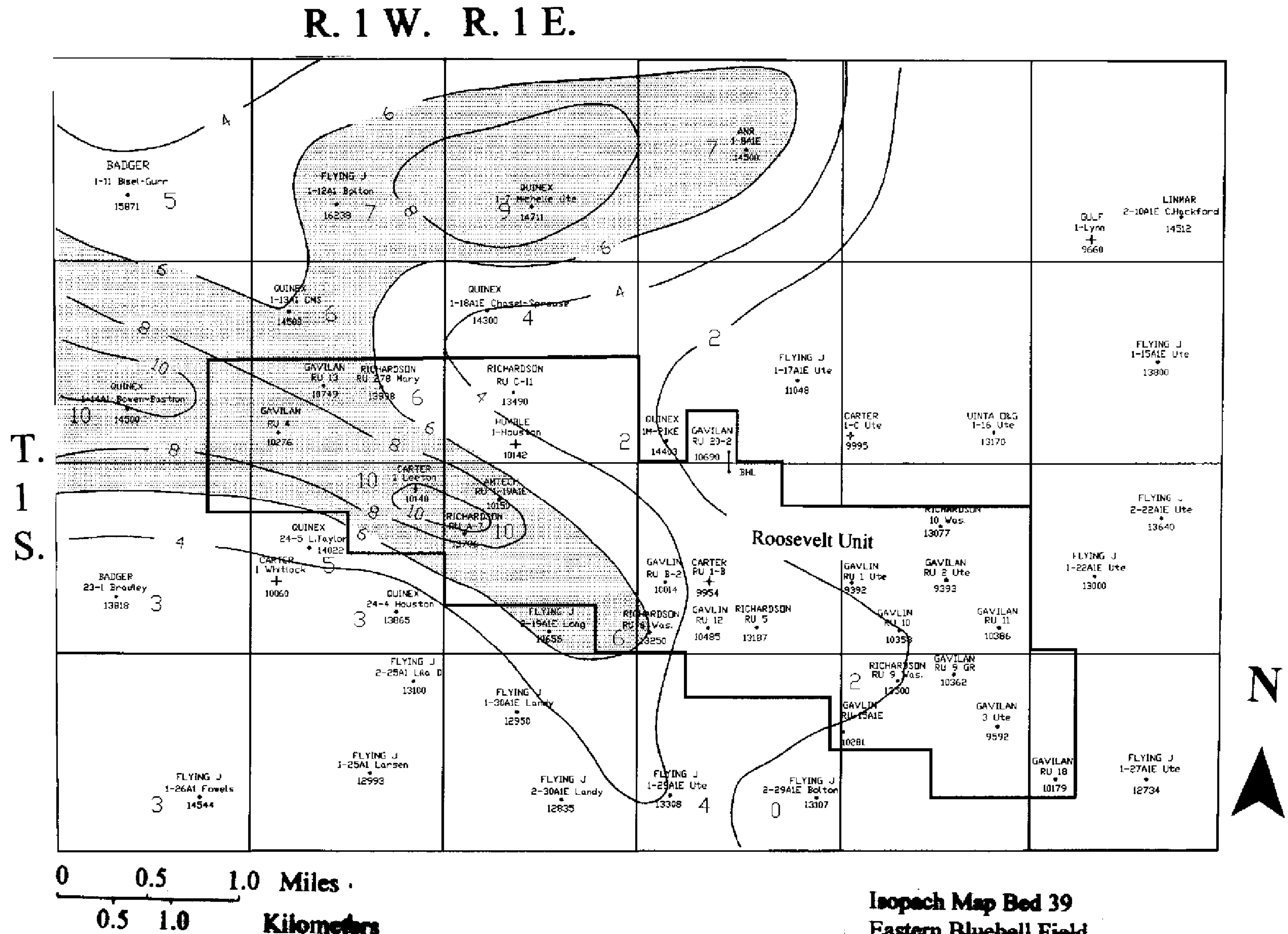

Isopach Map Bed 39
Eastern Bluebell Field
Uintah County, Utah

Contour interval 2 feet
Shaded areas are 6 feet or thicker
Bed thickness is defined by

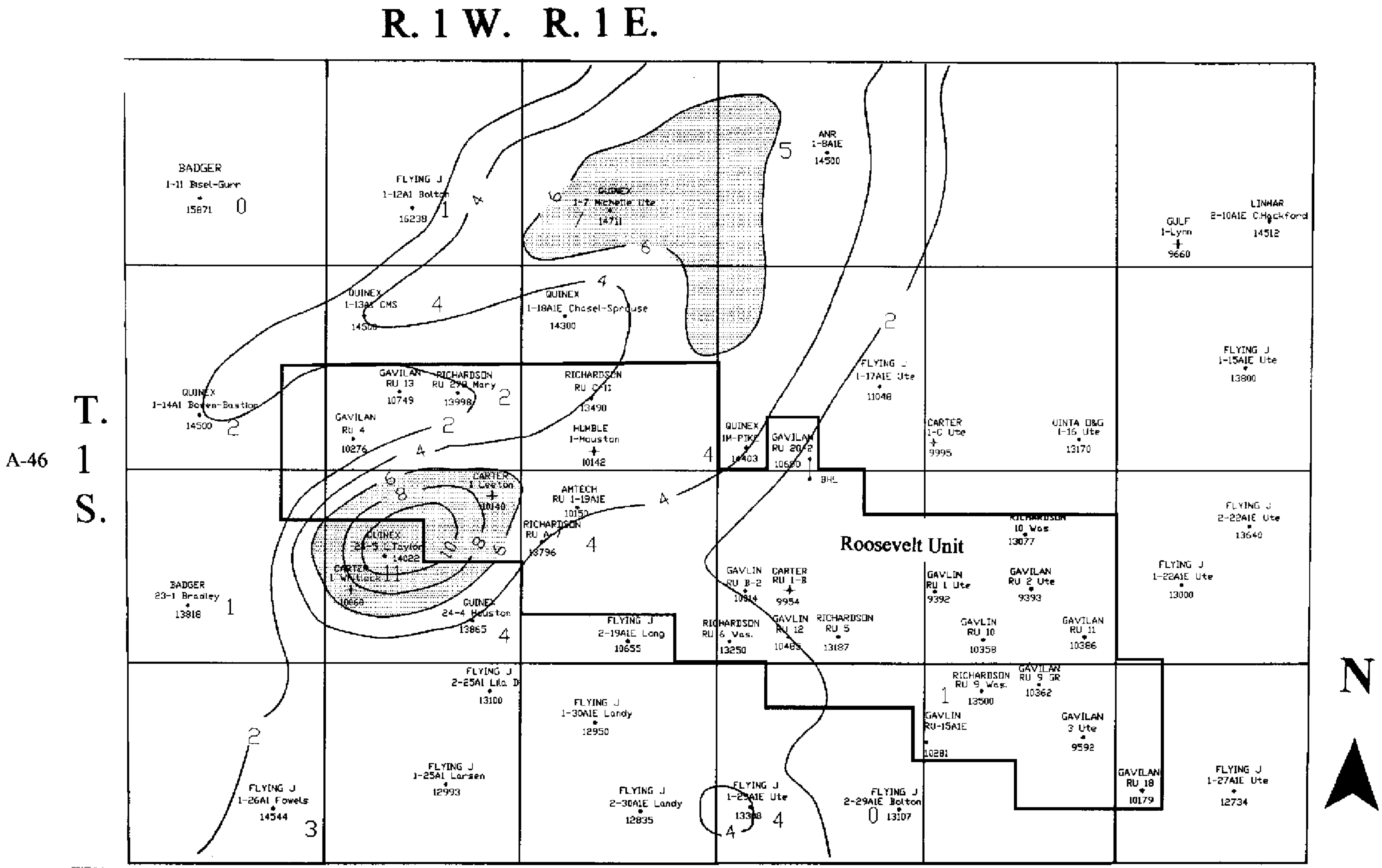

0 0.5 1.0 Miles
0.5 1.0 Kilometers

Isopach Map Bed 40
Eastern Bluebell Field
Uintah County, Utah

Contour interval 2 feet
Shaded areas are 6 feet or thicker
Bed thickness is defined by

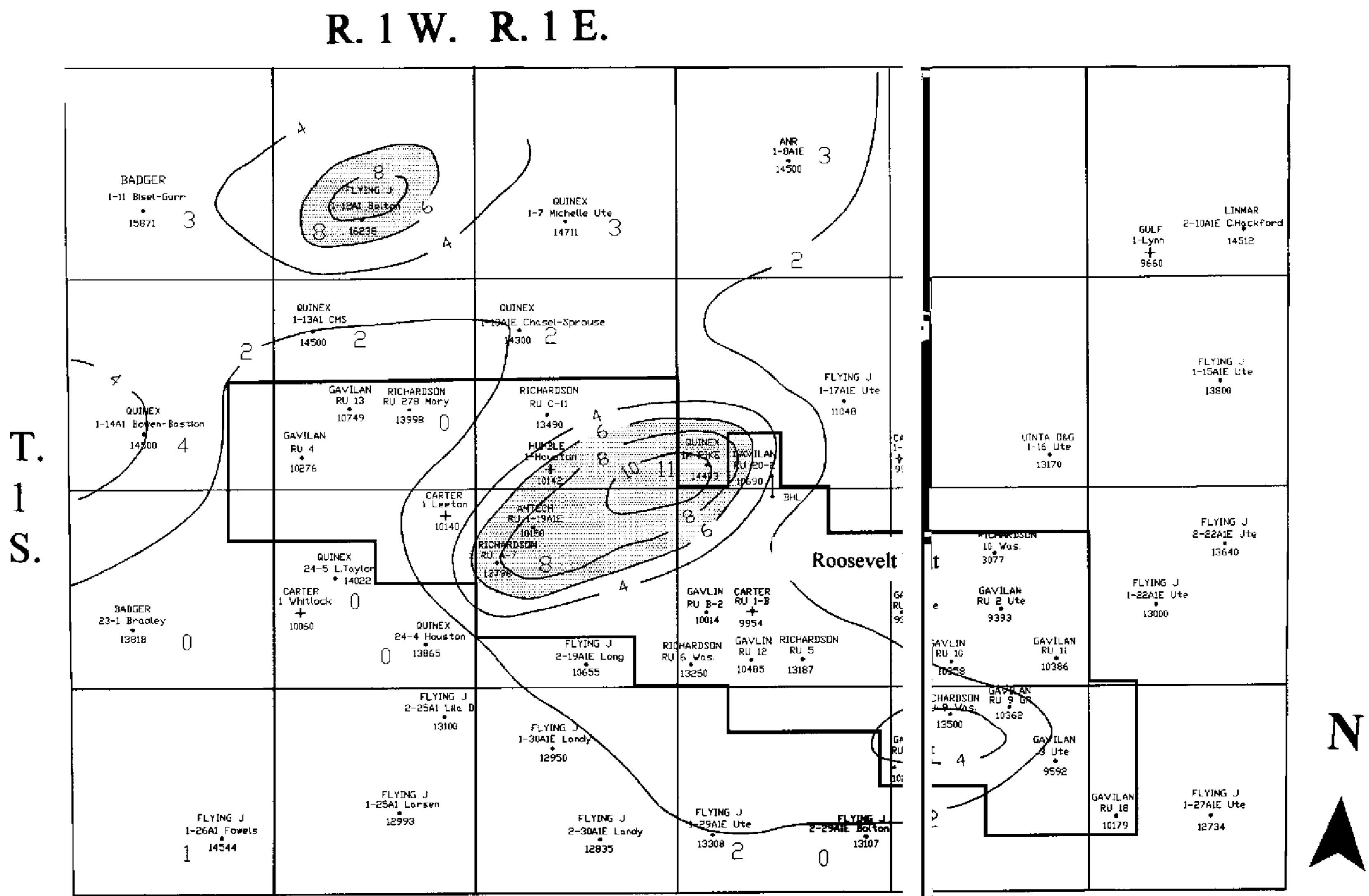

0 0.5 1.0 Miles
0.5 1.0 Kilometers

Contour interval 2 feet
Shaded areas are 6 feet or thicker
Bed thickness is defined by

opach Map Bed 41
astern Bluebell Field
Uintah County, Utah

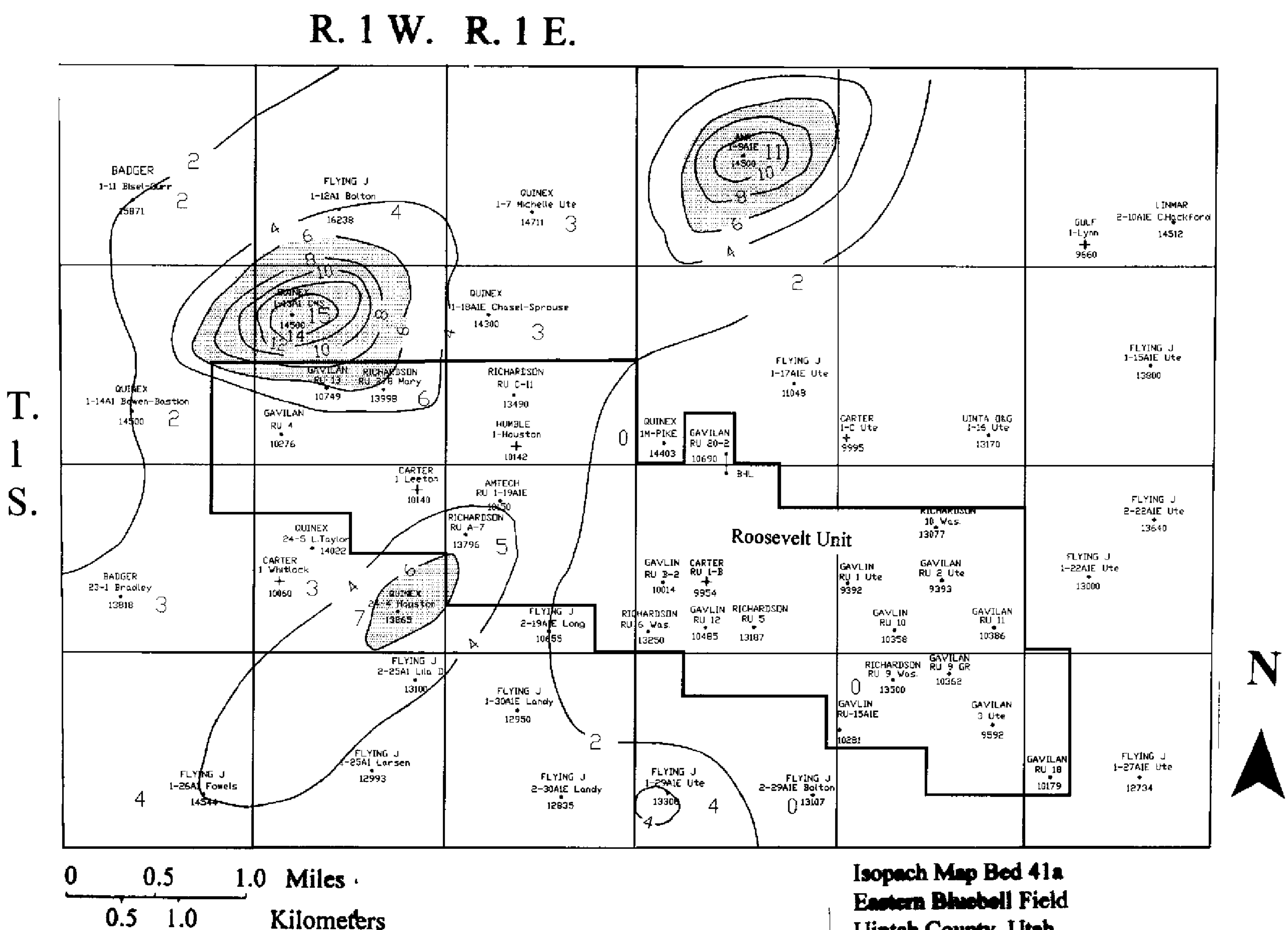

Isopach Map Bed 41a
Eastern Bluebell Field
Uintah County, Utah

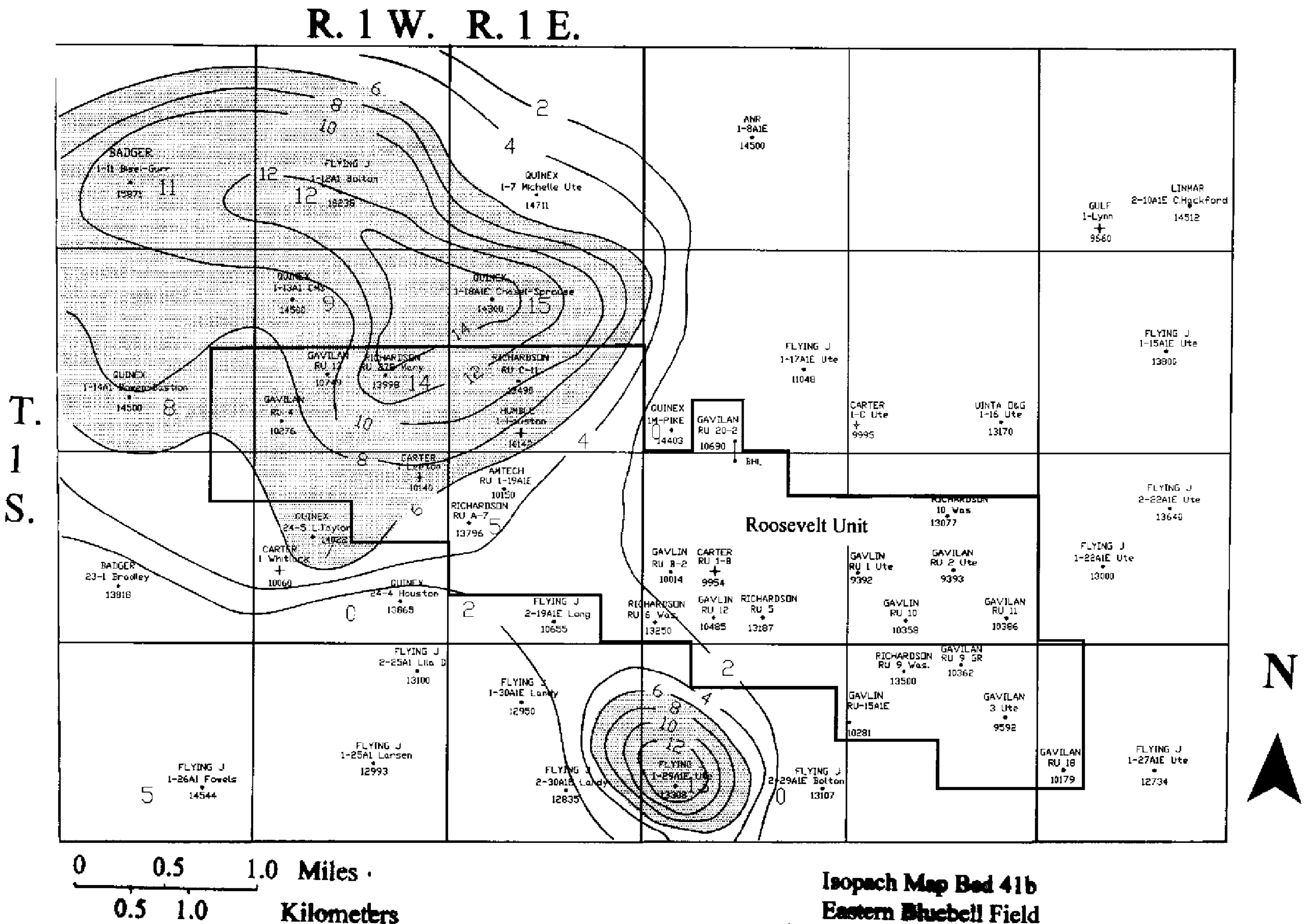

Isopach Map Bed 41b
Eastern Bluebell Field
Uintah County, Utah

Contour interval 2 feet
Shaded areas are 6 feet or thicker
Bed thickness is defined by